AN INVESTIGATION INTO JUNCTION TEMPERATURE OF GREEN AND BLUE LEDs

A Thesis

By

Burak Özlük

Submitted to the

Graduate School of Sciences and Engineering

in Partial Fulfillment of the Requirements for

Degree of

Master of Science

in the

Department of Mechanical Engineering

Özyeğin University

January 2019

Copyright © 2019 by Burak Özlük

AN INVESTIGATION INTO JUNCTION TEMPERATURE OF GREEN AND BLUE LEDs

Approved by:

Prof. Dr. Mehmet Arık (Advisor)

Department of Mechanical Engineering
Özyeğin University

Assist. Prof. Dr. Mete Budaklı

Department of Mechanical Engineering
Turkish-German University

Assist. Prof. Dr. Cenk Demiroğlu

Department of Electrical & Electronics Engineering
Özyeğin University

Date Approved: January 4, 2019

To My Family..

ABSTRACT

As more advanced technologies are developed, energy considerations are becoming more serious. This is also true for lighting systems that play a crucial role in worldwide energy consumption consisting of 15% of general consumption. Hence, integrating improved LED systems into today's lighting applications has become a critical task to build a greener future because of their high efficacy and less energy consumption. They also offer a wide variety of color options applicable for general lighting, backlighting, mobile devices, medical services, automotive lighting, display and a number of niche applications. Although the light output from LEDs is the most efficient at a narrow optical spectrum compared to conventional lighting sources, they are still not adequate to satisfy consumer demands due to considerable amounts of lost energy and emerging thermal issues. Degradation of LED components with generated heat is one of the most critical issues that directly affect the efficiency and lifetime of LEDs. Actually, while approximately 45% of electrical energy is converted into heat directly at an LED die, this becomes around 70% after considering additional heating inside an LED package. This is mainly attributed to excessive heat generation at the p-n junction region and resulting rise in the junction temperature. Among various factors, the temperature rise of the junction region has been shown as the primary cause of the degradation due to the heat generation that occurs in the package and mainly due to noncombined radiation in the die region and re-absorption of back scattered light in the package.

Accomplishing an effective thermal solution is possible if the LED junction temperature is precisely determined. A number of techniques have been proposed for the junction temperature measurement such as forward voltage change (FVC), IR thermal imaging, and Raman Spectroscopy. Since the wavelength shift method was not found accurate enough, this study focused on the first two techniques. Due to fast and reliable aspects of

the forward voltage method, it has been defined as the basic method for measuring the junction temperature in the current study and the findings have been compared experimentally using the infrared thermal imaging technique. Moreover, experimental results have been validated by means of ANSYS Icepak computational models for green and blue LEDs. Consequently, junction temperature results of green LEDs have been compared with blue LEDs and it has been determined that both LED types are sensitive to junction temperature showing a considerable change from 200 mA to 500 mA.

The effect of lens over junction temperature and optical extraction has also been investigated in the current study by comparing thermal and optical properties of an LED package in different cases including lens and without lens configurations. A detailed study is necessary to determine the transmission value of the LED lens. It may bring some uncertainties and restricts the practicality of the IR imaging technique. However, removing the lens offers some advantages such as enabling direct access to the chip. It is found that impact of LED lens is significant in heat dissipation from the junction region. In fact, blue LEDs are more affected by the lens as the junction temperature increased by 7.1 ºC compared to 4.8 ºC in green LEDs at 500 mA.

As the final step of the work, an experimental setup for the junction temperature measurement was produced by the help of experience obtained in manually conducted junction temperature measurements and the interpretation of measurement results given in the thesis. The first proposed model of the setup is working based on (FVC) method and it is designed to realize the calibration and test phases respectively with automation. The junction temperature results of T_j measurement setup have been determined properly for green and blue LEDs and compared with the results of manual T_j measurement. Consequently, variances of junction temperature results measured in both manual and produced auto setup were observed in an acceptable range with 6%.

ÖZETÇE

Teknoloji geliştikçe enerji konusundaki hassasiyetler daha da önemli hale gelmiştir. Bu durum, dünya genelinde önemli rol oynayan ve enerji tüketimi % 15'ten fazla paya sahip olan aydınlatma sistemleri için de geçerlidir. Bu sebeple, yüksek verimli ve düşük enerji tüketimli LED sistemlerin aydınlatma uygulamalarına entegrasyonu yeşil bir aydınlık gelecek için kritik öneme sahiptir. Aynı zamanda LED sistemler geniş ve farklı renk opsiyonlarıyla genel aydınlatma uygulamalarında, cep telefonlarında, medikal uygulamalarda, otomotiv aydınlatmasında, televizyon gibi birçok ihtiyaç duyulan alanda faaliyet göstermektedir. Elde edilen ışık miktarı ve görüntü kalitesi bakımından diğer ışık kaynaklarına göre daha verimli olan LED sistemler, yüksek miktarda enerji kaybına sebep olan termal problemler sebebiyle hala müşteri ihtiyacını karşılayabilecek seviyede değildirler. Kullanım ömrünü ve performansını azalttığı gibi, LED komponentlerinde meydana gelen bozulmalara sebep olan ısı oluşumu bu sistemlerdeki en kritik problemdir. LED sistemlere uygulanan elektrik gücünün %45'i direkt olarak ısıya dönüşürken, bunlara LED paketinin içindeki ısınmayı arttırıcı diğer faktörler eklendiğinde ısıya dönüşen enerji miktarı %70'lere çıkmaktadır. Diğer faktörler de göz önünde bulundurulduğunda, bu durumun en büyük etkisinin ısının ilk açığa çıktığı nokta olarak bilinen p-n jonksiyon noktasındaki elektron kombinasyonunu sağlayamayan elektronların ve geri yansıyan fotonlardan kaynaklanan radyasyon enerjisinin ısıya dönüşmesi sonucu meydana gelmektedir.

Etkili termal çözümler üretebilmenin tek yolu ise p-n jonksiyon noktasının sıcaklığını kesin bir şekilde ölçülmesidir. Önceki çalışmalarda bu noktanın ölçülmesiyle ilgili çeşitli yöntemler geliştirilmiş olup bunlardan bazıları şöyledir: İleri voltaj değişim yöntemi, Termal görüntüleme, Raman spektroskopi. Raman spektroskopi yöntemi her ölçüme uygun olmadığı ve sonuçlarında yeterli kesinlik bulunmadığı için bu çalışmada diğer iki

yöntem dikkate alınmıştır. İleri voltaj değişim yöntemi hızlı olması ve güvenilir sonuçlar vermesinden dolayı, bu çalışmada temel jonksiyon ölçüm yöntemi olarak belirlenmiştir. Bu iki yöntemin deneysel sonuçları kıyaslanmış, buna ek olarak deneysel sonuçların validasyonu için ANSYS Icepak kullanımı ile modellemeler yapılmıştır. Yeşil ve mavi LED'lerin jonksiyon sıcaklıklarının sonuçları birbirleri ile kıyaslanmış olup, sonuçlara bakıldığında tüm LED çeşitlerinin 200 mA'den 500 mA'e arttırılan akım değerleri arasındaki gözle görülür farktan dolayı jonksiyon sıcaklığındaki değişime olan hassasiyetleri gözlenmiştir.

Yürütülen çalışmanın diğer bir bölümünde, karşılaşılan belirsizlikler ve sınırlamalardan dolayı termal görüntüleme yönteminin uygulanabilmesi için LED çipler üzerinde bulunan silikon lens komponentinin çıkarılmasının gerektiği sonucuna varılmıştır. Lens etkisinin LED sitemler üzerindeki termal ve optik performanslarına olan etkisinin araştırılması için, silikon lens çıkarma işlemi gerçekleştirilip, çalışmalar lensli ve lenssiz LED'ler üzerinde ayrı ayrı yapılmıştır. Silikon lensin çıkartılması direkt olarak chip yüzeyinin ölçülmesine olanak sağlamış ve LED chip üzerinde bulunan bu lensin ısı yayılımına ve jonksiyon sıcaklığı üzerindeki etkisi gözlemlenmiştir. Sonuç olarak, 500 mA uygulanan akım koşulunda lens çıkarma işleminden en çok etkilenen LED tipi 7.1ºC artış ile mavi LED olarak belirlenirken, yeşil LED tipinde ise bu artış 4.8ºC yeşil LED gözlemlenmiştir.

Çalışmanın son bölümünde, yapılan tüm deneysel çalışmalar ve elde edilen sonuçlar ışığında, jonksiyon sıcaklık ölçümü yapabilen kompak bir deneysel setup üretimi ve testleri ile ilgili çalışmalar yürütülmüştür. Çalışma prensibi ileri gerilim (FVC) yöntemine dayandırılan sistem, kalibrasyon ve test evreleri arası otomatik geçiş yapabilecek şekilde ayarlanmıştır. Son haline getirilen sistemde gerekli deneyler yeşil ve mavi LED'ler için gerçekleştirilmiş ve jonksiyon sıcaklık sonuçları manuel olarak yapılan deney sonuçlarıyla kıyaslanmıştır. Sonuç olarak, manuel ve otomatik jonksiyon ölçüm

methodları arasında fark % 6 olarak ölçülmüş ve kabul edilebilir bir aralık olduğu sonucuna varılmıştır.

ACKNOWLEDGEMENTS

Initially, I would like to express my appreciation to my dear advisor, Prof. Dr. Mehmet Arık, for changing my life with a magic touch and giving me the opportunity to improve myself under his supervision, he advised me for the duration of the whole my master years and offered productive criticism. Also special thanks to the Engineering Faculty for giving me the chance to work as research assistant and being a part of Özyeğin University.

Secondly, I am grateful to all of my colleagues at EVATEG and ARTgroup for their help and support throughout my study. I have benefited a great deal from our individual meetings and your technical expertise and creativity. Specially, I would like to thank my colleague Ahmet Mete Muslu for his contributions to improve my abilities. I really appreciate all the technical discussions we have had during our one to one meetings.

I also want to thank to TÜBİTAK for the partial support during my research under the contract number of 217M357. Financial aid from Ozyegin University and utilization of laboratories as well as computational resources from EVATEG Center has been exceptionally helpful for part of my research.

Lastly, I would like to thank my family and my girlfriend for all sacrifices you have made. I am really appreciative for always supporting me to achieve my goals and allowing me to pursue my dreams. I am truly lack of words to express my feelings come from my heart.

Thank you all.

TABLE OF CONTENTS

LIST OF FIGURES

LIST OF TABLES

NOMENCLATURE

h	[W/m^2-K]	Heat transfer coefficient
Q	[W]	Heat transfer
T	[°C]	Temperature
g	[m/s^2]	Gravitational acceleration
R	[K/W]	Thermal resistance

Special characters

k	[W/m-K]	Thermal conductivity
α	[m^2/s]	Thermal diffusivity
V_f	[V]	Forward Voltage Value
A	[m^2]	Total convective area
T_s	[°C]	Surface temperature
T_j	[°C]	Junction temperature
T_w	[°C]	Wall temperature
T_a	[°C]	Ambient temperature

CHAPTER I

INTRODUCTION

1.1 Historical Evolution of Lighting Technology

Lighting has become one of the crucial inventions throughout humankind and it has been effectively used in various means as the technology progressed over the past years. Considering the historical background, an oil lamp was the first used light producing product and gas lighting systems were utilized to generate light for many years. Over the last several decades, new scientific approaches were carried out with the contribution of advanced technologies in material, optics and electronics science. In fact, novel approaches led to significant improvements in incandescent lamp, fluorescent tube light and CFL lamp technologies [1]. Although all of these systems have been utilized for a long time, these types of lighting systems still remain insufficient in current applications since they offer lower efficiency and shorter lifetime compared to novel counterparts [2],[3]. These shortcomings made scientists look for more effective solutions and they discovered the use of semiconductor materials in LEDs for light generation [4],[5].

LED systems consist of many LED chips that are made of two semiconductor materials and they are classified as N-type and P-type since they contain additional negatively charged electrons and electron holes respectively. Light is produced as a result of recombination of these free electrons and electron holes at the junction region of P and N type materials when electrical potential is applied [6].

The first running LEDs were created in 1907 by H.J. Round, who performed his studies with a silicon carbide (SiC) substrate, and realized that electrical potential difference between two sides of a semiconductor material caused a shift in the color of emitted light depending on its magnitude [7].

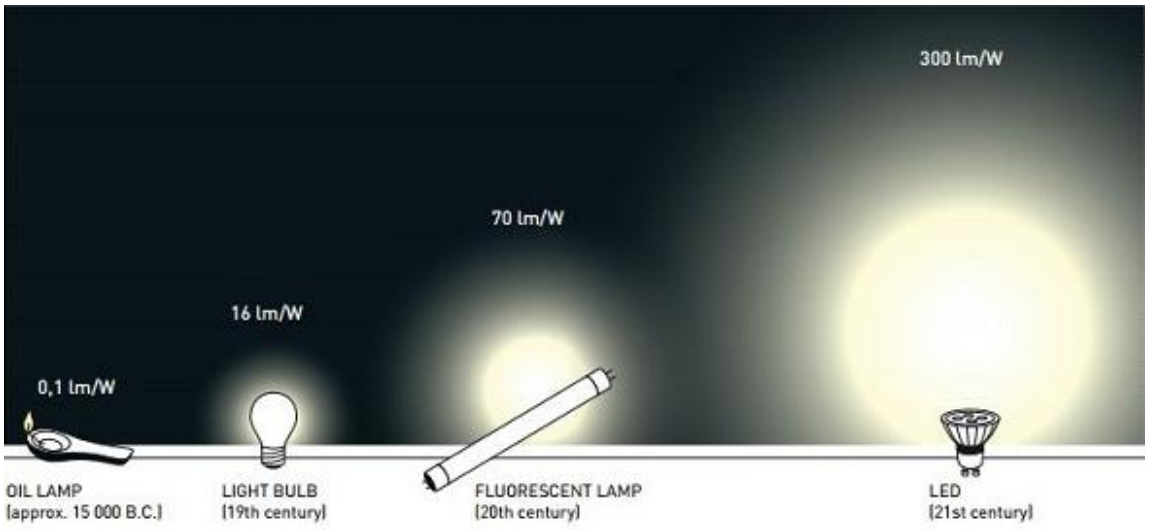

Figure 1.1 Historical evolution of lighting technology [8]

During the following years, the electroluminescence phenomena was studied by Soviet physicists in 1920s and 1930s. The first electronic transistor was invented at Bell Telephone Laboratories while they were investigating characteristics of semiconductors in 1947 [9]. A further research has focused on the electroluminescence path during the 1950s and clarified the interaction of holes and electrons in a p-n junction. Then, Shockley and Brattin received the Nobel prize for their research on semiconductors after the invention of transistor effect.

Infrared LEDs whose p-n junctions are made up of GaAs were created in 1962 by Nick Holonyak [10],[11]. After the invention of infrared LEDs, these lighting systems have long been used in various systems for indicator and signal applications. By the end of 1960s, GaP-based red and green LEDs were investigated by many researchers. At the time LEDs were producing red light, they were emitting 0.001 lumens per device [12]. Development of LEDs has continued in the following years especially after significant improvements in material science. Thus, they have offered enhanced efficiency, reliability and various color options. However, a typical LED was still inefficient compared to its counterparts until the development of AlGaN devices on sapphire by

Nakamura in 1996 [13]. This serious improvement on LED systems had attracted competitive companies' notice and it had accelerated the development of LEDs until a typical LED system's efficiency reached up to 50%. The most critical advancement was the widespread use of blue LEDs for general lighting applications [14] . The process of producing white light by utilizing LED chips can be categorized in two ways: the integration of red, green and blue lights in a package and utilization of additional phosphor material on blue LED chips. In the beginning of 2000s, the first high efficiency device was introduced by Lumileds at high operational currents. This system was the first commercial high power LED with 1W and $1mm^2$ footprint area. The performance of the high power LED systems was approximately double of an incandescent lamp [15]. In addition to high performance characteristics of LED systems, a significant lifetime period of 50,000 hours was another advantage if they operate under appropriate conditions. Further developments resulted in a 100 lm/W luminous efficiency for red LEDs, while it was 138 lm/W for white LEDs [16]. These outstanding results have showed that they were much more efficient than incandescent lamps and fluorescent lamps whose luminous efficiencies were 15 lm/W and 90 lm/W respectively. Efficiency of LED lighting systems has been recently raised over 120 lm/W due to innovative solutions.

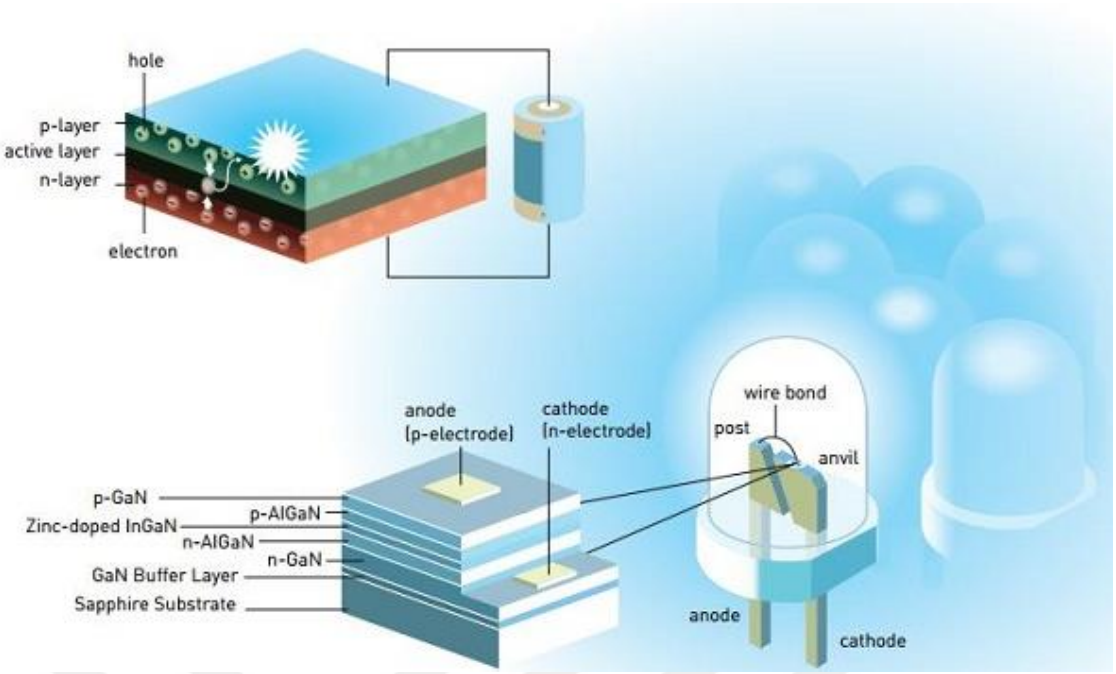

Figure 1.2 Semiconductor LED system layers [8]

Recent improvements in the performance of LED systems have put them in a significant place in the market although these systems were only used as signal or indicator lamps previously. In addition, their advantages in efficiency, durability, lifetime and flexibility have extended their potential applications in projectors, cell phones, television, cameras, toys, automobiles, computers, watches, advertising signboard, indoor and outdoor lighting systems [11].

It is also proposed that AlGaN/GaN LED systems will be used in the future to purify water by emitting some ultraviolet light that destroy bacteria and viruses [8]. Moreover, latest advancements in smart lighting industry indicated that integration of IoT systems into LED products will become a prospective technology in the era of internet of things [6], [17].

1.2 Thermal Management of LED systems

LEDs with their superior characteristics and outstanding growth potential have been considered by many researchers over the last two decades. It has been reported that lighting industry can play a very significant role in sustainability due to the fact that lighting for indoor and outdoor applications constitutes over 15% of total energy consumption [18]. Hence, integrating these lighting systems into today's lighting industry has become inevitable once considering their high efficiency, exceptional reliability, low power consumption and environmentally friendly nature. However, high power flux requirement of LED systems is the most critical problem in LED system technology. A typical high power LED has a 1 W heat generation on a 1 mm^2 surface, requiring more operating power to reach high levels of lumen outputs that cause high temperatures [12]. Characteristics of an LED system can easily be changed by temperature due to semiconductor chip material. Moreover, since LED systems do not have enough space to cool the package, problem solving becomes much more difficult [19],[20]. Therefore, in order to have more efficient LED systems, LED design from system and chip level should be handled by thermal engineers with some specific criteria's. Thermal management plays a critical role in the creation of efficient, durable and reliable LED systems. To be practical for general illumination, LED system should reach over 600 lumens for general illumination except for MR16 low lumen lamp, junction temperature should be kept below 120 ºC and lifetime should be over 50,000 hours. And this is only possible if thermal management solutions can be addressed effectively by a careful consideration of LED chips, package and system levels. The invention of high brightness LEDs raised considerable concerns about the thermal management and performance issues due to higher operating currents. In fact, the first packaged system in the size of 5 mm was subjected to higher operating currents and greater power consumption resulted

in a limitation of removing heat with a thermal resistance of 240–275 K/W [19]. However, the thermal resistance of a power LED package was necessary to keep under 20 K/W in the package to system level of thermal management [12]. In the chip scale thermal management, the contact area from silicone sub-mount to the die must be maximized in order to elevate the heat extraction and it can only be possible with increasing the size and/or a number of electrical interconnects in the LED packages [21]. As a result, a well designed LED chip and the package can result in the lowest temperature and that would end up with more effective, reliable and durable systems. On the other hand, a poor chip design with packaging defects can cause critical problems for both optical efficiency and system reliability.

Although LED systems are known with their high efficiency, around 80% of the applied electrical power on LEDs is released as heat while the remaining 20% is converted into visible light [22]. Approximately an 80% lost energy constitutes a huge developmental potential for white LEDs if their thermal issues are addressed effectively.

p-n junctions of LED systems are the most critical regions where a significant amount of heating occurs (see Figure 1.3). Furthermore, it is crucial to determine the temperature of this active region to meet the performance and lifetime goals. Increasing temperature of this region lowers total efficiency of the system and causes optical loses, while reducing the device lifetime and reliability. In addition, vast of the operated power energy converts into heat because of uncombined electron holes. Thus, it is a critical task to keep the temperature of LED modules below junction temperature limits.

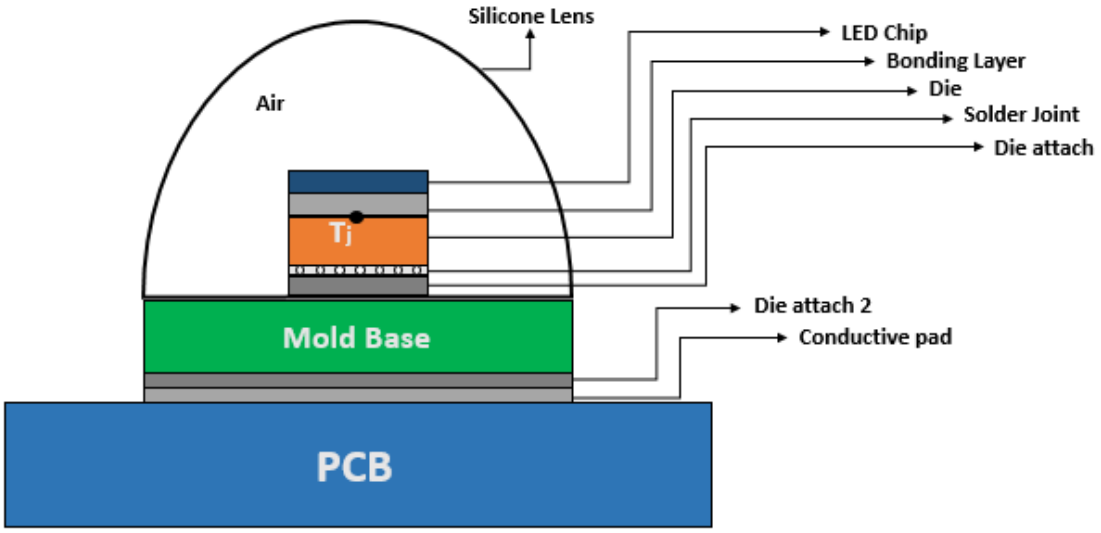

Figure 1.3 Layers of LED package [23]

In an experimental study, the effect of increased junction temperature on the efficiency of the LED system with the effect of over lifetime has been analyzed. According to the study, if the junction temperature of the LED system can be controlled below 80 °C, the lifetime of the system will be over 50,000 hours [24]. In addition, the tendency of recent electronic systems having more power consumption leads to significant local heating problems, which draw more attention to thermal management. [19], [20].

In another study, the relationship between junction temperature and lifetime sensitivity of the LED system was analyzed by Barbosa. et. al. [23]. The lifetime of the LED system is significantly reduced by the increased junction temperature as shown in the Figure. 1.4 [25]. Therefore, it is a difficult task to determine the junction temperatures of LED systems to calculate performance behavior and lifetime.

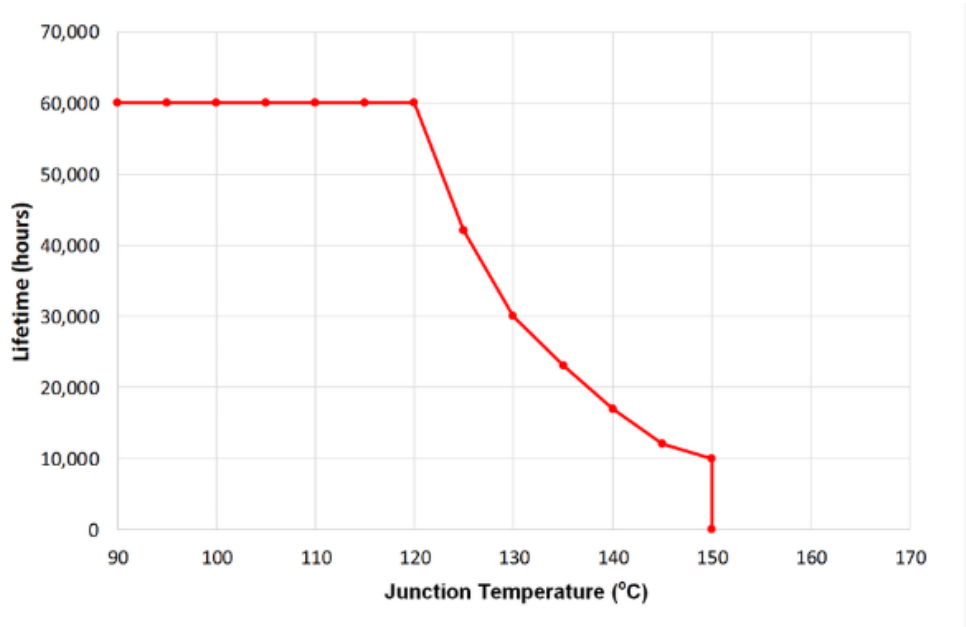

Figure 1.4 Relationship between junction temperature and lifetime (HP-LED) [25]

In addition to electrical and optical properties of LEDs such as luminous flux, correlated color temperature (CCT) and color rendering index (CRI) can also be affected by the increase in the junction temperature. Thus, it is a critical task to perform the correct temperature measurements.

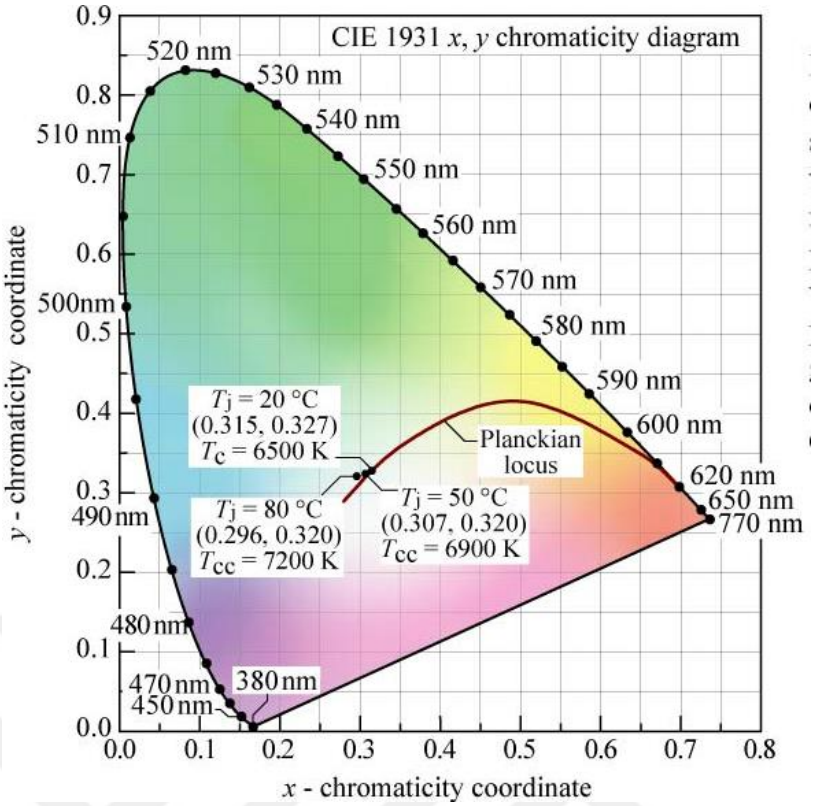

Figure 1.5 Relationship between T_j and lifetime (HP-LED) [25]

Experimental and numerical studies can be helpful approaches to reach optimum solutions in order to determine thermal characteristics and to come up with alternative thermal designs of LED systems. The challenging task is to control the thermal resistance between LED board and junction region at a value as small as possible by using various techniques [26], [27]. High thermal conductivity materials have been utilized during manufacturing of these systems and numerous studies have been evaluated to meet thermal resistance requirements. Thus, measurement of junction temperature is the most critical task to meet thermal management requirements and it is only possible with the measurement of p-n junction region accurately by suitable methods.

1.3 Junction Temperature Measurement Methods

Estimation of the thermal resistance of LEDs is closely related with the reliably determined junction temperature for high power LEDs [28],[29]. The junction temperature is determined accurately by monitoring the device temperature at the junction region, but it is not effective and requested method. Secondly, determination of junction temperature could be reached using temperature sensors by placing close point to the region, however larger size of sensors compared to junction region can be resulted in an additional error to the measurement [30]. Thus, other measurement methods have been recently developed in order to obtain junction temperature of LED systems accurately and found to be more effective.

In literature, there are three widely accepted methods for the measurement of junction temperature which can be listed as Forward Voltage [31], Raman Spectroscopy [31],[32], [33] and Infrared (IR) Imaging techniques [31]. Among the proposed methods in previous studies for the junction temperature measurement, the forward voltage method has been identified as the most accurate, reliable and suitable one for typical LED chips.

1.3.1 Forward Voltage Method

Forward Voltage method is conducted based on the forward voltage drop of an LED subjected to a temperature rise in vicinity of the so-called p-n junction. The correlation between the voltage drop and junction temperature demonstrates a strong linear trend as shown in Figure 1.6 [34]. The forward voltage of an LED chip drops linearly while the junction temperature is increasing. Relying on this electrical behavior, the FVC technique was developed in order to measure the junction temperature of LEDs operating at a specified current. The method typically consists of two main steps that aim to construct a transfer function (calibration phase) and then determine the junction temperature (test phase).

In the calibration process, the primary goal is to set a relationship between the junction temperature of an LED and its forward voltage. A temperature-controlled oven system has been used to provide a controlled thermal condition in which uniform temperature distribution is achieved during the experiments. The aim of the test phase is to obtain the junction temperature of an LED chip using the transfer function determined in the calibration phase. Also, it is crucial to perform the test phase in an integrating sphere system in order to determine the optical attributes and understand how the thermal state of the LED chip affects its optical findings [35].

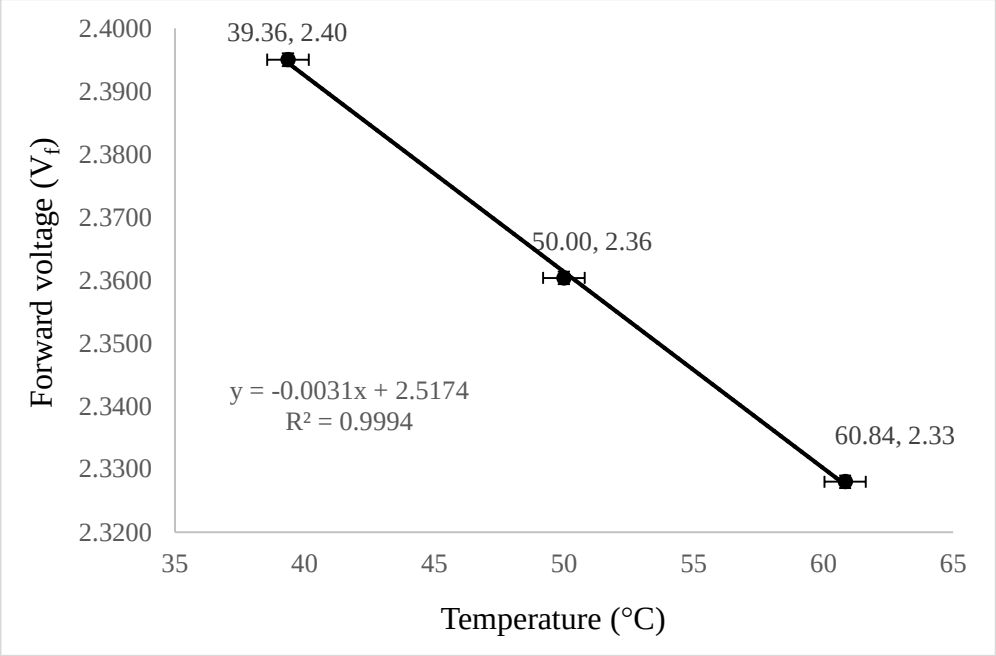

Figure 1.6 Example calibration equation of a green LED

In addition, determining the forward voltage at a certain oven temperature or junction temperature is not possible without driving the LED at a certain current, but it also causes heat generation and a rise in chip temperature. Thus, it is critical to choose a current value as small as possible so that its effect on junction temperature can be considered negligible. As presented in other studies, identification of proper pulse time and pulse duration has been studied by Tamdogan et al [35]. The forward voltages were measured at constant currents increasing from 1 mA to 450 mA for different pulse durations between 1 ms and

20 ms as shown in Figure 1.7. The highest change in voltage drop was observed in the first few seconds. Thus, in order to determine the effect of pulse width accurately in the millisecond scale, Figure 1.8 was created between 1 ms and 10 ms. Since negligible self-heating effect was observed at the junction, LEDs are operated at 1 mA pulsing current at a pulse duration of 1 ms after reaching the steady state condition. In addition, identification of proper pulsing time and pulse duration has been also mentioned in JEDEC standards [14],[36].

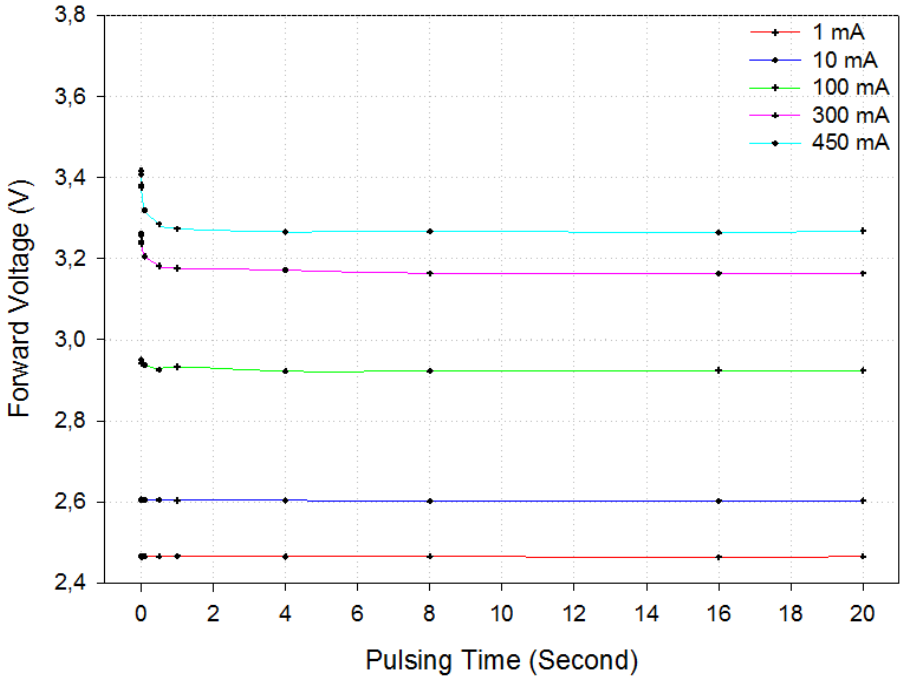

Figure 1.7 Variation of forward voltages (coarse-scale) [33]

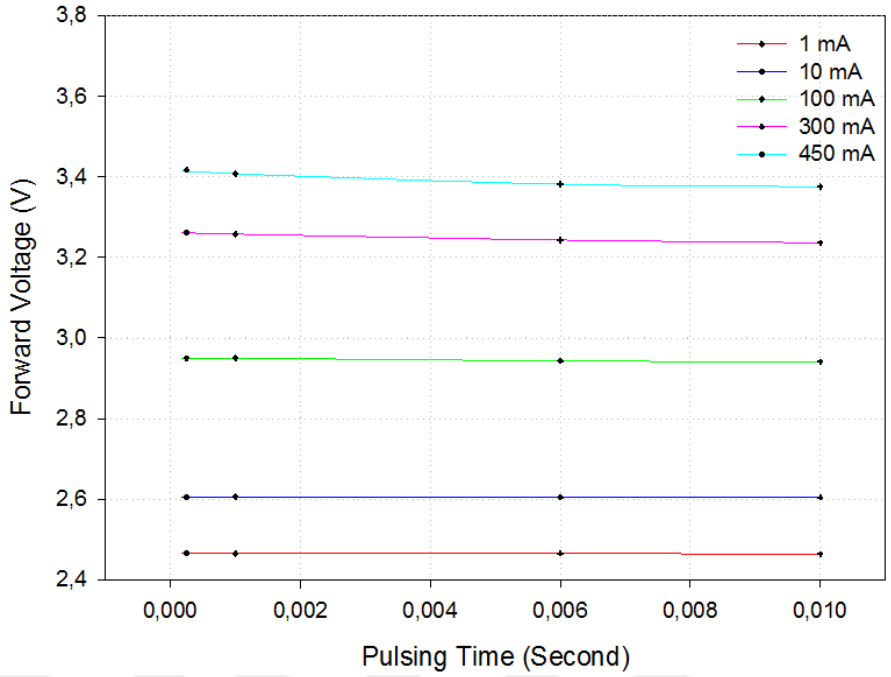

Figure 1.8 Variation of forward voltages (Fine-scale pulse duration and current) [33]

1.3.2 Thermal Imaging Method

The solid objects emit a particular amount of energy as radiative and convective heat because of their temperature. As the temperature of the objects is increasing, the transmitted radiation also increases as clarified by the principle of Planck's law of blackbody radiation. A measurement of electromagnetic radiation using IR camera is the key to determine the temperature distribution over the surface of the objects since they allow us to detect invisible infrared radiation absorbed and emitted by objects [30]. However, the measurement of bare LED die is not easily defined by using IR thermography, but this method is still used to determine junction temperature of LED systems. In fact, the infrared thermal imaging is an expensive but much practical technique if results are shown sufficient accuracy compared to other methods.

Thermal imaging method was performed by Arik et al. [31] in order to determine junction temperature of a blue LED system by using a FLIR SC3000 IR camera with the wavelength spectrum range of 8-9 μm.

In the study, the temperature distribution over a sapphire layer on top of a GaN junction (1x1 $mm^{2)}$ of a blue LED has been obtained under steady-state operating conditions of an LED. As a result of the study, junction temperature of GaN and sapphire layers has been estimated through a simple analytical conduction model. The temperature results have been measured as 40.4 ℃ and 41.26 ℃ under 100 mA operating current for sapphire and GaN layers respectively. A small variance has been observed between temperature of chip (GaN) and sapphire external surface due to the uncertainty value used for the sapphire surface for 8-9 μm range.

In another study, an experiment have been conducted for uncoated and coated blue LED chips by Tamdogan et al. [35] using a Quantum Focus Instrument (QFI) Infra Scope II system. Initially, emissivity correction was adjusted automatically at 70ºC by the QFI system. Measurements has been repeated at various times to reduce the uncertainty rate of the experimental study. Then, a single average temperature reading for each separate case was determined. Finally, maximum junction temperature results of an uncoated package have been measured as 77℃, 85℃ and 95 at 150 mA, 300 mA and 450 mA applying conditions respectively. On the other hand, unlike uncoated chips, the coated chip measurements have shown a non-uniform temperature distribution over the chip surface.

1.3.3 Raman Spectroscopy Method

Raman spectroscopy is an optical scattering method developed to capture molecular vibrational energies of optical phonons in Raman active materials. Raman scattering method captures the molecular vibrational energy that is transferred either from the incident photon to the molecule (Stokes) or from the molecule to the scattered photon (anti-Stokes) by measuring the energy difference between the incident light and radiation

scattered from the sample. While this technique was based on non-interacting randomly oriented molecules in gas or liquid phase, in solid samples such as semiconductors the phonons are also observable [35].

Measurements of junction temperature for coated and uncoated blue LED chips were performed by Tamdogan et al. [33]. In the comparative study, three different measurement techniques were investigated in order to determine the most suitable junction temperature method. Eventually, uncoated bare chips were measured accurately with all three methods and results were found to be in close proximity, while the coated packages have shown variances due to non-uniform thermal distribution. Due to extensive range of light extraction from the coated package, the Raman spectroscopy was not able to capture the peaks to the corresponding temperatures. Therefore, Raman Spectroscopy method was found unsuitable for measuring junction temperature of the LED systems under all conditions, and it can be only useful for specific junction measurements.

In another study, a non-contact method for measuring junction temperature of phosphor-converted white LEDs has been performed by Gu et al. [32]. This method has been developed by observing changes in the ratio of the total radiant energy (W) emitted by a white LED to the radiant energy within the blue emission (B). As a results of the method the change in W/B ratio can be used as a direct measure of the junction temperature. Besides, three different manufacturing samples showed a linear relationship between junction temperature and W/B ratio and this holds for any commercial white LED of this type. Eventually, researchers claimed that it could be possible to make LED life predictions based on junction temperature and short wavelength amplitude.

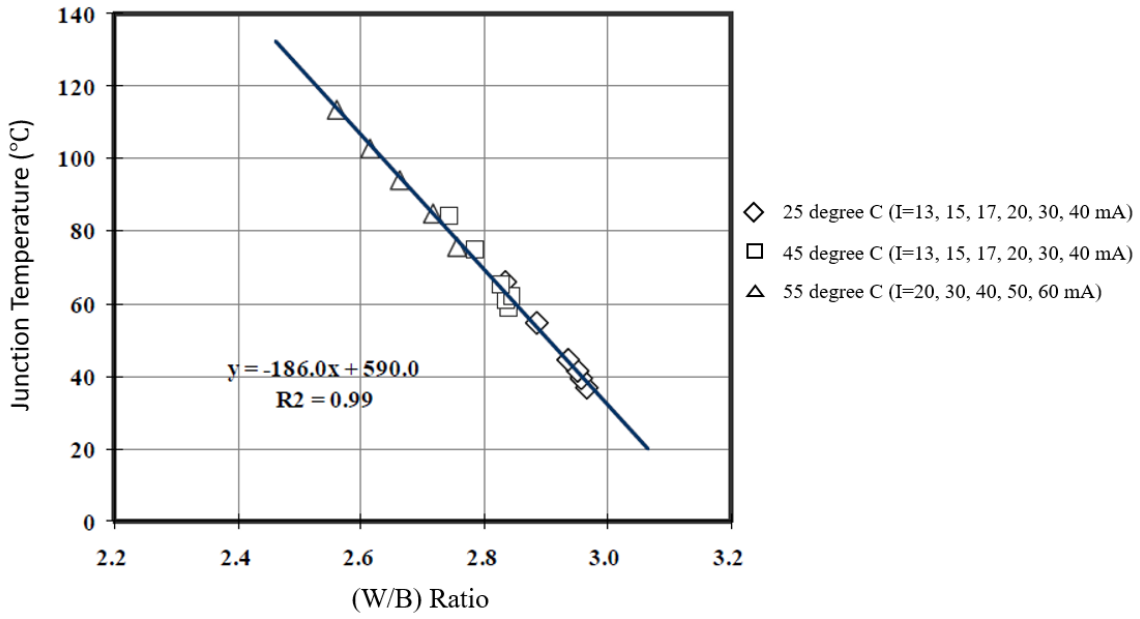

Figure 1.9 Relationship between junction temperature and W/B ratio [32]

1.4 Junction Temperature Measurement Test Systems

Existing products that stand out in measuring the junction temperature of LEDs in the market are “T3ster” from Mentor Graphics (USA) and “TRA-200 LED Thermal Resistance Structure Analyzer” from Everfine (China). Junction temperature measurements in these products are based on determination of thermal resistances part-wise [37]. Once the LED and thermal interface material properties, general dimensions and geometries are defined, thermal capacity and thermal resistance values can be determined. The first step in measuring the thermal resistance is to obtain the time dependent heating curve of the LED. In line with this method, the speed of sampling and data collection of the device must be considerably high in order to accurately obtain the heating curve of LEDs having a small structure. At the same time, following these calculations, a “structure function” which describes the relationship between thermal resistance and thermal capacity is defined and a high measurement frequency and accuracy are required since complex calculations such as convolution, inverse convolution and Fourier transformation are required.

T3ster, one of the existing devices, produces information such as properties of thermal resistance, heat flow path, thermal interface material in addition to “junction” temperature [38]. Increasing cost as a result of the complexity of the device makes this product very expensive for users who want to measure the junction temperature. At the same time, features such as high sampling rate and data acquisition resolution (1µs) were found to be as a factor to increase the product costs more than needed for the junction temperature measurement. In addition, thermal characterization is made by assuming a one dimensional heat flow path with “structure function”. However, the presence of parts such as phosphor and lens on the LED package often prevents the symmetrical spread of heat flow [39],[40]. Thus, the accuracy and reliability of the junction temperature measurements carried out in this way also raise doubts. Determining the thermal conductivity of the thermal interface material as a factor affecting the measurement result, or the necessity of using a reference thermal interface material in the measurement system, also appears as other factors that increase the device costs. In addition, the actual thermal resistance is determined by obtaining thermal power as a result of subtracting the radiation power from supplied electrical power. Thermal resistances determined without performing the photometric measurements are not also real values but can be defined as the reference thermal resistance [37].

The produced device does not have the requirements for the time-dependent measurements, determination of the material properties of the sample, and the calculation of the thermal resistance. Calibration measurements in steady state and thermal equilibrium, instead of short time-based measurements, eliminate the costly processes that previous devices have. Thus, instead of a sampling rate of 1 µs, a measurement data is collected at a rate of 1 ms in accordance with the previous work [39]. The appropriateness of this frequency was also proven in an earlier study at the EVATEG

Center [35]. Applications that increase the measurement uncertainty such as determining the thermal conductivity of the thermal interface material, have also been avoided. Furthermore, since the thermal characterization of the LEDs is made based on the measured forward voltages obtained in steady state and thermal equilibrium conditions, the heat flow assumption in one dimension is not made. In this way, the most crucial parameter that affects the LED chip performance, junction temperature is measured reliably and automatically without increasing the costs with the proposed device in the study.

1.5 Operating Parameters and Boundary Conditions

In this study, boundary conditions have been set under the consideration of a fixed ambient temperature of 25℃ and are given according to operating parameters of experimental studies, which are performed at three different input powers corresponding to 200 mA, 350 mA, and 500 mA driving currents. In the current study, the performance of a 1 W CREE Xlamp XP-E2 high power 520 nm green and 455 nm blue LED chip have been evaluated using various junction temperature measurement techniques. The related junction temperatures are measured for three different configurations of LEDs which can be listed as LED with a lens, without lens and painted (without lens). The results are compared to understand suitability and performance of each technique when it is used for measuring the LED junction temperature. Moreover, a set of numerical studies were performed with ANSYS Icepack in order to verify experimental results. Besides, an integrating sphere system were utilized to determine optical characteristics of LEDs for each case individually, since the aim of the test device is to measure efficiency of the lighting systems under thermal and optical conditions reliably. As a result, optical and thermal characteristics of high power LEDs were determined and compared with each other.

1.6 Scope of the Current Research

Main objective of the thesis was to investigate junction temperature measurement and modeling of for green and blue LEDs. In addition, a numerical study was carried out in order to develop and validate the predictive ability of experimental results. Finally, the junction measurement test setup has been developed by the integration of the optimal junction temperature method for fast measurements with less uncertainty.

Historical evolution of LEDs in the lighting, thermal problems in the LEDs and available products that measure the junction temperature of the LEDs in the market have been explained in Chapter 1. In Chapter 2, Forward Voltage Change (FVC) method and Integrating Sphere system technique have been introduced. The key point of the method and the important details were indicated by experimental data. Finally, the results of the forward voltage method were evaluated using graphs and tables, also the optical properties of the LEDs were determined.

In Chapter 3, thermal imaging technique which is known to be expensive but a practical method has been presented. The method principle has been described and illustrated by detailed pictures of a test vehicle. Silicon lens removal techniques for green and blue LEDs were performed and the most applicable method for further study was determined. Eventually, the results of the junction temperature measurements using an IR camera were evaluated for green and blue LEDs.

In Chapter 4, numerical simulations were performed to verify the results of the experiments study. All relevant dimensions and working boundary conditions of the study have been defined. Mesh sensitivity of green and blue LEDs and face alignments have been evaluated and the results of the numerical study have been discussed. Finally, a comparative study has been performed to confirm the FVC method with thermal imaging and numerical results.

In Chapter 5, a series of technical details and the production process of the T_j measurement setup have been described. The working principle of the system have been explained in a detailed schematic diagram. Finally, junction temperature results of the green and blue LEDs have been presented and compared with the results of manually measured junction temperature. In Chapter 6, the main findings of the thesis, future directions and contributions have been summarized.

CHAPTER II

EXPERIMENTAL STUDY

In this chapter, a series of experimental studies has been presented to measure the junction temperature and optical attributes of green and blue LEDs. Experimental procedure of forward voltage change (FVC) method has been introduced first and the method has been performed in both manual and automated test system, then the results have been shared and compared in order to understand reliability of measurement method and reliability of test approach. A further study has been performed with the introduction of infrared imaging technique and its results.

2.1 FORWARD VOLTAGE METHOD STUDY

In literature, there are commonly utilized methods for the determination of junction temperature. Forward Voltage method has been identified as one of the most suitable measurement techniques among numerous studies [34]. Moreover, this method has been reported the most accurate one with an error range of ±3°C [31]. In the current study, determination of junction temperature has been performed experimentally by using forward voltage technique.

The experimental study has been conducted for green and blue LEDs. In addition, obtaining various optical attributes of LED systems plays crucial role for identifying efficiency rate and thermal behavior of this system. Besides that, it is important to determine optical parameters accurately with appropriate devices. For this reason, in the current study, an Integrating Sphere system has been used in order to monitor changes in a set of optical properties such as radiant power, dominant wavelength, peak wavelength, CRI, CCT, and color spectrum depending on a range of applied current levels to correlate junction temperatures.

Forward Voltage method is known as an electrical technique in literature since it is based on forward voltage drop of an LED chip. The main idea of this technique is related with the developing relationship between forward voltage drop and junction temperature. While the junction temperature is increasing, forward voltage of an LED drops linearly. Previous studies indicated that correlation between voltage drop and junction temperature demonstrates a strong linear trend [34]. The method typically consists of two main phases that aims to derive the calibration equation (calibration phase) and then determine junction temperature (test phase).

2.1.1 Experimental Setup

In this study, a pulse meter (Keithley 2602B Source Meter) and an integrating sphere were used respectively in order to determine junction temperature of LEDs and their optical properties. Each phase of experimental study and test system have been described in the following sections with some pictures and schematics.

2.1.1.1 Calibration Phase

A temperature controllable oven is connected to a DC power supply and a data acquisition system as seen in Figure 2.1. While two DC power supplies are used in order to control the thermoelectric modules which is used to generate constant temperature surface under the LEDs and around the oven to set the control the ambient temperature. Two separate data acquisition systems provided necessary feedbacks for running the thermoelectrics properly. As temperature data is obtained by using T-type thermocouples, thermoelectric modules are adjusted at the prescribed condition accordingly in order to keep the oven temperature constant at a set value. Communication between DC power supplies and data acquisition system is established through a Labview program.

To ensure a uniform temperature distribution inside the oven, thermoelectric modules are placed on both outer walls of the chamber and below the LED system together with T-type thermocouples. After setting the oven temperature, a sufficient time is required for the system to reach steady state and thermal equilibrium conditions. For this experiment, the steady state condition is defined as approximately ± 0.1 ˚C fluctuation between the maximum and minimum temperatures over the board where the LED system is placed.

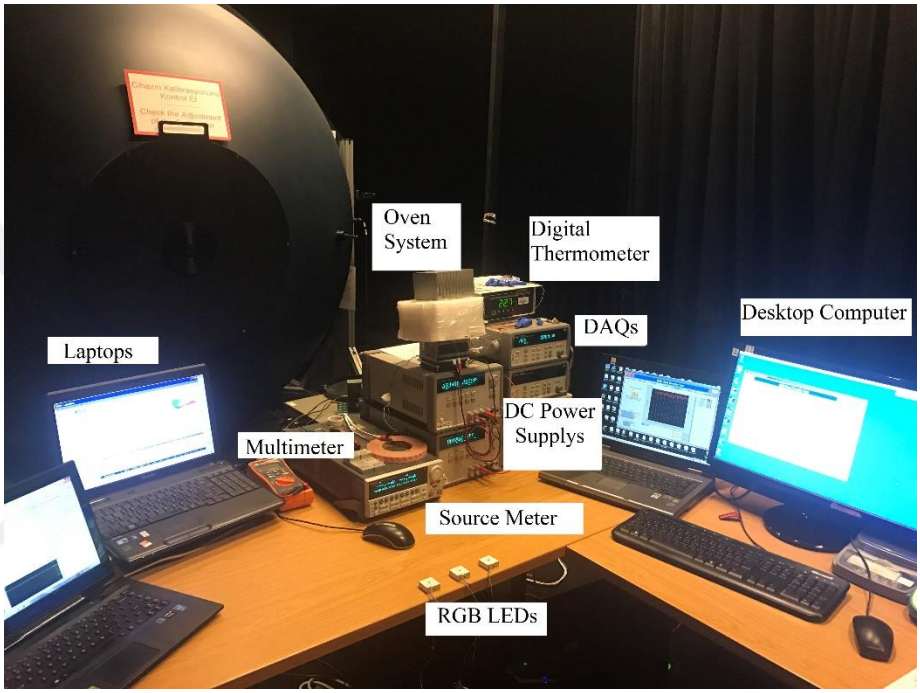

Figure 2. 1 Experimental setup of calibration phase

Once required condition is satisfied inside the oven for a set temperature, a pulse current is given by the source-meter to the LED chip in order to read corresponding forward voltage value at that temperature. It is important that given pulse current should not produce any extra self-heating on p-n junction in order to keep junction temperature constant in thermal equilibrium conditions; therefore, a pulse current with 1 mA width has been applied on LEDs for very small duration 1 ms [35].

After operating LEDs under proper conditions, the forward voltage results were determined at three different selected temperatures (40°C, 50°C and 60°C). As a result, a

calibration equation was derived using calibration readings to determine junction temperature of LEDs.

Lastly, accuracy of pulse currents and acquisition of the corresponding forward voltages of the LEDs was handled with a particular attention that is detailed in the section followed.

2.1.1.2 Accuracy of Experimental Study

2.1.1.2.1 Accuracy of Pulse Current

In order to analyze accuracy of the given pulse current used for both calibration and pulse phases as well as defining their effect on the measurement results, the process of selecting the operating pulse current was determined by an experimental study. Since any self heating generated from the pulse magnitude or duration can affect measurement results by increasing the junction temperature.

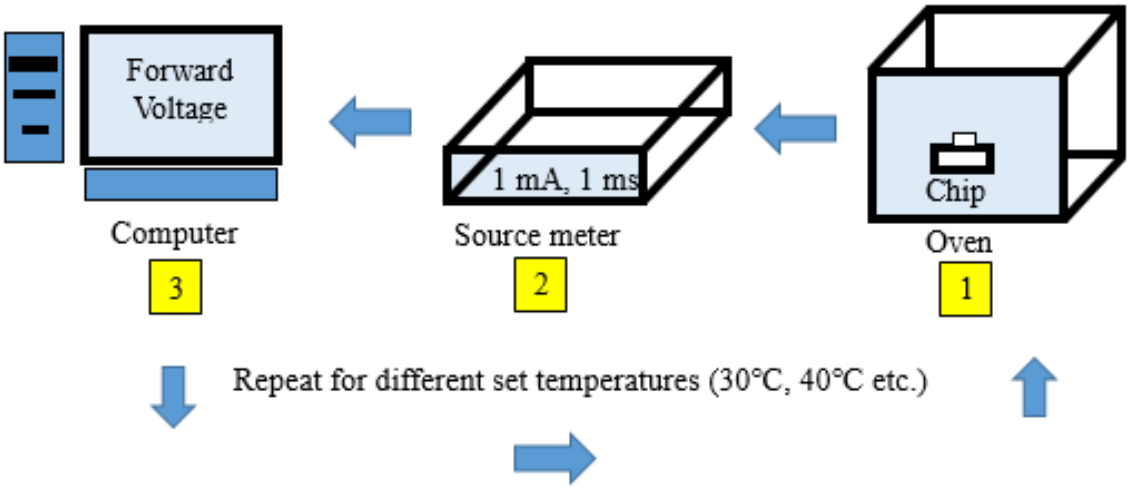

Figure 2. 2 Block diagram for the experimental procedure of forward voltage method

A number of criterias' should be considered while selecting of pulse magnitude and duration for operating currents as studied in a previous study [35]. In this study, forward voltages have been measured at constant operating currents increasing from 1 mA to 450 mA for different pulse magnitude between 1 ms and 20 seconds as shown in Figure

2.3 and Figure 2.4. The FVC was observed in the first couple of seconds as shown in Figure 2.3. [33]. In order to gain an insight about the effect of pulse magnitude, the scale of the graph was extended and pulse duration between 1 ms and 10 ms determined as shown in Figure 2.4 [33]. Since any self-heat generation at the junction was observed as also proposed in JEDEC standards [41], [42] 1 mA magnitude of operating current at a pulse duration of 1 ms was selected for entire measurements settings. The calibration process was completed, then the LEDs were operated with the selected currents (200-350-500 mA) then the corresponding forward voltages have been determined.

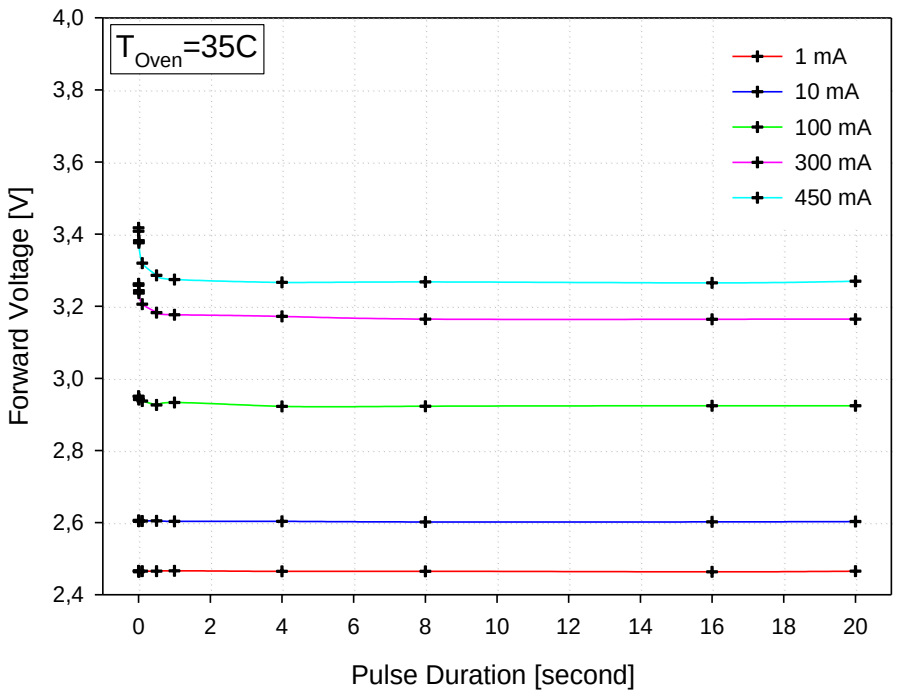

Figure 2. 3 Variation of forward voltages (Coarse scale) [33]

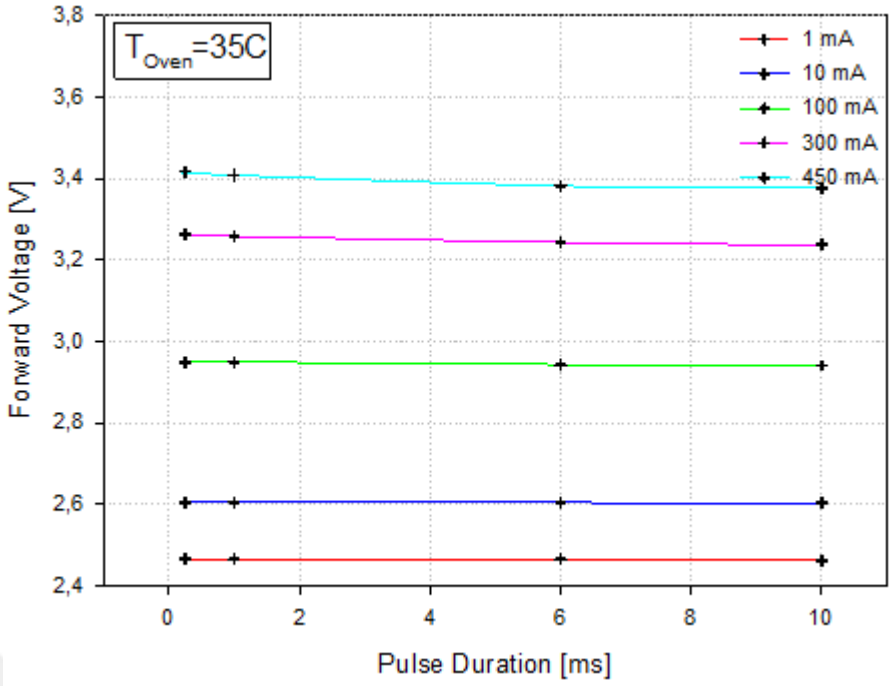

Figure 2. 3 Variation of forward voltages (Fine scale pulse duration and currents) [33]

2.1.1.2.2 Accuracy of Forward Voltage Measurements

In open literature, precision level of the repeated forward voltage method has not been studied previously. Therefore, duration requirements between the repeated forward voltages of both the calibration and the pulse phase were investigated. First, the steady state range and thermal equilibrium conditions of an LED chip were determined approximately 0.2°C at each oven temperature (see Figure 2.5).

It was observed that even 0.001 V difference in average forward voltage readings of calibration phase results in 0.3°C and 0.8°C differences in junction temperature calculations of green and blue LEDs respectively [34].

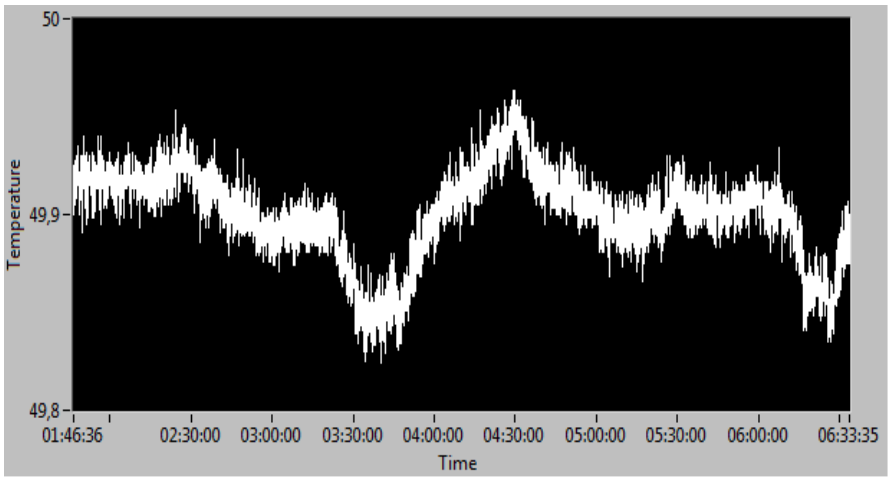

Figure 2. 4 Fluctuations in temperature at a steady state condition of calibration phase

Therefore, it was noticed that taking repeatable forward voltage readings while the system reached at steady state without any change in four digits after decimal mark and matching the corresponding oven temperature precisely for that experiment is very important. Instead of having large time gaps between applied pulse currents that could increase the possibility of variation between forward voltage results during a 0.2˚C range, a small time gap (one second) that does not introduce any heating at the junction was preferred [34].

2.1.1.3 Pulse Test Phase

The purpose of performing pulse phase is to measure junction temperature of LED systems as they are operating under suitable conditions utilizing the transfer function determined in the calibration process.

Green and blue LEDs were positioned into an integrating sphere system as shown in Figure 2.6, and T-type thermocouples were placed at the proper positions in order to monitor ambient and LED board temperature through connected Agilent data acquisition system. A Keithley 2602B source meter was also connected to operate green and blue LEDs at a selected pulse current once the system is achieved at steady state condition.

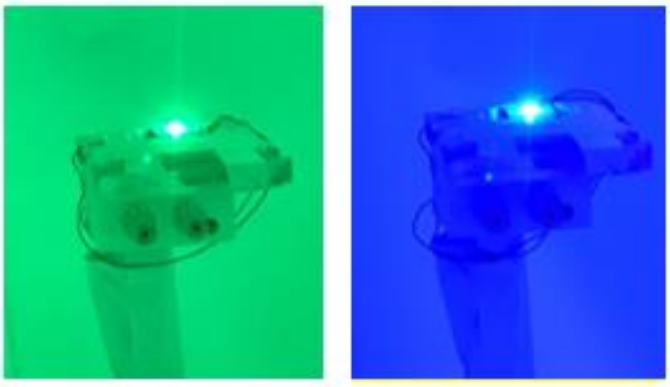

Figure 2. 5 Green and blue LEDs inside the integrating sphere [34]

The purpose of using an integrating sphere system was to determine optical characteristics of LED systems such as the radiant power, dominant wavelength and color spectrum change. The Integrating sphere system is a 2-meter diameter sphere whose internal wall is covered by a specific reflective paint which has a reflectivity of over 0.98 [43].

The LED systems were positioned at the center of the sphere and emitted lights are reflected over the reflective surface of the system when an electrical power was operated on LEDs. Finally, the reflected lights were detected by sensors located at one side of the internal wall. The received information by the sensor is converted into a digital data which can be seen in special integrating sphere computer software.

When preparing the setup inside the sphere, it is very important to adjust the height of the light source inside the sphere in order to prevent the light beams reach the detector directly. In addition, LED chips should be fixed well enough such that any motion during the measurements is avoided. Insulating LED chips well around their edges is also important in order to prevent heat dissipation around edges other than p-n junction side.

Figure 2. 6 EVATEG optical laboratory integrating sphere system

After setting up the experimental requirements, the test phase of the study was started with the calibration of system in order to introduce LED system and its position to the sphere. A selected operating currents (200 mA, 350 mA and 500 mA) were respectively applied to the LED system until they were achieved steady state condition. Once the steady state condition was met, operating currents were suddenly dropped to the current value at 1 mA magnitude for 1 ms duration, then corresponding forward voltage values were measured. The aim of dropping forward voltage was to have comparable data with the determined from calibration phase. It is important to remember that the transfer function (calibration equation) were derived at 1mA and 1ms duration in the first phase. Finally, forward voltage results that measured in pulse phase were directly put in the calibration equation for calculating junction temperature of LED systems.

While forward voltage results were measured during the pulse phase, radiometric measurements were conducted simultaneously for obtaining optical attributes of LED systems.

The procedure was applying for three different selected operating currents and differences of optical attributes of LEDs can be obtained at certain junction temperature.

Finally, radiant and electrical power measurements were determined by the sphere system and source meter in order to calculate dissipated heat converted from electrical energy. Also, determination of this converting rate enables to define efficiency of LED system. As a result, optical behaviors of green and blue LEDs for three different junction temperatures were identified by comparing the percent change in radiant power, wavelength shift, junction temperature and dissipated heat from LEDs.

2.1.2 Experimental Study Results

Experimentally measured forward voltage, junction temperature and optical attributes of green and blue LEDs were presented. Initially, calibration process was performed in order to derive required transfer function for pulse current phase. After that, determination of junction temperatures, optical measurements in the integrating sphere was conducted for the current study. Finally, forward voltage (V_f), junction temperature (T_j), electrical power (P), radiant flux (Φ_e), dissipated heat (Q), and dominant wavelength (λ_{Dom}) change behaviors of green and blue LEDs between three operating currents were analyzed and compared with details in later sections.

2.1.2.1 Calibration Phase Results

Before starting the experimental study for the calibration phase, experimental setup and accuracy of pulse were prepared as it is explained in the previous sections. Experiments were repeated three times to ensure the desired accuracy of the results were achieved. Test results with the lowest standard deviation were chosen to derive the calibration equation. Then, measured forward voltages were averaged and presented as shown in Table 2.3 and Table 2.4 with the selected oven temperatures so that the standard deviation was reduced as small as possible in the experimental study.

During the experimental study for the calibration phase, oven temperatures were adjusted approximately 40°C, 50°C and 60°C and forward voltage results for each LED were presented below.

Table 2. 1 Forward voltage results (V) of three experiments for green LED

Experiment	Set temperature (°C)		
	40	50	60
1	2.39503	2.36034	2.32799
2	2.39506	2.36037	2.32795
3	2.39504	2.36030	2.32797

Table 2. 2 Forward voltage results (V) of three experiments for blue LED

Experiment	Set temperature (°C)		
	40	50	60
1	2.39760	2.37979	2.36221
2	2.39767	2.37977	2.36226
3	2.39761	2.37976	2.36220

The average value of measured forward voltages was considered in all analytical calculations. It is important to mention that four digits after decimal mark were critically selected for all measurements in order to increase accuracy of the transfer equation.

Table 2. 3 Calculated average forward voltage (V) for a green LED at 40°C

Pulse Duration (ms)	Pulse Current (mA)	Forward Voltage (V)	Standard Deviation (V)	Average (V)
1	1	2.39503	1.52753E-05	2.3950433
1	1	2.39506		
1	1	2.39504		

Table 2. 4 Calculated average forward voltage (V) for a blue LED at 40°C

Pulse Duration (ms)	Pulse Current (mA)	Forward Voltage (V)	Standard Deviation (V)	Average (V)
1	1	2.39760	3.78594E-05	2.3976266
1	1	2.39767		
1	1	2.39761		

The average of measured forward voltage values of each LEDs were embedded into graph to make them presentable. Thus, calibration equations of green and blue LEDs were derived by utilizing average forward voltages. Three forward voltage values were determined for three different set temperatures and the slope of the derived equation was found to be more than 0.995 (R^2). The correlation of the oven temperature and forward voltage results can be seen in Figure 2.8 and 2.9.

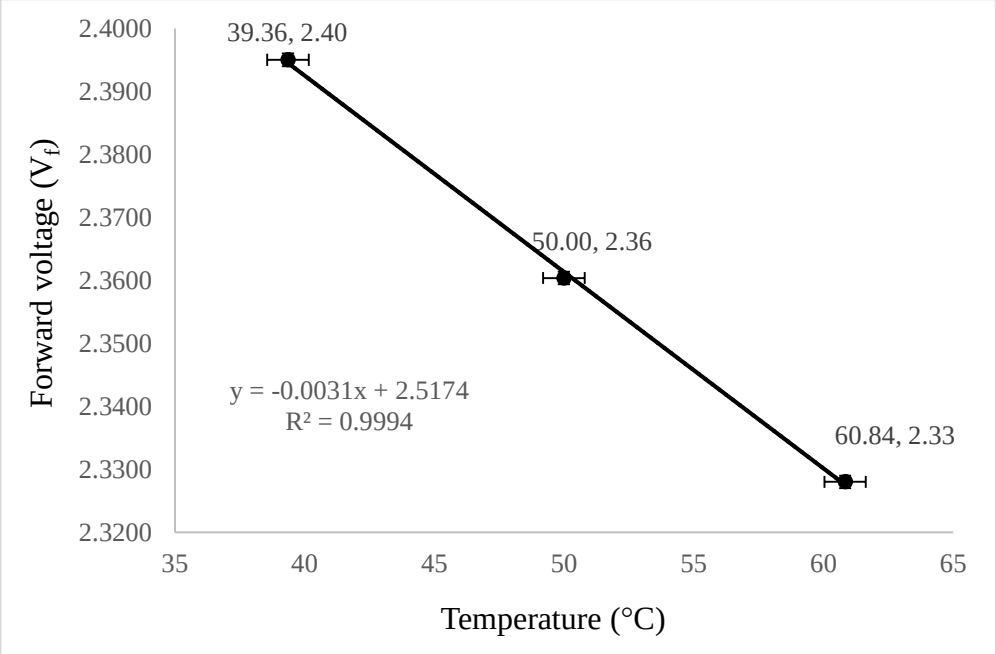

Figure 2. 7 Calibration equation for a green LED chip

2.3950 V, 2.3603 V and 2.3279 V forward voltage results were determined respectively in 39.36°C, 50.00°C and 60.84°C oven temperatures for a green LED chip. The R^2 value

on chart was identified as 0.9994, which is in the acceptable range in terms of the linearity of the experimental data.

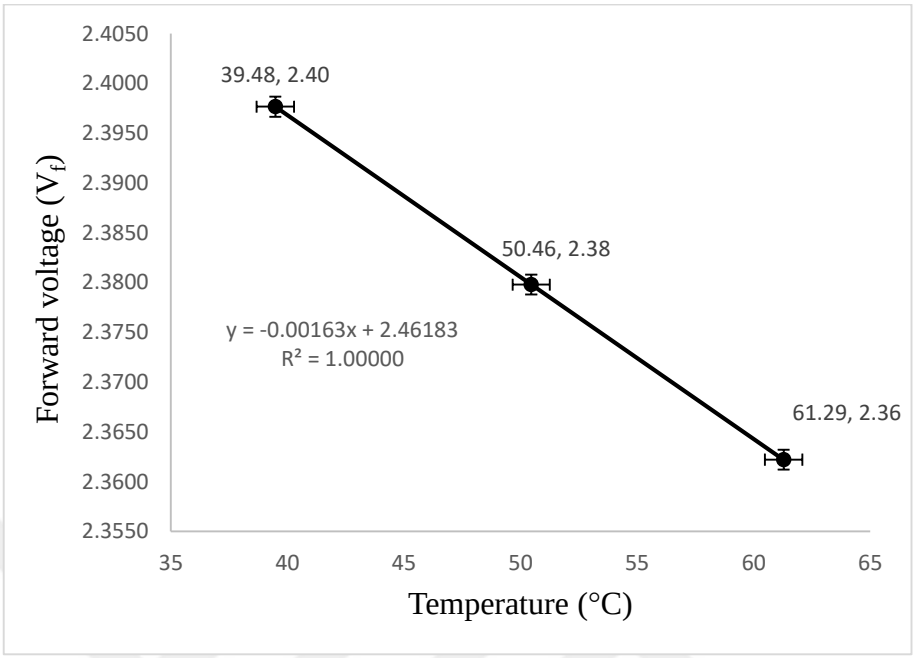

Figure 2. 8 Calibration equation for a blue LED chip

2.3977, 2.3798 and 2.3622 V forward voltage results were obtained respectively in 39.48°C, 50.46°C and 61.29°C oven temperatures for a blue LED chip. The R^2 value on chart was found to be 1 that indicates high prediction capability for the calibration equation. Besides that, the slope ($R^{2)}$ of this equation for the blue LED chip was noted as the biggest one compared to green LED chip.

2.1.2.2 Pulse Phase Results

The aim of the second phase of method was to obtain forward voltage readings under real operation conditions of LED chips. Thus green and blue LEDs were positioned in the integrating sphere system respectively and connection of the Keithley 2602B Source meter was done in order to provide a pulse current. Finally, T-type thermocouples were placed under the LED chip board and inside the sphere system in order to monitor temperature of the LED chip board and ambient by using a DAQ system. Each LED chip

were exposed to 200 mA, 350 mA and 500 mA operating currents and dropping operating currents to 1 mA magnitude was performed after a steady state condition was met in order to determine the corresponding forward voltage values which were used for obtaining junction temperature of LEDs. The same process was repeated three times for each LEDs and averaged for reaching requirement of accuracy.

In addition, selection of time interval between pulse currents (1 mA) was determined over 30 seconds in the experiment to make sure that the steady state condition was under control. As a result of experimental study, four digits of forward voltages after decimal mark was found the same for a 30 seconds time gap.

As forward voltage readings of LEDs were getting sensitively, optical attributes of these systems was also identified since it was positioned inside the integrating sphere system. After requirements of calibrating sphere system was performed, optical measurement readings were obtained utilizing LightMtrX software under steady state condition. Thus, spectrum flux graphics, radiant flux and dominant wavelength of green and blue LEDs were extracted. In the following section, the electrical, optical and thermal behaviors of green and blue LEDs will be presented as their operating currents increasing from 200 mA to 350 mA and 500 mA.

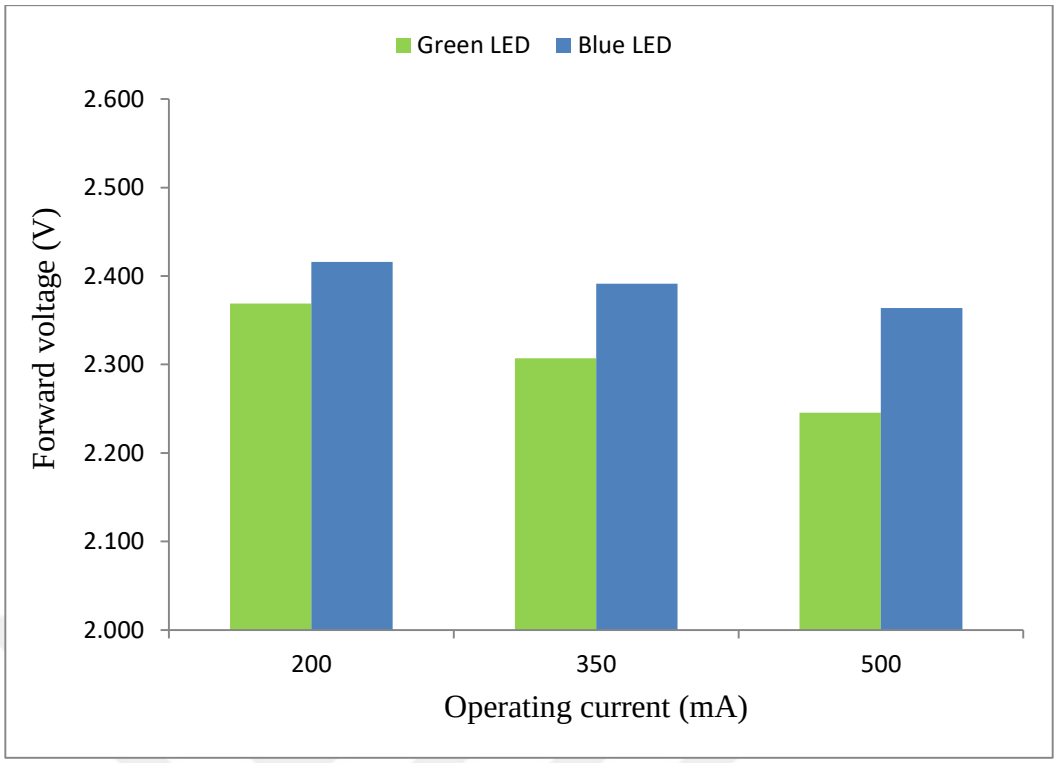

Figure 2. 9 Variation of forward voltage (V) for green and blue LEDs

The forward voltage changes of green and blue LEDs were shown in Figure 2.10 for operating currents of 200 mA to 350 mA and 500 mA. It is important to clarify that the forward voltage change of the green LED was determined by 1.47 % from 200 mA to 350 mA and 1.39 % from 350 mA to 500 mA. While it is 0.77 % and 0.79 % for the blue LED at increasing applying current from 200 mA to 350 and 350 mA to 500 mA respectively.

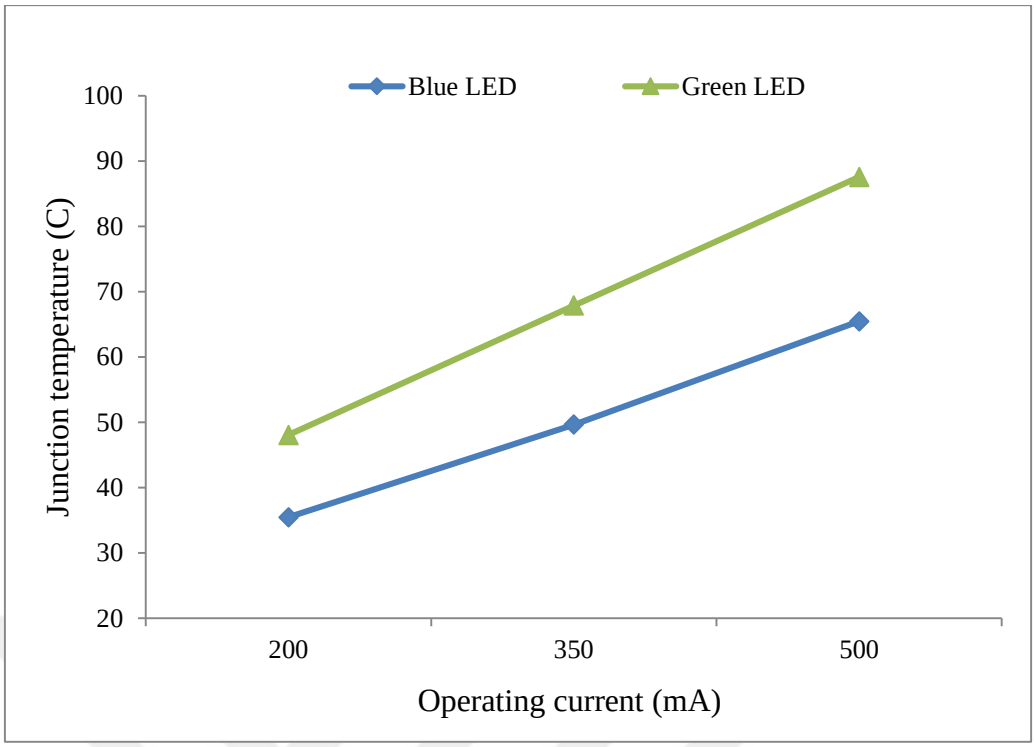

Figure 2. 10 Variation of junction temperature for green and blue LEDs

Figure 2.11 indicates the junction temperature results of green and blue LEDs for 200 mA, 350 mA and 500 mA operating currents. When the operating currents increased from 200 mA to 350 mA, the change in T_j values were measured in the green LED chip by 19.8°C, while it is 14.1°C for the blue LED chip. In addition, the change in T_j values were identified by 19.6°C and 15.8°C for the green and blue LED chips respectively, once the operating currents are elevated from 350 mA to 500 mA.

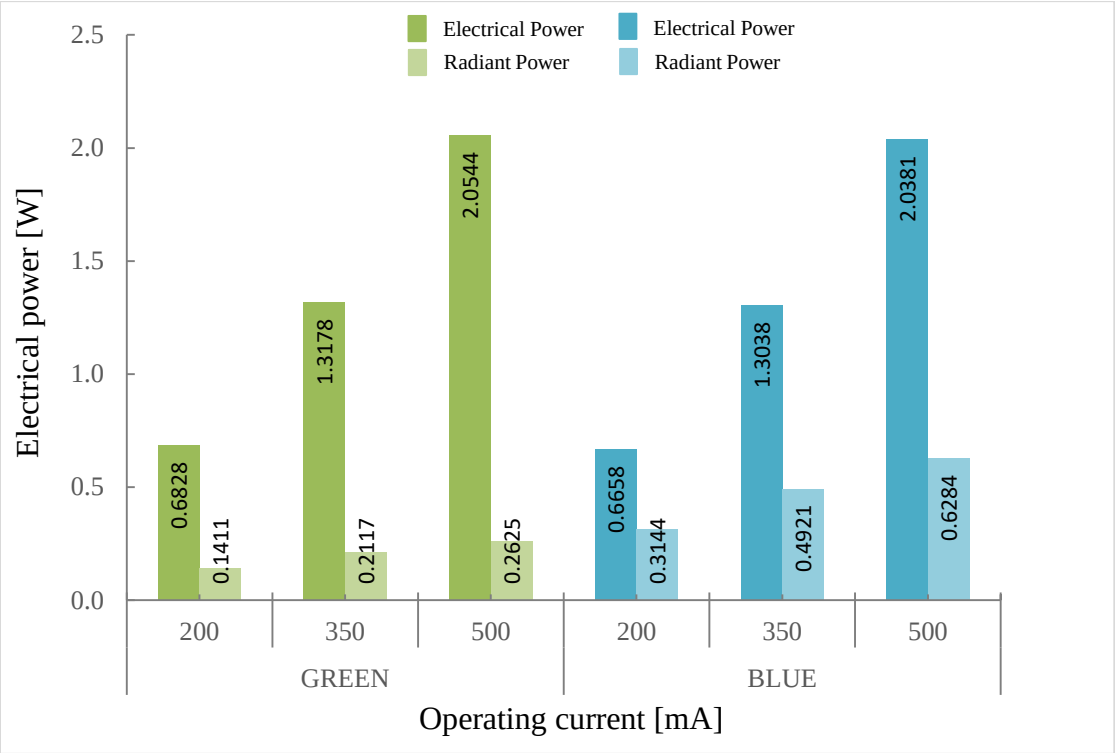

Figure 2. 11 Conversion rate from electrical to radiant power (W) for green and blue LEDs

Green and blue LEDs were respectively operated under 200, 350 and 500 mA during the pulse test phase. Input electrical powers were obtained proportionally at respective operating currents as shown in Figure 2.12.

Figure 2.12 shows radiant power outputs of green and blue LEDs as operating currents are increasing from 200 to 350 and 500 mA in order to insight relationship between junction temperature and radiant energy. When increasing the operating currents from 200 mA to 350 mA, the change in radiant energy were noted in the green LED chip by 50 %, while 56.5 % for the blue LED chip. In addition, increasing the operating currents from 350 mA to 500 mA led to the change in radiant energy by 23.9 % for green LED chip and 27.6 % for blue LED chips respectively.

On the other hand, the rate of converted heat from electrical energy was calculated. The amount of heat dissipation from 200 to 350 mA was determined 0.564 W for the green LED chip and 0.460 W for the blue LEDs respectively. The amount of heat dissipation

from 350 to 500 mA was also found to be 0.685 W and 0.598 W for green and blue LEDs respectively.

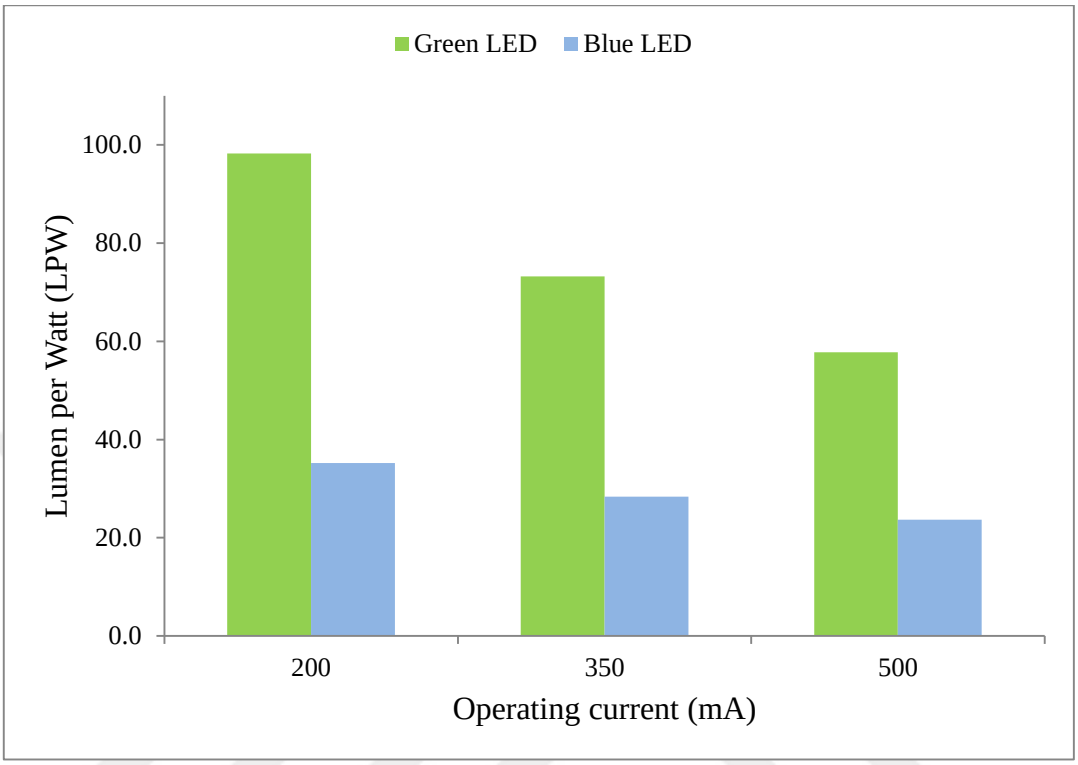

Figure 2. 12 Variation of dominant wavelength (nm) for green and blue LEDs

Figure 2.13 shows the efficiency rate of green and blue LEDs as increasing their operating currents. In other words, the value of lumen (radiant power) was indicated per 1 W in Figure 2.13. When operating currents are increasing from 200 to 350 mA, reduction in LPW value was observed by 34.1 % for green LED and 24.1 % for blue LED respectively. The amount of decrease from 350 to 500 mA was also determined 26.7 % and 19.8 % for green and blue LEDs respectively. Finally, electrical, thermal and optical results for green and blue LED chips can be summarized in Table 2.5 and Table 2.6 as below.

Table 2. 5 Electrical, thermal and optical results for a green LED chip

Parameter	Operating current (mA)		
	200 mA	350 mA	500 mA
V_f (V)	2.3689	2.3071	2.2457
T_j (˚C)	48.0563	67.8865	87.5551
P (W)	0.6828	1.3178	2.0544
Φ_e (W)	0.1411	0.2117	0.2625
Q (W)	0.5417	1.1061	1.7918
LPW	98.2242	73.2367	57.7793
P. W. (nm)	526.5	524.8	524.0
D. W. (nm)	534.6	532.0	530.2
CCT(K)	7185	7376	7495

Table 2. 6 Electrical, thermal and optical results for a blue LED chip

Parameter	Operating current (mA)		
	200 mA	350 mA	500 mA
V_f (V)	2.4158	2.3912	2.3639
T_j (˚C)	35.4573	49.6382	65.4619
P (W)	0.6658	1.3038	2.0381
Φ_e (W)	0.3144	0.4921	0.6284
Q (W)	0.3514	0.8117	1.4098
LPW	35.2099	28.3644	23.6635
P. W. (nm)	468,4	468,3	468,5
D. W. (nm)	472.6	472,4	472,4
CCT(deg.K)	22000	22000	22000

2.1.3 Experimental System for the T_j Measurements

The produced first model of the T_j measurement experimental setup is existing of 20 mm thick aluminum blocks (chamber) where the LED samples are positioned and kept under desired thermal conditions. 6 heaters were located in each wall by grooving at all outer block surfaces and heating power of them is controlled by the use of PT-100 type

thermocouples positioned behind of the heaters and attached the walls. While these six thermocouples measure the temperature of the walls, other 4 PT-100 type thermocouples are located inside of the chamber in order to monitor the ambient temperature. Since the primary goal of the T_j measurement setup is to reach steady state and thermal equilibrium condition in the chamber, a PLC controller was utilized. The temperature of the air in the system is defined as the value of ±0.2˚C (can be adjust by user) variation by averaging 4 PT100 thermocouples via PLC system. The outer surfaces of all over the wall were covered with the insulation material in order to minimize heat losses. A sourcemeter is utilized as another critical part of the device in order to supply a very small magnitude (1 mA) current for a very short time duration (1 ms) in calibration phase of the measurement. All test settings such as set temperature, sensitivity of steady state condition, forward voltage range, operating pulse currents are adjusted before the measurement is initiated by the user and the measurement process can be easily monitored. The each controlled heaters by a PLC system have 150 W heat capacity and they provide full of power once the system initiate to heat until reaching the set temperature defined by user.

The maximum temperature inside the chamber was limited with the value of 100˚C because of safety reasons related to maximum temperature LEDs can stand for. An LED is positioned at the bottom surface of the chamber by using adhesive epoxy material. The device software also enables to follow the temperature variation at different places transiently in the chamber by monitoring temperature results of 10 thermocouples to check steady state condition. Some operating conditions can be either chosen default or user defined in the software. Those selections include temperatures at which calibration equation is derived, temperature sensitivity at steady state, pulse current width and duration, delay time between measurements, forward voltage sensitivity between measurements, desired R^2 value for the relation between T_j and V_f and temperature at

which test phase of the measurements is conducted. Other than these selections, operating currents at which junction temperature is preferred to measure should be defined by the user only since it varies depending on the LED type.

A sourcemeter used as a part of the device is responsible for applying small pulse currents (1 mA) on an LED for short durations (1 ms) in calibration phase and supplying an operating current in test phase for much larger durations. Application of the direct current on LED in these phases can be adjusted in a desired configuration through the software but measurements are repeated until a certain desired R^2 value is met in the calibration relation and 0.0005 V sensitivity is obtained between forward voltage results. It was shown in a previous study that 0.001 V variation in forward voltage reading corresponds to 0.3 - 0.8˚C change in junction temperature. Thus, meeting these conditions would ensure the measurement results are reliable. 1 ms frequency of the temperature measurement of the device also enhances the reliability. Safety measures are taken for the system including emergency button, maximum temperature, voltage and current limit sets.

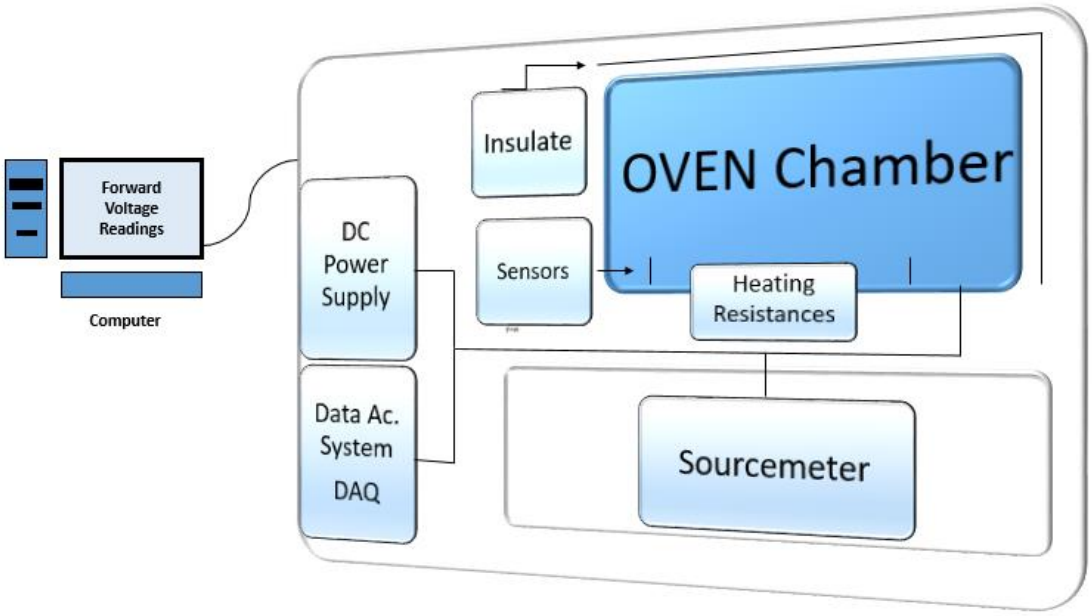

Figure 2. 13 Scematic diagram of the junction temperature setup

2.1.4 Experimental Results

In the current section, results of the measurement setup for green and blue LEDs were presented. Calibration process was initiated according to the user defined settings shown in Table 2.7 in order to derive the required calibration function.

Table 2. 7 Calibration phase settings of green and blue LEDs

	Green	Blue
Set temperature ℃	30 - 40 - 50	30 - 40 - 50
Pulse magnitude(mA)	1	1
Pulse duration (ms)	1	1
Delaying time (s)	3	3
V_f readings range	0.0005	0.0005
Steady state range (℃)	0.2	0.2
R^2 value	0.985	0.985

Secondly, the requirements of pulse phase were also inputted by the user as shown in Table 2.8 to determine the junction temperature. Consequently, forward voltage and junction temperature results of green and blue LEDs were depicted between three operating currents in Table 2.9 and Table 2.10.

Table 2. 8 Pulse phase settings of green and blue LEDs

	Green	Blue
Operating current (mA)	200 - 350 - 500	200 - 350 - 500
Delaying time (s)	60	60
Oven temperature (℃)	-	-
V_f readings range	0.0005	0.0005
Number of Avg. V_f	10	10

Table 2. 9 Results of automated experimental setup for green LED

Parameter	Operating current (mA)		
	200 mA	350 mA	500 mA
Forvard voltage (V)	2.3808	2.3225	2.2612
Junction temperature (˚C)	44.25	62.94	82.06
Board temperature (˚C)	34.7	44.1	53.2
Ambient temperature (˚C)	23.3	23.3	23.3

Table 2. 10 Results of automated experimental setup for blue LED

Parameter	Operating current (mA)		
	200 mA	350 mA	500 mA
Forvard voltage (V)	2.4085	2.3875	2.3620
Junction temperature (˚C)	32.83	45.80	61.48
Board temperature (˚C)	30.84	38.17	46.26
Ambient temperature (˚C)	23.4	23.4	23.4

Finally, a comparison of measurement results was shown both manually and automatically in Table 2.11 in order to validate reliability and accuracy of the automated the experimental setup.

Table 2. 11 Comparison of results determined manually and automatically

Current [mA]	Manual		Auto	
	Green LED	Blue LED	Green LED	Blue LED
200	48.056	35.45	44.25	32.83
350	67.886	49.65	62.94	45.80
500	87.555	65.46	82.06	61.48

In the light of results given in Table 2.11, junction temperatures in both manual and automatic results were found to be in a close proximity. For instance, at 200mA applying condition, the junction temperature was found to be 48.05 ℃ for manual measurement, while 44.25 ℃ for automatic measurement of the green LED. The junction temperature results of the blue LED were also defined as 35.45 ℃ and 32.83 ℃ for manual and automatic measurement under 200 mA operating currents respectively. Thus, variances of the junction temperature results were observed in an acceptable range with 6 % between manual and automatic measurements. It is crucial to result that produced the measurement experimental setup have a change to become essential for the measurement studies if it could have produced as fully automated and higher performance.

2.2 THERMAL IMAGING METHOD

Altough there are numerous methods for the junction temperature measurements, some of them have been identified as proper techniques in literature. One of those, thermal imaging method, has been selected as much practical method and utilized during the different phases of the study. However, in order to guarantee that the results obtained from the thermal imaging method are reliable, comparison has been made in the current study with the forward voltage method results.

The thermal imaging method is aimed to investigate the capability of a high resolution IR camera to measure the junction temperature of a LED. An infrared (IR) thermal camera has been utilized to measure the junction temperature of LEDs, although the temperature of LED chip surface is directly measured by IR method after a process for removing silicon lens.

Removing the lens was advantageous in terms of having more accurate measurements during infrared thermal imaging technique, since the emitted radiation energy from the LED chip surface will be directly measured. Alternatively, another study would be necessary to determine the transmission value of the LED lens and this brings additional uncertainties and restricts the practicality of the technique. Previous studies have shown that a siginificant amount of heat collected at the junction region. A recent study is reported about the impact of the LED lens [44]. Thus, a rise in the junction temperature has been expected due to lack of an effective conductive path leading to relatively high thermal resistance between chip surface and ambient. Measurements of the chip temperature were made more reliably by utilizing IR thermal imaging technique in this study. If this technique were utilized for the LED with a lens, temperature distribution would be measured over the lens surface, and this would cause considerable errors while determining the chip temperature.

Measurement of electromagnetic radiation using IR camera is key to determine the temperature distribution over the surface of the objects since they allow us to determine invisible infrared radiation absorbed and emitted by objects [31]. As infrared radiation is able to transmit through a number of materials; this method is used to determine the junction temperature of LEDs, because the emitted infrared energy increases with rising object temperature [45]. As the temperature of the objects is increasing, the transmitted infrared energy also enhances as clarified by the principle of Planck's law of blackbody radiation. IR cameras mainly consist of a special lens to focus IR on a detector, electronics and software in order to convert the radiated thermal energy into electrical impulses and the final colors in display for the corresponding temperature values.

In current study, CREE XP-E2 high power green and blue LED chips were studied for various configurations which can be listed as: an LED with lens, an LED without lens (bare chip) and a painted LED without lens as shown in Figure 2.15. A process for removing the lens over green and blue LEDs were developed. The primary reasons for removing the LED lens are related to the investigation of the lens effect on the thermal and optical attributes of the LED chip as well as direct access to the chip during infrared thermal measurements.

In the next section, green and blue LED chips were used for the painted and unpainted surface of an LED without lens in order to demonstrate the rate of converted energy into heat.

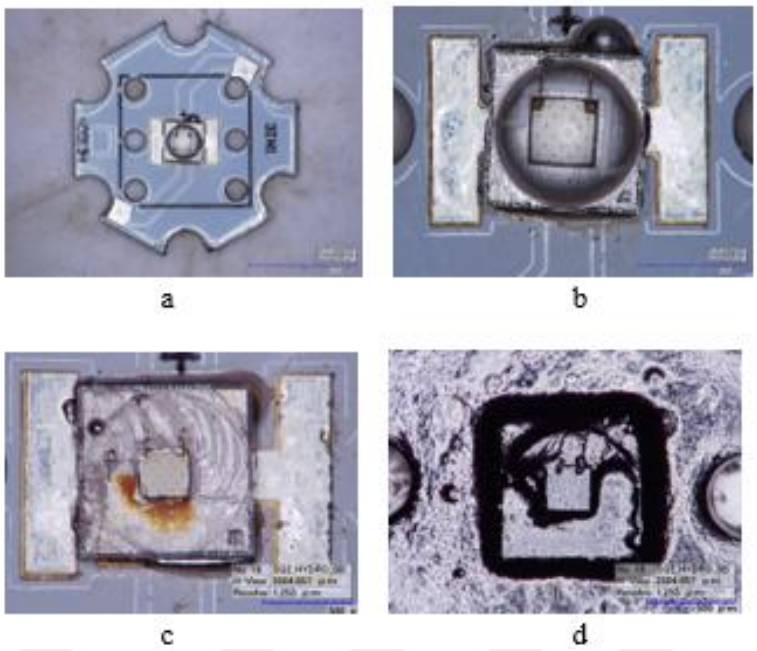

Figure 2. 14 CREE XLamp XP-E2 high power LED chip, (a) unpainted LED with lens, (b) unpainted LED with lens (closer), (c) unpainted LED without lens, (d) black painted LED without lens [46]

2.2.1 Test System

A cooled mid-wave FLIR SC5000 camera was utilized in order to measure the junction temperature of green and blue LEDs. It operates in between 2.5-5.1 µm wavelength and have a resolution of 640x512, the camera also offers a measurement area of 3.2 x 2.4 mm by using a microscopic G3 lens. The measurement uncertainty for the camera is given as ±1˚C. Experimental system consisted of an IR camera, a DC power supply, a heater, four thermocouples, a data acquisition system and a software (see Figure 2.16).

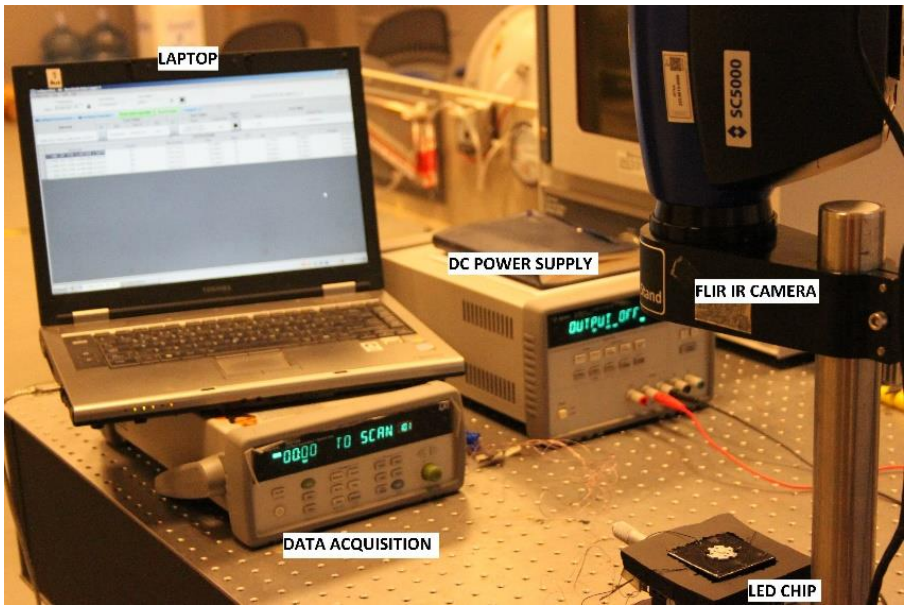

Figure 2. 15 Experimental setup for thermal imaging measurements

A special test vehicle was designed and manufactured as shown in Figure 2.16 in order to validate temperature distribution obtained by the IR camera and four T-type thermocouples. A 40x40x5 mm^3 large aluminum block was grooved from four different paths at dimensions of 2x20 mm^2 in order to position the T-type thermocouples. These thermocouples were connected to the data acquisition system for monitoring temperature of the aluminum block and the LED board. As shown in Figure 2.17, a heater was placed under the aluminum block and controlled by the DC power supply in order to calibrate the surface temperature of the LED measured by both IR camera and thermocouples. The chip was placed on the aluminum block with two screws and it was securely fixed to prevent any movement during the experimental study.

Thermal imaging measurements may be affected by a number of parameters include the emissivity, transmissivity, atmospheric attenuation and any reflections over the region [47]. In addition, keeping the IR camera position parallel to the surface was critical that was assured by using a special holder apparatus. Thus, it is provided that all radiated thermal energy from the measured surface was perceived by the IR camera sensors. The

exact positioning of the IR camera can be seen in Figure 2.16. Besides that, in order to prevent surface reflections, the objects which are more likely to cause any reflection are either removed around the experimental setup or painted black. Lastly, atmospheric attenuation was automatically adjusted.

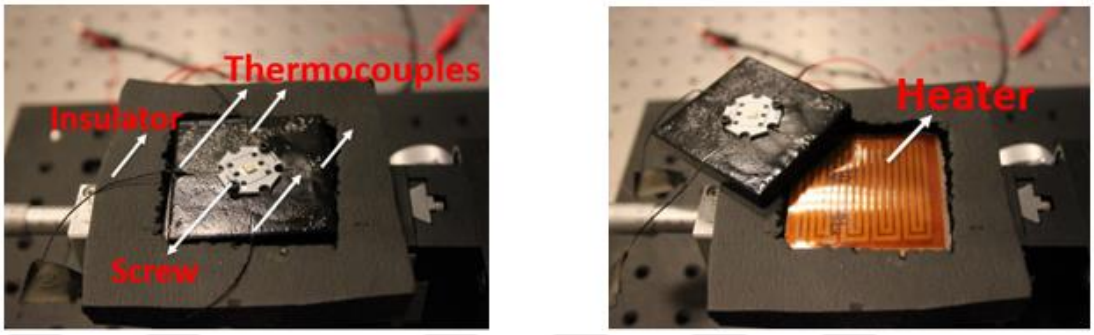

Figure 2. 16 Positioning of thermocouples and heater for verification study

A calibration process was performed between thermocouple readings and IR local temperatures in order to confirm that the specified emissivity is correct. For this purpose, a heater connected to the DC power supply was adjusted at seven different selected temperature points linearly increasing between 35°C and 105°C. The first selected temperature reading (aluminum board and LED chip) was achieved by a thermocouple, and then the emissivity value was adjusted through the software in order to achieve the closest possible reading of IR camera with the results of thermocouple. The measurement was performed for each selected temperature and the results were plotted in Figure 2.18.

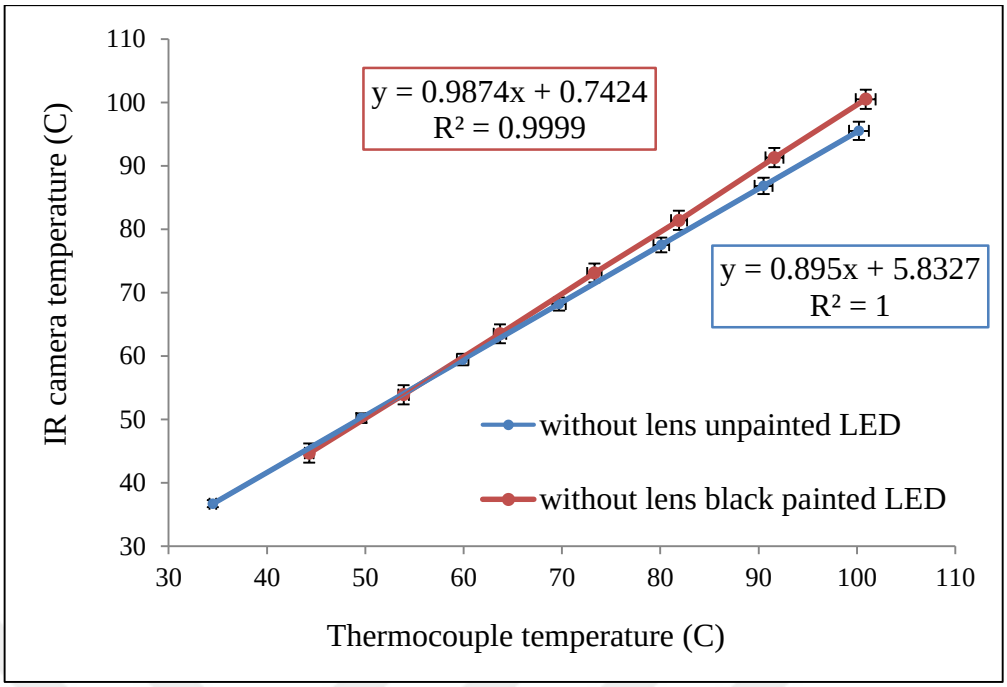

Figure 2. 17 Calibration between T type thermocouples and IR results

2.2.2 Process Development for Removing Silicone Lens

In the literature, although there are a few techniques for removing silicone lens over LED systems, an accepted technique does not exist. In most processes while removing the lens over an LED chip, wire bonding are damaged as presented in the previous studies [12]. In addition, once this process is performed, the LED chip stays unprotected and wire bonds of the chips become open to external conditions. Thus, a special care should be given to the LED chip even if the LED lens is removed safely.

The lens removal process was performed over 10 Cree XP-E2 green and blue LED packages in order to investigate the effect of a lens on LED performance and specifically its effect on the junction temperature. Two different techniques were developed and the more feasible one was selected.

Initially green and blue LED chips with lens were kept for 45 minutes in a container filled with ethyl alcohol. After 45 minutes, the decomposed silicone lens was removed by scratching on top of the LED package. However, the wire bonding connecting the LED

chip was barely connected (80% lost electrical connection). Although the chip seemed working well, a digital microscope was utilized in order to confirm whether the LED chip was in a good state or not. The particles of the residual silicone were accumulated on the junction region as it is shown in Figure 2.19. Due to the residual silicone on top of the junction region, thermal and optical losses led to a significant decrease in the LEDs efficiency.

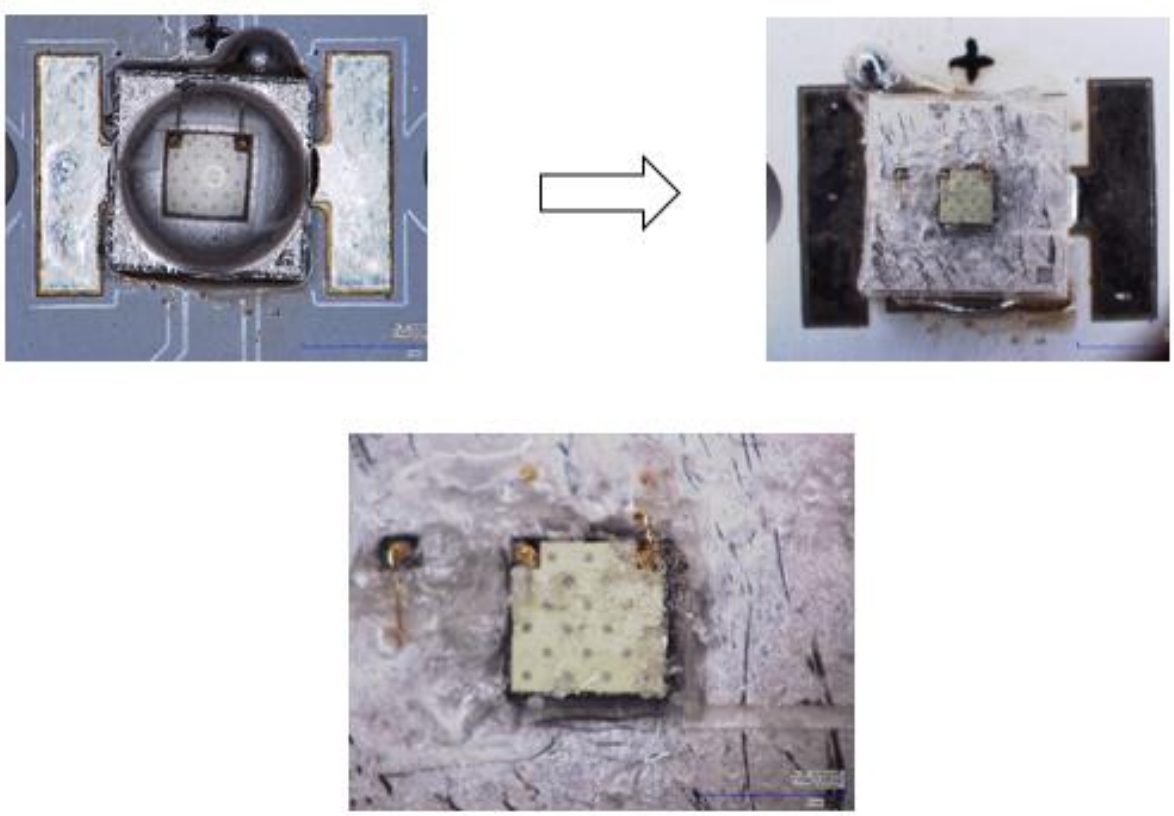

Figure 2. 18 A process for removing lens with the first technique on green LED chips

According to the literature, the melting temperature of the silicone is found to be around 60°C [48]. As a second technique, a hot gun WXR3 was utilized in order to reach that temperature without damaging the LED chip as shown in Figure 2.21.

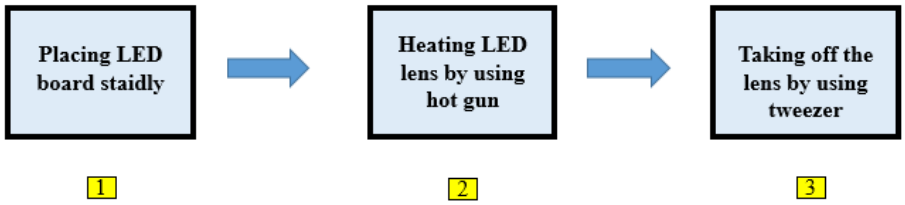

Figure 2. 19 Schematic of a process for removing LED lens

A heating process was initiated until the silicone lens became softer. After obtaining a sufficient amount of softness, the silicone lens was removed by utilizing a tweezer gently. Once the air inside the lens came out, the lens was removed easily. The process for 10 LED packages was performed by the same removal technique and a 90 % yield is achieved. After applying this technique, it was observed that 9 LED chips did not experience any broken wire bonding, and they were working smoothly without any residual silicon particle on the junction area as shown in Figure 2.22. After the process for removing the lens, the unprotected LED chips were kept under special conditions to avoid any external damage.

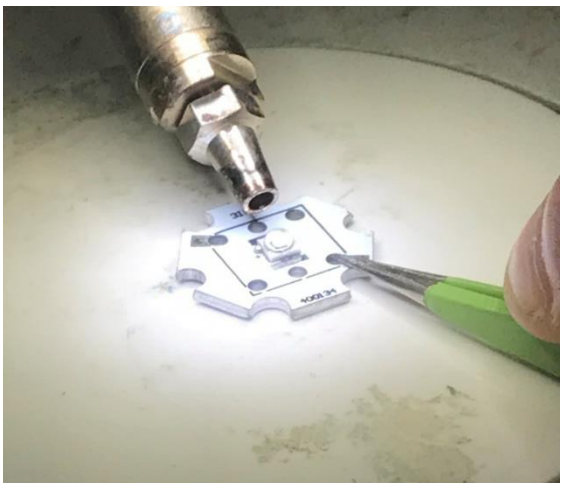

Figure 2. 20 Lens removal process by use of hot gun WXR3 [46]

The same removal process was performed for green and blue LEDs. The satisfactory rate was determined 90 % for all color type of LED chips [46]. The results of removing

process for LEDs are presented below, as it can be seen from figure, residual silicone does not exist on surface of the junction region and wire bonding are unbroken. In order to make sure that the LED chips (without lens) are working well the experimental study was performed and the results were found to be satisfactory.

The same procedure was conducted for green and blue LED chips after a process for removing silicone lens was performed successfully as shown in Figure 2.23.

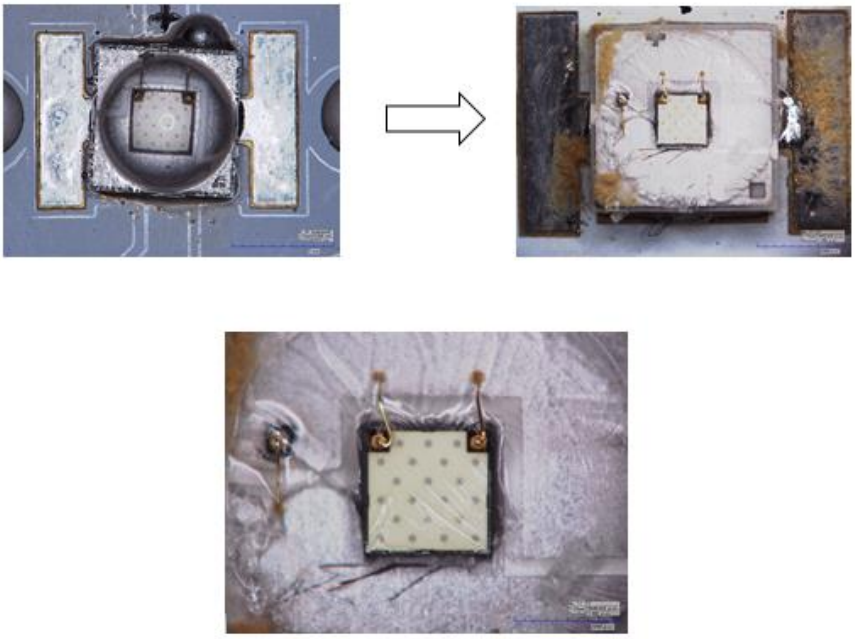

Figure 2. 21 A process for removing lens with the second technique on green LED chips

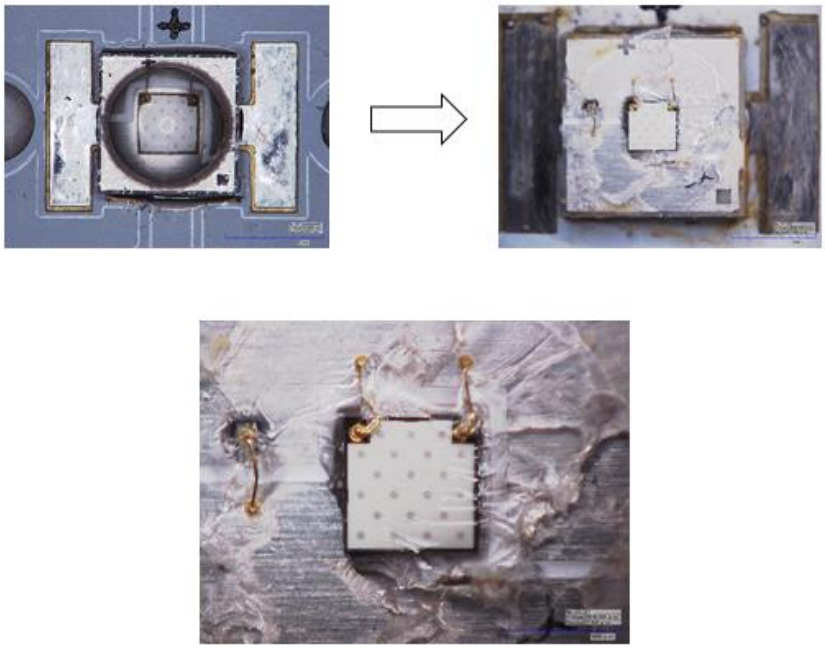

Figure 2. 22 A process for removing lens with the second technique on blue LED chips

2.2.3 Thermal Imaging Results

2.2.3.1 A Silicone Lens Effect on LED Performance

The forward voltage (FVC) method was utilized in this section in order to obtain a silicone lens effect on LED performance. Therefore, junction temperatures of green and blue LEDs were measured for both with a lens and without a lens configuration. Junction temperature results for a green LED with lens utilizing FVC technique are shown in Table 3.1. The process for removing silicone lens was completed then measurements were conducted again in order to demonstrate the effect of the lens over a green LED performance. Eventually, junction temperatures, electrical and optical behaviors of the green LED without lens for three different operating currents (200 mA, 350 mA and 500 mA) were given in Table 2.12.

Table 2. 12 Forward voltage results of a green LED with a lens

V_f [mW]	Electrical power [W]	Radiant power [W]	T_{base} [°C]	T_j [°C]	T_j @40°C [°C]
2.369	0.683	0.141	35.8	48.056	52.256
2.307	1.318	0.212	44.93	67.886	62.956
2.246	2.054	0.263	54.33	87.555	73.225

Table 2. 13 Forward voltage results of a green LED without a lens

V_f [mW]	Electrical power [W]	Radiant power [W]	T_{base} [°C]	T_j [°C]	T_j @40°C [°C]
2.363	0.597	0.082	36.5	49.994	53.494
2.297	1.058	0.124	45.6	70.99	65.39
2.231	1.516	0.154	57.6	92.4	74.808

FVC method was conducted again before and after the silicone lens is removed for a blue LED. Junction temperature results of a blue LED with lens are presented in Table 2.13. Thermal, optical and electrical behaviors of blue LED without lens are listed in Table 2.14 for three different operating currents (200 mA, 350 mA and 500 mA).

Table 2. 14 Forward voltage results of a blue LED with a lens

V_f [mW]	Electrical power [W]	Radiant power [W]	T_{base} [°C]	T_j [°C]	T_j @40°C [°C]
2.416	0.666	0.314	31.520	35.457	43.937
2.391	1.304	0.492	38.500	49.638	51.138
2.364	2.038	0.628	46.030	65.462	59.432

Table 2. 15 Forward voltage results of a blue LED without a lens

V_f [mW]	Electrical power [W]	Radiant power [W]	T_{base} [°C]	T_j [°C]	T_j @40°C [°C]
2.410	0.578	0.227	32.440	39.031	39.031
2.381	1.038	0.366	40.720	55.270	55.270
2.351	1.501	0.457	49.500	72.560	72.560

A process for removing the silicone lens from an LED chip led to an increase in the temperature of the junction area. The differences between junction temperatures of configurations with lens and without lens for green and blue LEDs can be seen clearly in Figure 2.24 and Figure 2.25 respectively.

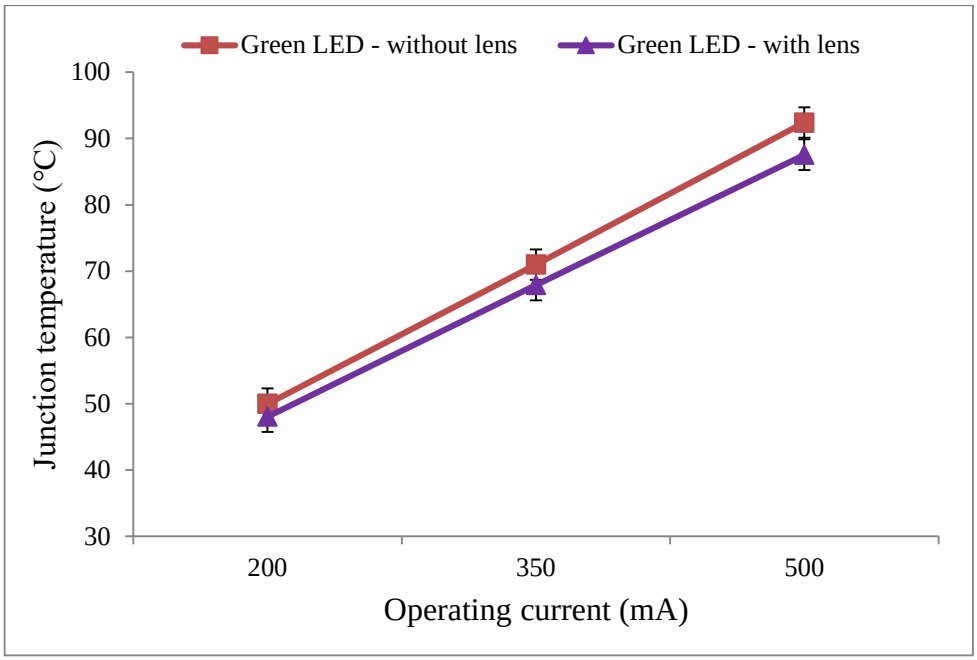

Figure 2. 23 Lens effect on the junction temperature of a green LED

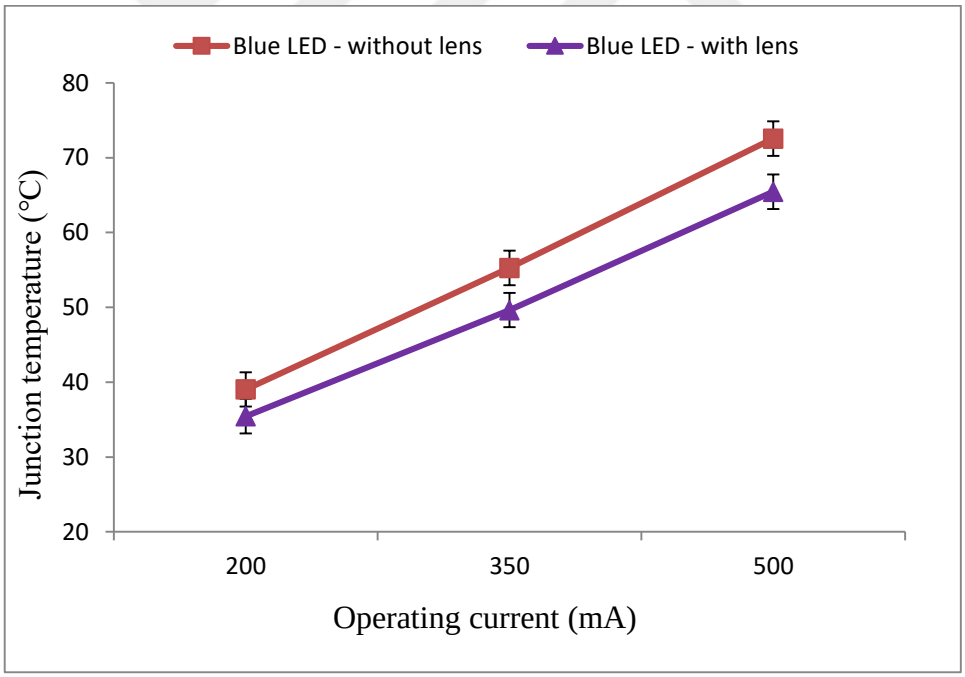

Figure 2. 24 Lens effect on the junction temperature of a blue LED

The existence of a lens on top of the LED chip caused to more heat transfer from the junction region to the lens by heat conduction [44]. Therefore, the generated heat around the junction area was transferred through the lens instead of remaining at the junction and

increasing temperature. On the other hand, once the process for removing the silicone lens was performed, the generated heat was not dissipated from the upper path due to high resistance from the chip surface to the ambient. This eventually resulted in a junction temperature rise considerably. While the junction temperature difference of green LED was found to be 1.93°C, 3.1°C and 4.85°C for operating currents of 200, 350 and 500 mA respectively. Junction temperature variance of a blue LED was determined by 3.57°C, 5.63°C and 7.09°C under the same applied currents of 200, 350 and 500 mA respectively. According to variance results in the junction temperature values of green and blue LEDs, it is clear to observe that the blue LED were attained to be the most sensitive to the process of removing silicone lens, while the green LED were found to be the less sensitive one as shown in Table 2.16.

Table 2. 16 The junction temperature differences for green and blue LEDs after a process for removing silicone lens

Current [mA]	Green		Blue	
	with lens	without lens	with lens	without lens
200	48.056	49.994	35.457	39.031
350	67.886	70.990	49.638	55.270
500	87.555	92.408	65.462	72.560

In addition to the investigation for the effect of LED lens on the junction temperature of a green LED, its effect over optical and electrical behavior was also analyzed in the current study. The differences in the chip efficiency of the green and blue LEDs for various conditions can be seen with details in the following section.

As mentioned before, the current study was conducted for 200, 350 and 500mA respectively. Given data in figures indicate the lens effect over electrical and optical powers of the LED depending on the operating currents. Primarily, once the operating current is increased from 200mA to 500mA, the chip efficiency decreased and a lower amount of electrical energy was converted into radiant energy. Secondly, the lens has led to considerable differences on the ratio of emitted radiant to electrical power of LED chip as shown in the graphs for three different LED types.

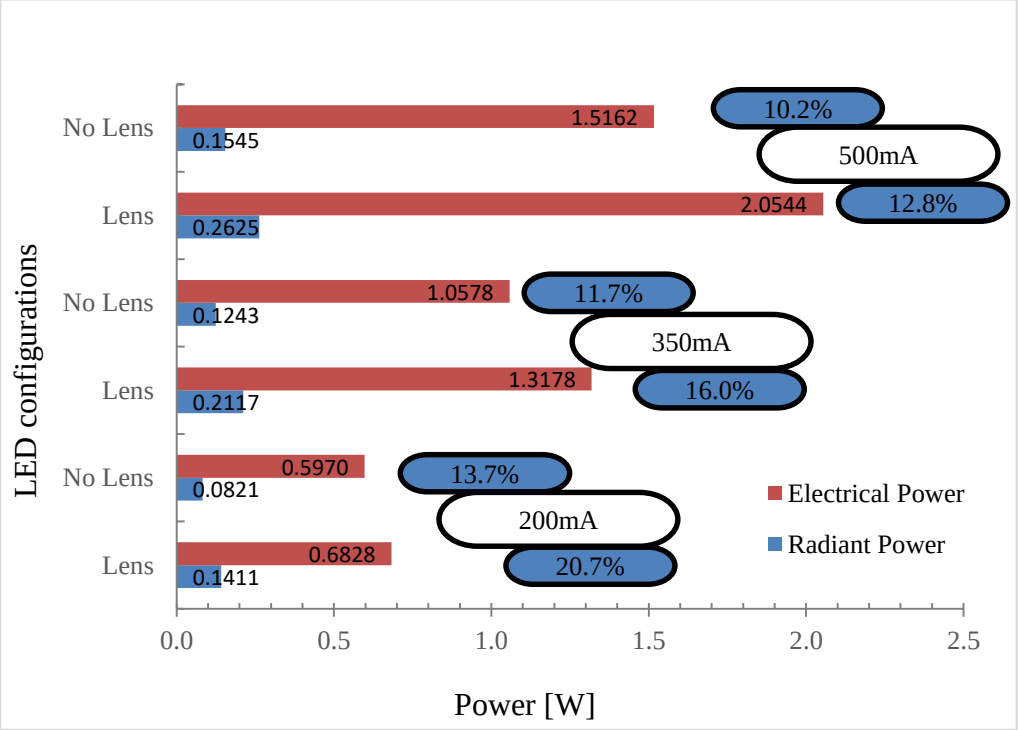

Figure 2. 25 Conversion efficiency rate (converted energy from electrical to optical energy) of the applied current of a green LED

Before and after LED lens was removed for the green LED, the differences of conversion efficiency were observed by 7 %, 4.3 % and 2.6 % for driving currents of 200, 350 and 500 mA respectively. The electrical power variance was also determined by 12.5 % at 200 mA, it lowers to 26.1 % once the applied current is increased to 500 mA (see Figure 2.26).

For the blue LED, decrease of the electrical power was determined by 12.5 %, 19.7 % and 26.1 % for 200, 350 and 500 mA currents respectively. As there is a difference of

7.8 % in conversion efficiency between the LED with and without lens at 200 mA, it drops to 0.4 % when the operating current is increased to 500 mA (see Figure 2.27).

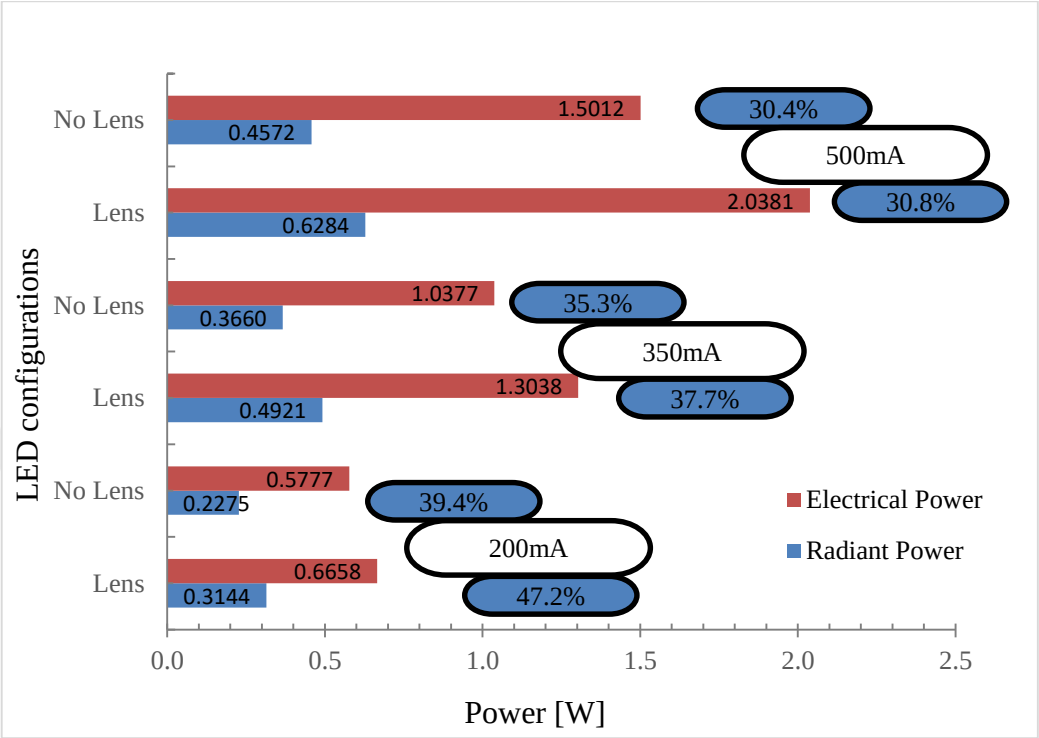

Figure 2. 26 Conversion efficiency rate (converted energy from electrical to optical energy) of the applied current of a blue LED

As a result, the converted energy from electrical into radiant energy was found to be higher for the all type of LEDs with lens at all three operating currents compared to the LED without lens. It is also worth noting that as the operating current increases, the positive impact of a lens on the conversion efficiency becomes less sound or optical losses become more dominant.

Another observation was a decrease in the electrical power of the LED due to the drop in the forward voltage. When the process for removing silicone lens was completed, the junction temperature increase led to a drop at forward voltage although the same current is applied with the LED with lens case.

2.2.3.2 Investigating Painting Effect

In this part of the study, the measurement of the junction temperature of green and blue LEDs and its thermal behavior were investigated using an IR camera. It is known that conventional LEDs spread most of its applied electrical power as heat and the rest of the energy is converted into visible light. The study was conducted for the painted and unpainted surface of green and blue LEDs without lens in order to demonstrate the rate of converted energy into heat.

The junction temperature of green and blue LEDs was first determined by utilizing an IR camera under selected operating currents of 200, 350 and 500mA. After the process for removing lens was completed, measurements were conducted with the unpainted surface of a green LED first. Later on, the painted surface of a green LED was prepared in order to demonstrate the amount of radiant energy converted into heat. The obtained junction temperature results of green and blue LEDs by an IR camera can be seen in Figure 2.28, and Figure 2.30.

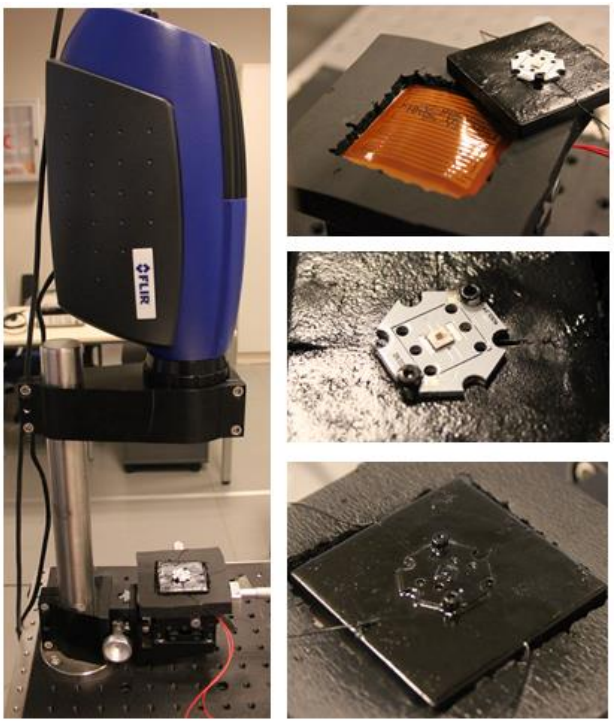

Figure 2. 27 Experimental setup with unpainted and painted LED chip samples

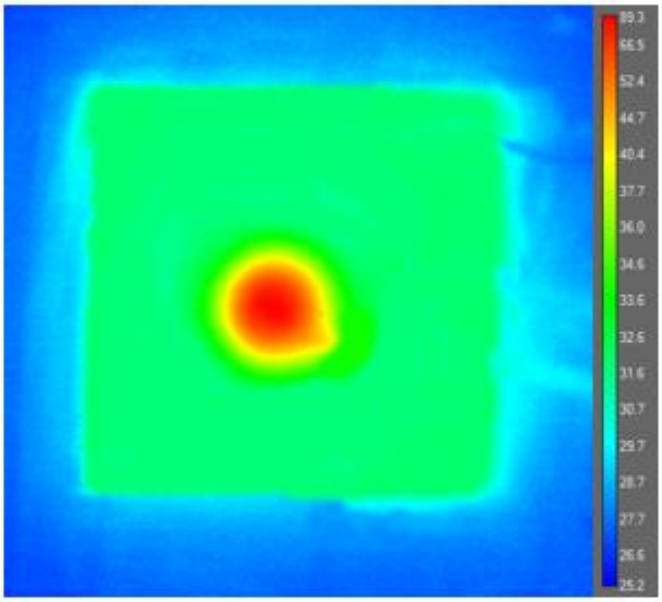

Figure 2. 28 The temperature distribution of the unpainted green LED without lens running at 500 mA operating current

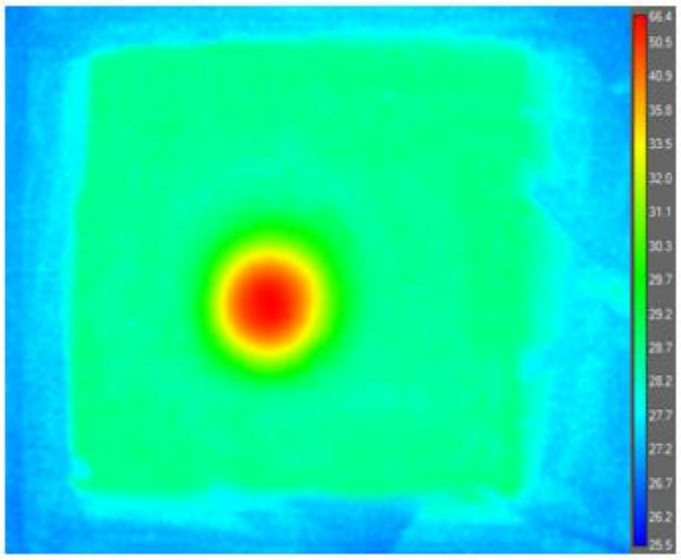

Figure 2. 29 The temperature distribution of the unpainted blue LED without lens running at 500 mA operating current

As the temperature distribution of green and blue LEDs was attained by thermal imaging method, the junction temperature results were also measured accurately utilizing FVC method and the variance between two configurations of without lens (painted and unpainted) shown in detail from Table 2.17, Table 2.18 for a green LED and Table 2.19, Table 2.20 for blue LED.

Table 2. 17 A green LED without lens (unpainted)

V_f [mW]	Electrical power [W]	Radiant power [W]	T_{base} [°C]	T_j [°C]	T_j @40°C [°C]
2.363	0.597	0.082	36.500	49.994	53.494
2.297	1.058	0.124	45.600	70.990	65.390
2.231	1.516	0.154	57.600	92.400	74.808

Table 2. 18 A green LED without lens (black painted)

V_f [mW]	Electrical power [W]	Radiant power [W]	T_{base} [°C]	T_j [°C]	T_j @40°C [°C]
2.352	0.594	-	39.080	53.449	54.369
2.279	1.050	-	51.440	76.822	65.382
2.208	1.502	-	63.880	99.456	75.576

Table 2. 19 A blue LED without lens (unpainted)

V_f [mW]	Electrical power [W]	Radiant power [W]	T_{base} [°C]	T_j [°C]	T_j @40°C [°C]
2.410	0.578	0.227	32.440	39.031	39.031
2.381	1.038	0.366	40.720	55.270	55.270
2.351	1.501	0.457	49.500	72.560	72.560

Table 2. 20 A blue LED without lens (black painted)

V_f [mW]	Electrical power [W]	Radiant power [W]	T_{base} [°C]	T_j [°C]	T_j @40°C [°C]
2.393	0.572	-	37.720	48.660	50.940
2.352	1.020	-	50.170	71.976	61.806
2.312	1.470	-	61.870	95.036	73.166

The amount of heat generation was determined for the unpainted LED with and without lens by subtracting the radiant power from electrical power while it was determined for the painted LED without lens by taking the electrical power directly since it is all

converted into heat due to 100 % absorbing nature of the black paint over the chip. In order to demonstrate the junction temperature variance of green and blue LEDs over the ambient temperature with respect to the net power, the results are shown in Figure 2.31 and Figure 2.32.

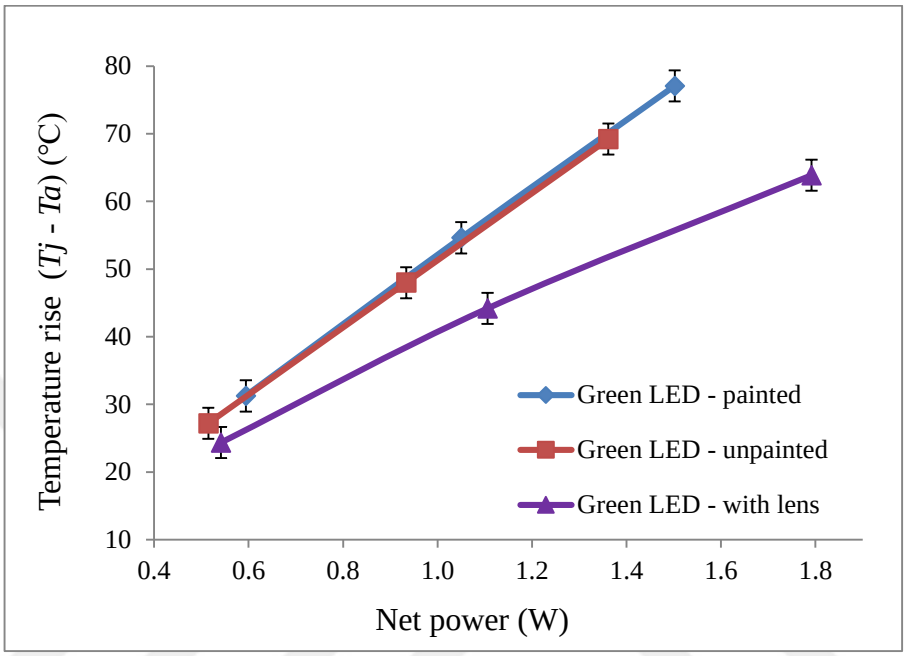

Figure 2. 30 Change in the junction temperature over the ambient temperature with respect to the net power for green LED

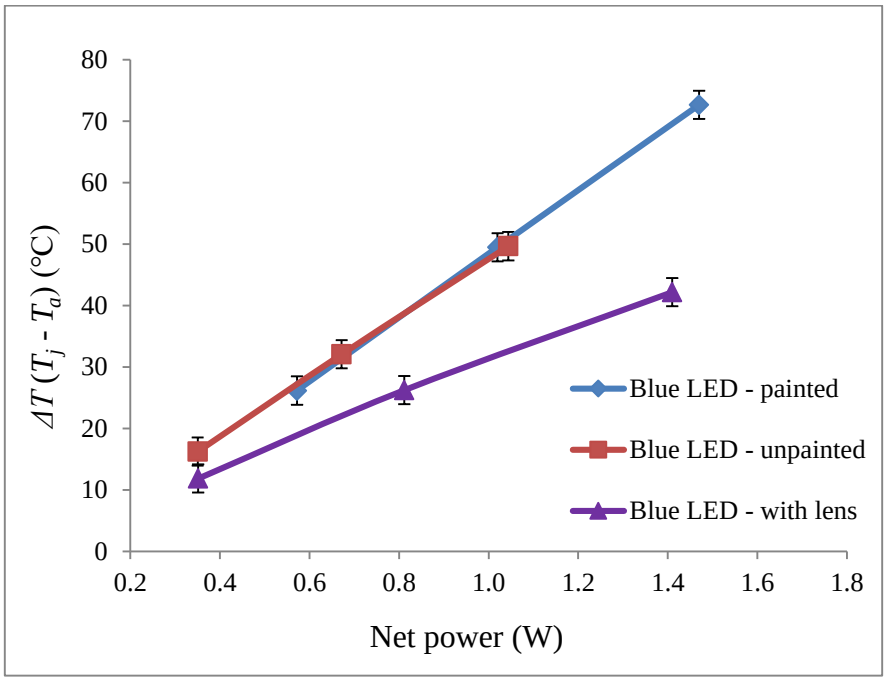

Figure 2. 31 Change in the junction temperature over the ambient temperature with respect to the net power for green LED

As expected, the slope of temperature rise curve was found to be very close to each other for unpainted and painted LED without lens. On the other hand, the LED with lens has shown a different trend. It is observed that the curve for the painted LED without lens is a slightly shifted as a result of the increase in junction temperature after painting. However, the LED with lens has a less temperature rise in the junction region for the same generated heat amount as expected.

CHAPTER III

COMPUTATIONAL STUDY

Computational approaches are very helpful in engineering design to provide pre or post design conditions. It is rather a simpler and cheaper approach to develop numerical models and provide further insights without going through expensive and time consuming experimental studies. Numerical models have been developed by using ANSYS Icepak [49] in order to both validate experimental results and establish a numerical approach that enables a user to determine the junction temperature of LEDs in various conditions.

The study is critical to understand the lens and painting effect on various traits of an LED system using the CFD model. The models with and without lens were thus created related to the features of green and blue LEDs in the first case. The models with and without painted surface were also carried out in the second case. The aim of painting surface of the junction area is both to see the painting effect on the junction temperature and to have more accurate results with a known emissivity value (0.95).

3.1 Boundary Conditions

The basic LED chip model created by using ANSYS Icepak software for green and blue LEDs as shown in Figure 3.1. Furthermore, a set of features for the components of the model were listed in Table 3.1.

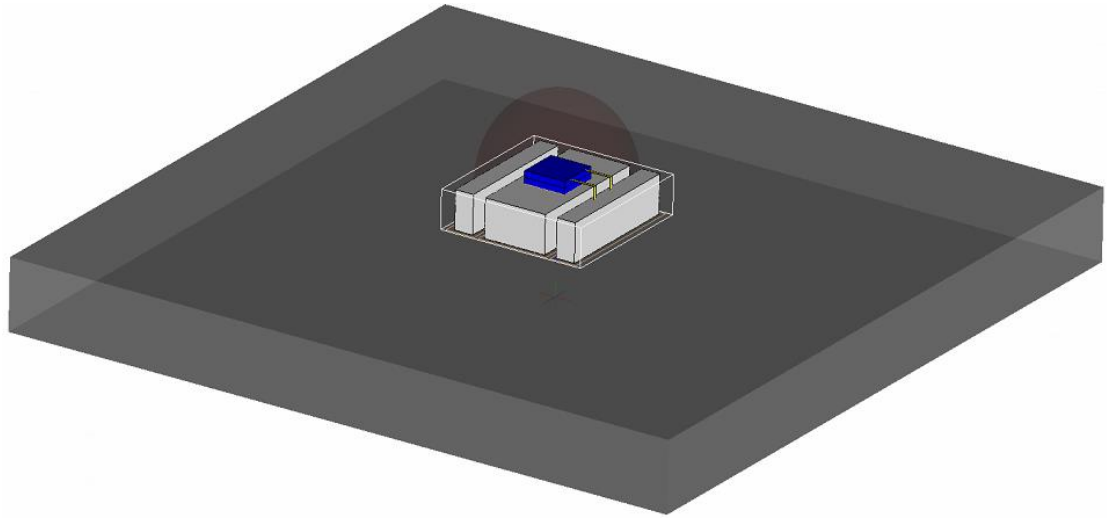

Figure 3. 1 CFD model of a LED chip with a PCB

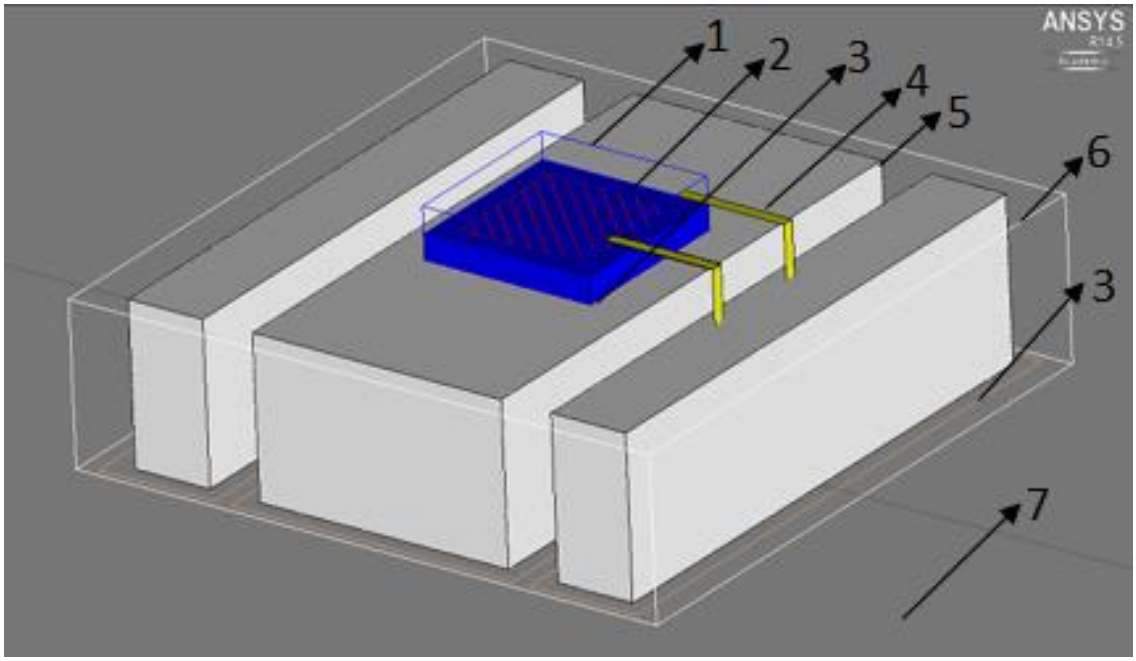

Figure 3. 2 CFD model of an LED chip with components

Table 3. 1 Properties of the LED components for CFD simulations

Component	Material	Conductivity [W/m-K]	Dimensions [mm^3]
Chip blocks (1)	Si - typical	180	1 x 0.15 x 1
Source (2)	-	-	0.75 x 0.75
Wire bondings (4)	Au - typical	313	0.65 x 0.07
Inner lead (5)	Al Die Cast90	105	1.5 x 0.92 x 3.2
Mold base (6)	Mold material	0.8	3.5 x 0.92 x 3.5
Die attache (3)	Die attach mat.	2.5	1 x 1
PCB (7)	Al die-cast 90	105	16.5 x 1.7 x 16.5

For each case, the given driving currents of 200, 350 and 500 mA were studied according to actual experiments. A certain amount of converted electrical energy into heat was considered while an input power was entered for the unpainted surface in the CFD model. On the other hand, for the painted LED surface, overall electrical energy was entered as an input power because all the radiant energy converts into heat. In addition, for each operating current, ambient and board temperatures were directly taken from experimental data. The detailed boundary conditions of each LED has been shown in Table 3.2 and Table 3.3.

Table 3. 2 Boundary conditions of green LED

with a lens				without a lens			
Electrical power [W]	Heat generation [W]	T_{base} [°C]	T_{amb} [°C]	Electrical power [W]	Heat generation [W]	T_{base} [°C]	T_{amb} [°C]
0.683	0.542	35.8	23.7	0.597	0.515	36.5	22.8
1.318	1.106	44.93	23.7	1.058	0.934	45.6	23.0
2.054	1.791	54.33	23.7	1.516	1.362	57.6	23.2

Table 3. 3 Boundary conditions of blue LED

with a lens				without a lens			
Electrical power [W]	Heat generation [W]	T_{base} [°C]	T_{amb} [°C]	Electrical power [W]	Heat generation [W]	T_{base} [°C]	T_{amb} [°C]
0.666	0.351	31.52	23.6	0.578	0.350	32.44	22.8
1.304	0.812	38.50	23.4	1.038	0.672	40.72	23.2
2.038	1.410	46.03	23.3	1.501	1.044	49.50	22.9

3.2 Mesh Sensitivity Study

In the present study, in order to optimize the mesh sensitivity of the CFD model, a grid dependency analysis was conducted for green and blue LEDs based on the maximum junction temperature and the number of elements as shown in Figure 3.3, Figure 3.4. Ambient temperatures, input powers and board temperatures were directly taken from experimental data, and applied for three different configurations and operation currents of 200, 350 and 500 mA in the numerical model.

The green LED system was simulated for a number of elements increasing from 109,606 to 3,552,674. The variation of junction temperature results was found to be less than 0.001 between 2,420,343 and 3,552,674 elements. Therefore, 2,420,343 elements were selected for the further study.

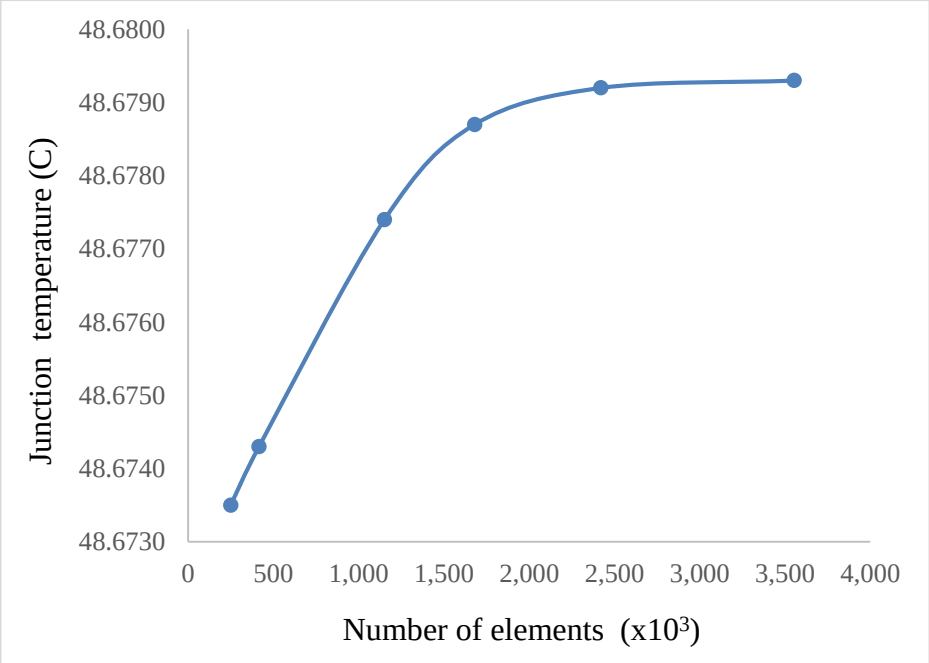

Figure 3. 3 Mesh sensitivity analysis of the green LED model (without lens) at 200 mA

The mesh analysis for the blue LED was also conducted by the number of elements until 1,743,555. The junction temperature differences were obtained by less than 0.001˚C

between 1,467,004 and 1,743,555 elements. Thus, the number of elements of 1,467,004 was utilized for the current study.

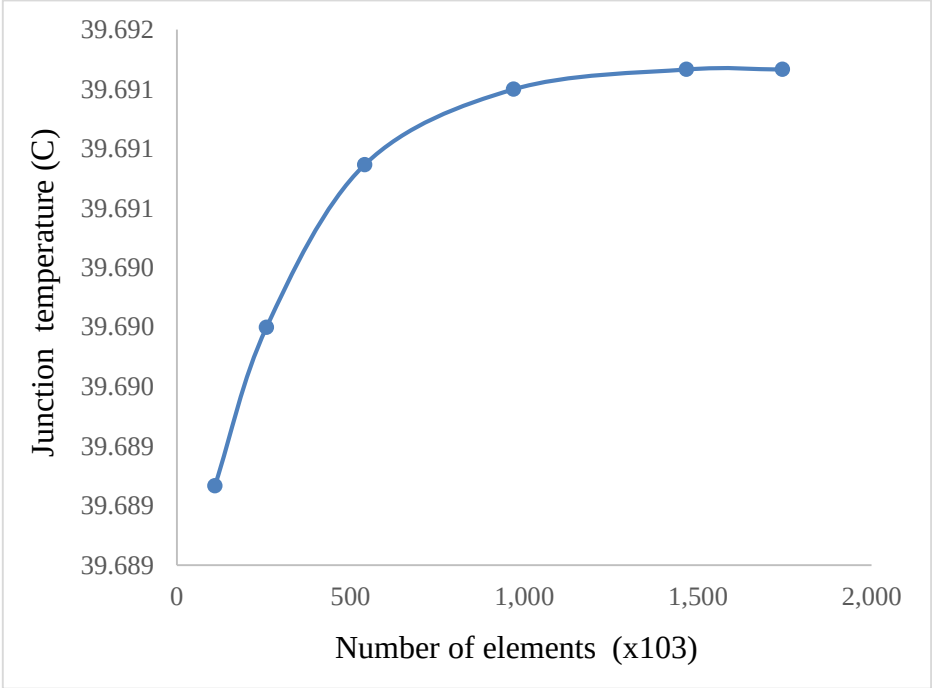

Figure 3. 4 Mesh sensitivity analysis of blue the LED model (without lens) at 200 mA

Overall mesh structure has shown a good quality with a high face alignment ratio (99.7 % of elements have a face alignment ratio in between 0.9 and 1).

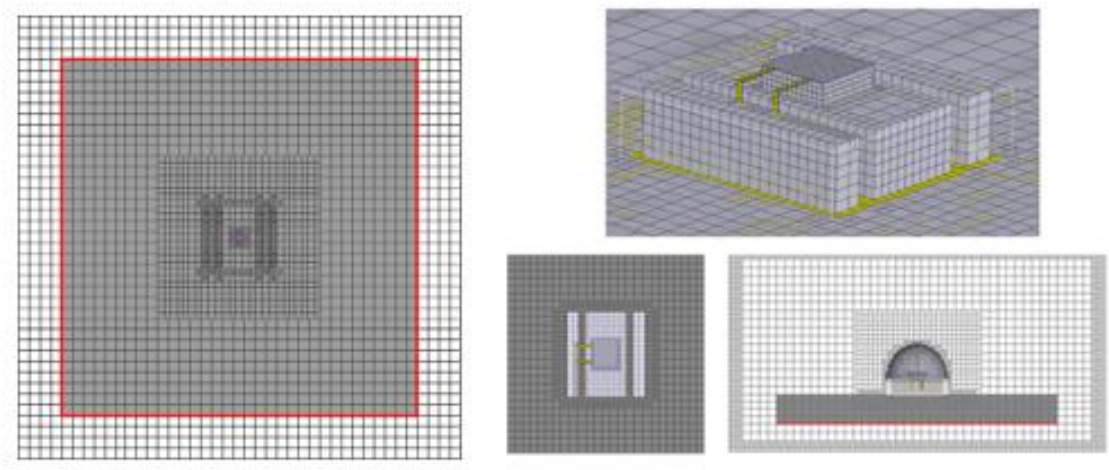

Figure 3. 5 The meshed model of blue LED with number of 1,467,004 elements

3.3 Computational Results

The purpose of a numerical study was to improve the estimation capability and validate test results obtained from forward voltage change and infrared imaging techniques. Two different cases were conducted in the current study. The first case focused on verifying the results for the lens effect, while the second one examined the experimental findings for the painting effect.

3.3.1 CFD Results Silicone Lens Effect over Junction Temperature

The green and blue LED chips were modeled in this section to validate junction temperature results obtained by FVC method as well as investigating the lens effect on LED performance. The junction temperature of green and blue LEDs was determined both with a lens and without lens configurations. The temperature distribution of the generated heat of the green LED can be seen clearly in Figure 3.6, and Figure 3.7. The junction temperature of the green LED with a lens was obtained as 45.87 ˚C under 200 mA operating current. It is not possible to observe the maximum temperature of the LED system due to the existence of silicone lens.

The model was resimulated under relevant boundary conditions of the second configuration to demonstrate the effect of the lens over the green LED junction temperature. Eventually, the junction temperature of the green LED without lens was observed as 48.70 ˚C under 200 mA applying current.

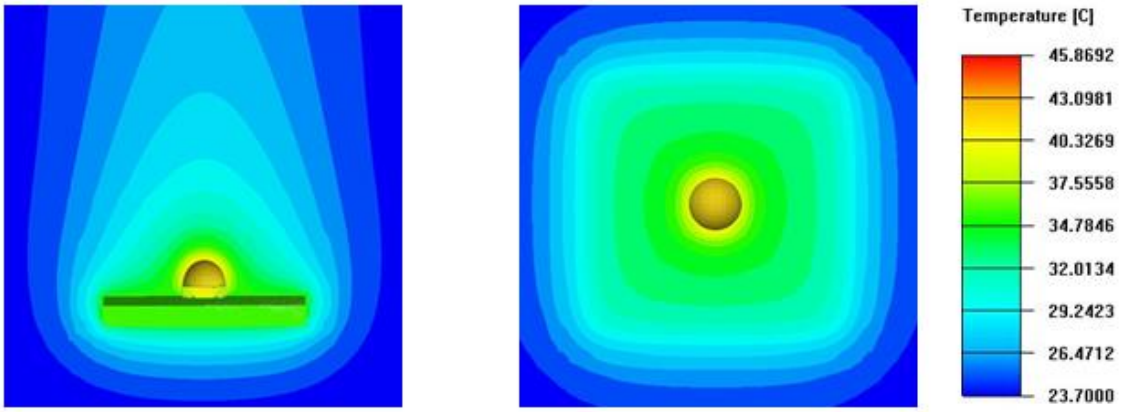

Figure 3. 6 Temperature distribution of a green LED with lens at 200 mA operating current

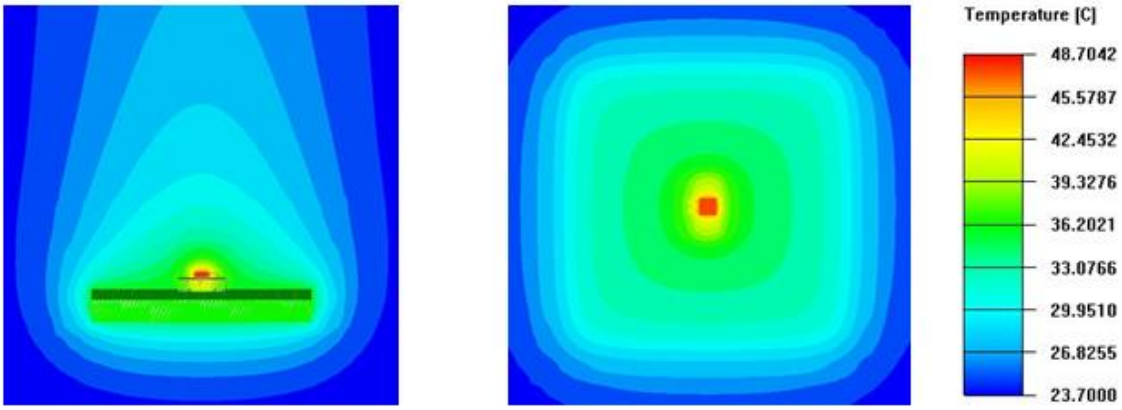

Figure 3. 7 Temperature distribution of a green LED without lens at 200 mA operating current

The CFD model of a blue LED was also created before and after silicone lens was removed and the temperature distribution was determined along with obtaining junction temperature. Eventually, the junction temperatures of the LED with/without lens were observed 35.81 ˚C and 39.69 ˚C respectively under 200 mA applying current.

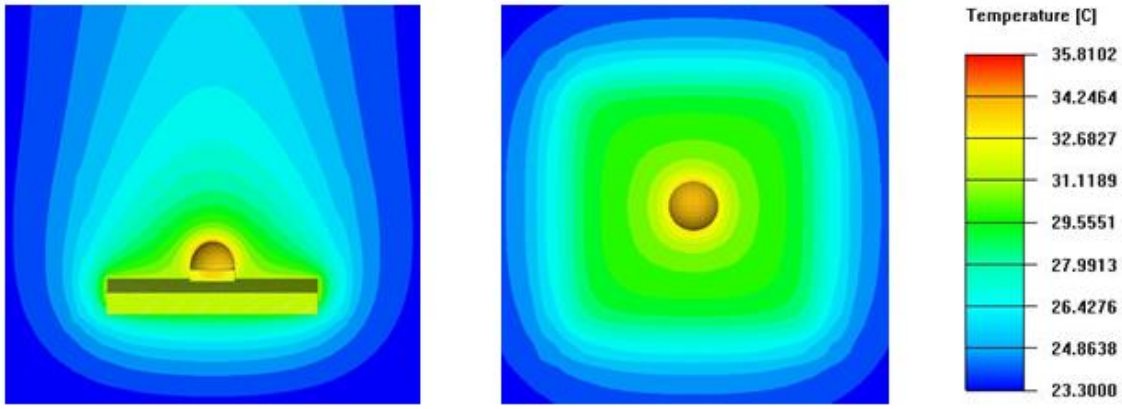

Figure 3. 8 Temperature distribution of a blue LED with lens at 200 mA operating current

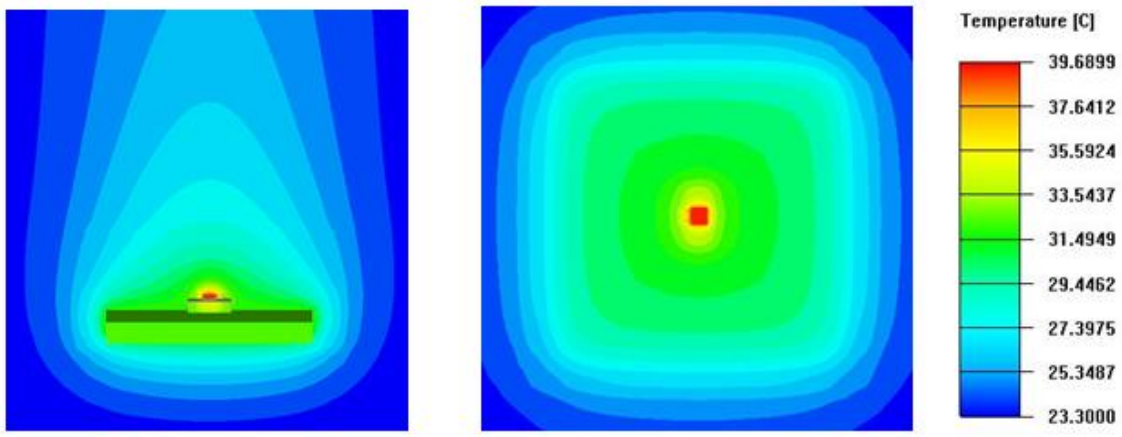

Figure 3. 9 Temperature distribution of a blue LED without lens at 200 mA operating current

3.3.2 CFD Results Painting Effect over Junction Temperature

In this section, green and blue LED chips were simulated to obtain the painting effect on the LED performance as well as measuring junction temperature with a known emissivity (black painting = 0.98). Conventional LEDs spread most of its applied electrical power as heat and the rest of the energy is converted into visible light. The study was conducted for the painted and unpainted surface of green and blue LEDs without lens in order to demonstrate the rate of converted energy into heat.

Table 3. 4 Boundary conditions of painted green and blue LEDs

Current [mA]	Green		Blue	
	Heat [W]	T_{base} [°C]	Heat [W]	T_{base} [°C]
200	0.597	39.080	0.578	37.720
350	1.058	51.440	1.038	50.170
500	1.516	63.880	1.501	61.870

The painted surface of LEDs was prepared in order to demonstrate the amount of radiant energy converted into heat. In addition, a certain amount of converted electrical energy into heat was considered while an input power was entered for the unpainted surface in the CFD model. The obtained junction temperature results of green and blue LEDs by numerical model can be seen in Figure 4.10 and Figure 4.11.

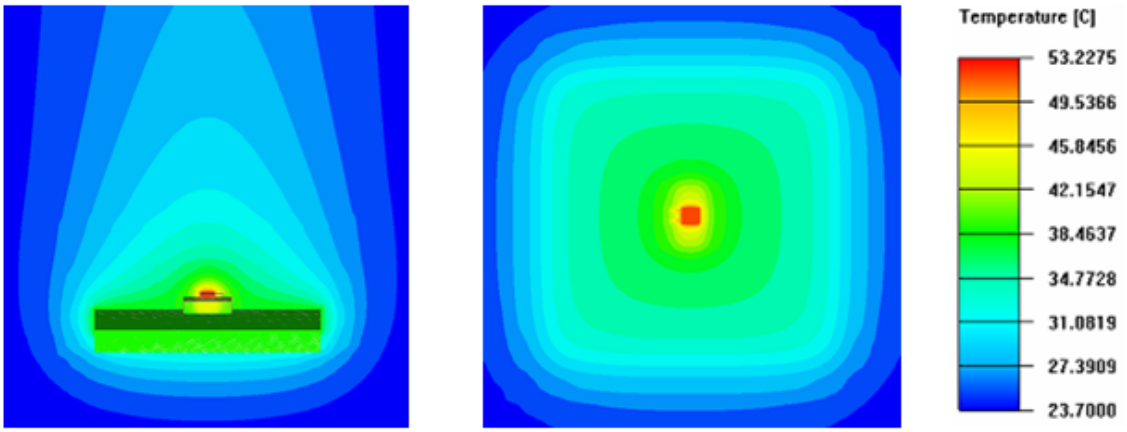

Figure 3. 10 Temperature distribution of a green LED painted configuration at 200 mA operating current

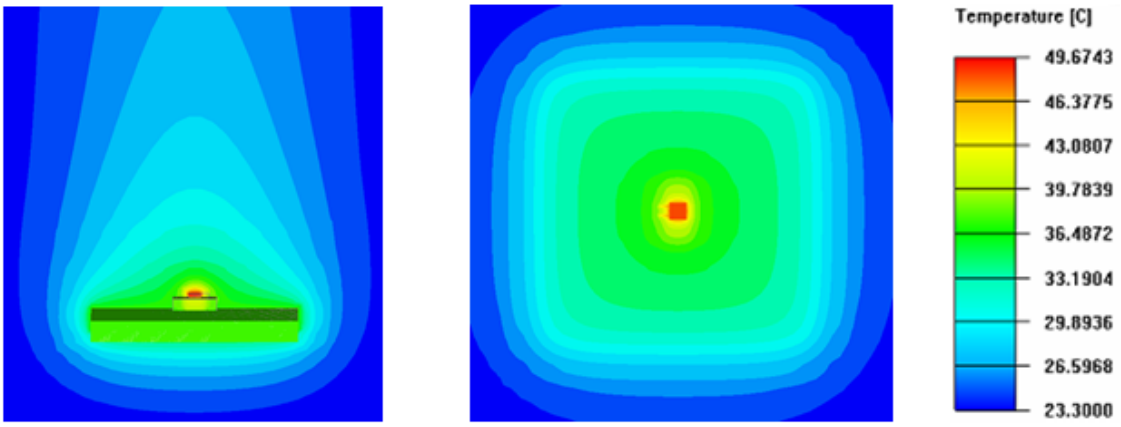

Figure 3. 11 Temperature distribution of a blue LED painted configuration at 200 mA operating current

According to the CFD results shown in Table 4.5 and Table 4.6, the process for removing silicone lens and painting the bare chip resulted in an increase in junction temperature. It is important to understand that the converted amount of radiant energy into heat led to more increase in junction temperature than the lens effect.

Table 3. 5 Computational results of the green LED for lens and paint effect on junction temperature

Pulse current [mA]	With lens	Without Lens	Black painted
200	45.82	48.67	53.15
350	65.56	69.26	76.28
500	87.50	89.86	99.35

The impact of painting over green LED chips was determined approximately by 8.41 % under 200 mA operating currents, 9.2 % and 9.5 % for 350 and 500 mA respectively.

Moreover, the rate of increasing junction temperature of unpainted LED was found to be 29.7 % between 200 and 350mA, 22.9 % between 350 and 500 mA. (see Table 4.5)

Table 3. 6 Computational results of the blue LED for lens and paint effect on junction temperature

Pulse current [mA]	With lens	Without lens	Black painted
200	35.81	39.68	49.67
350	48.43	54.62	71.7
500	63.29	71.13	92.99

The differences of the junction temperature for the blue LED were 20.1 % under 200 mA operating currents, 23.8 % and 23.5 % for 350 and 500 mA respectively after painting process was carried out. Besides that, the rate of increasing junction temperature of unpainted LED was found to be 27.3 % between 200 and 350mA, 23.2 % between 350 and 500 mA. (see Table 4.6)

3.4 Comparison of Junction Temperature Measurement Findings

In this section, numerical and experimental results were presented for junction temperature of green and blue LED chips to compare various techniques.

As given in Figure 3.12, junction temperatures in both numerical and experimental results were found to be in a close proximity. For instance, at 500 mA driving condition, junction temperatures of green LED were found to be 89.9 ˚C for numerical study, 92.4 ˚C and

88.5 ˚C for FVC and IR method respectively. Thus, it can be said that the accuracy of the technique is in a reliable range of 4%.

On the other hand, the junction temperature of the blue LED was measured at 71.1 ˚C using numerical study, 72.6 ˚C and 70.8 ˚C by FVC and IR techniques under 500 mA condition. Therefore, the reliability of the techniques for the blue LED is in an acceptable range of within 2%.

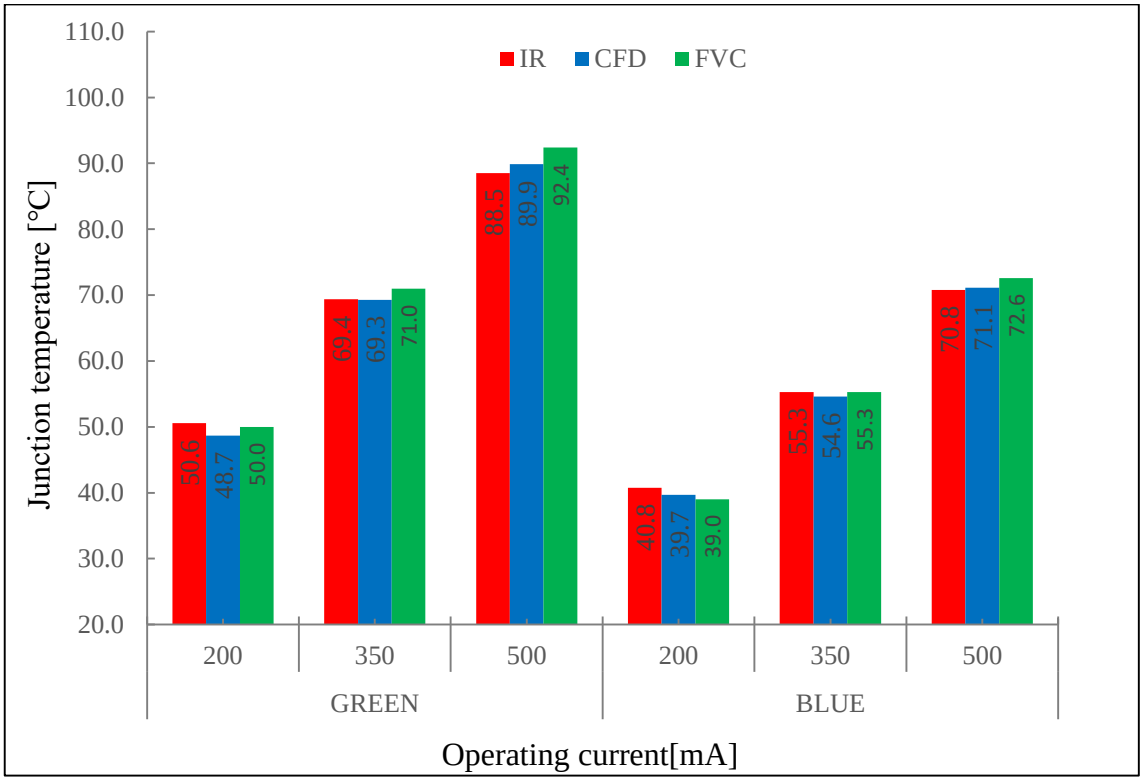

Figure 3. 12 Comparison of junction temperature results of green and blue LEDs without lens measured by IR, CFD and FVC methods

CHAPTER IV

SUMMARY AND CONCLUSIONS

The primary purpose of this thesis is to develop a method for measuring the junction temperature of green and blue LEDs and validating with numerical models as well as understanding the impact of a silicon lens over the junction temperature and optical extraction. Experimental and computational results are compared to demonstrate the junction temperature of green and blue LEDs. Furthermore, the performance of a 520 nm green LED and 450 nm blue LED was compared in order to pave the way of further studies for monochromatic LED systems.

The junction temperature of a green and blue LEDs has been obtained using FVC and IR imaging techniques. During the measurements of green and blue LEDs, it was noticed that a process for removing the LED lens is necessary for accurate measurement results. Since the lens causes a significant error in measuring the junction temperature by using an IR camera, measurements have been conducted for the LED without a lens. Because the existence of lens on LED system allows heat transfer by conduction to the top of the lens and it leads to a decrease in the junction temperature. Although configuration of LEDs with lens generates comparably more heat in junction compared to the cases without a lens, its junction temperature becomes rather low. Since IR camera measures the lens surface over the LED, thermal imaging technique is not found to be a suitable and reliable for the LED system with lens.

The junction temperature measurement methods have been compared in order to demonstrate the level of suitability of forward voltage method in terms of precision and practicability. Specific findings from current work can be listed as follows;

- The accuracy and reliability of the study for measurement of junction temperatures in both numerical and experimental results is in good agreement within 4%.
- Four significant digits are taken for repeatable forward voltage readings to achieve accurate results. Since it was found in the study that 0.001 V change in average forward voltage may result in 0.3 °C shift in junction temperature for LEDs.
- A proposed junction temperature measurement setup is running on the forward voltage change method and it is designed to realize calibration and test phases respectively with an automation.
- The infrared thermal imaging is defined as a much practical technique and its accuracy has been found adequate compared to forward voltage technique, but it is not suitable for measurement of an LED chip with lens.
- A novel process for removing silicone lens of green and blue LEDs has been applied in the current study and a 90% yield is achieved.
- The process for removing silicone lens and painting the bare chip resulted in an increase in junction temperature. It is important to understand that the converted amount of radiant energy into heat led to more increase in junction temperature than the lens effect.
- A green LED was highly sensitive to the change in junction temperature. When operating currents are varied from 200 to 500 mA, variation in junction temperature was found to be around 45%.
- The process for removing the lens affects the blue LED more severely from 200 mA to 500 mA. In fact, at 500mA operating current, removing the lens caused a rise in junction temperature by more than 7.1 ˚C for blue and 4.8 ºC in green LEDs.

SUGGESTIONS FOR FUTURE WORK

The junction temperature measurement methods have been studied in the current thesis for green and blue LED chips and categorized in terms of their capability, practicability and accuracy. In addition, the first measurement setup has been produced by the integration of FVC method to achieve more accurate results in a short time. A set of suggestions for next studies can be given as the following;

- As more advanced technologies are developed, compact and featured electronic products has become prominent. They are getting smaller and generated heat problems become more intense due to serious lifetime and performance issues. Therefore, the junction temperature measurement of a compact system such as LED package, FR4, laser etc. will be hot topics in a few years. In addition of the current thesis which focuses on T_j measurement of single green and blue LED chips, another study can be continued with T_j measurement of compact systems.
- It is not easy to measure junction temperature of a compact system as it is for a single chip. Therefore, the measurement approaches should be developed by increasing the measurement capability that enable to measure several points at the same time.
    - The advanced sourcemeter with multiple voltage outputs can be used in a system to measure a few touch points.
    - A robot arm conrolled by PLC system can be developed to measure several points simultaneously which can be very useful to measure junction temperature of compact system.

- The system capability can also be developed with modeling technology to make a quick prediction about thermal distribution of the compact system before the measurement is completed.
- Even though the first junction temperature measurement test system has reached some requirements of accuracy and reliability, the system still needs to improved by redesigning and adding new specifies. A brief list of suggestions for a true functional prototype system may have the following:
    - The dimensions of the measurement chamber can be optimized in terms of compact electronic products.
    - The device can be designed with the cooling system in order to achieve highly sensitive steady state and thermal equilibrium conditions in a shorter time.
    - PLC controlled heaters can be replaced with a more advanced product which enables us to control the given power of heaters.
    - Developing a sophisticated software system can be next step of the study in order to increase capability, reliability and speed of the measurements.
    - In addition to controlling thermal condition inside of the chamber, other weather conditions can be controlled using different type of sensors and technology.

REFERENCES

[1] Arik M, Setlur A, Weaver S, and Shiang J J, “Energy Efficient Solid State Lighting Systems,” 2012.

[2] D. A. Steigerwald *et al.*, “Illumination with solid state lighting technology,” *IEEE J. Sel. Top. Quantum Electron.*, vol. 8, no. 2, pp. 310–320, 2002.

[3] Tamdogan E, Arik M, Dogruoz M, “Direct Liquid Cooling of High Flux LED Systems: Hot Spot Abatement,” *ASME 2013 Int. Tech. Conf. Exhib. Packag. Integr. Electron. Photonic Microsystems*, vol. Volume 2:, p. 7 pages.

[4] J. R. Pryde, D. C. Whalley, and W. Malalasekera, “A review of LED technology trends and relevant thermal management strategies,” *Thermomechanical Phenom. Electron. Syst. -Proceedings Intersoc. Conf.*, pp. 31–38, 2014.

[5] K. D. Jandt and R. W. Mills, “A brief history of LED photopolymerization,” *Dent. Mater.*, vol. 29, no. 6, pp. 605–617, 2013.

[6] “LED Magazine.” [Online]. Available: https://www.ledsmagazine.com/articles/2004/01/what-is-an-led.html.

[7] “Light Emitting Diode.” [Online]. Available: http://www.wiki-zero.co/index.php?q=aHR0cHM6Ly9lbi53aWtpcGVkaWEub3JnL3dpa2kvTGlnaHQtZW1pdHRpbmdfZGlvZGU.

[8] L. Work, “Nobel Prize in Physics 2014 : Why Were Blue LEDs so Hard to Make ?,” pp. 1–7, 2014.

[9] *Physics of Semiconductor Devices*. 2006.

[10] B. S. F. Holonyak N., “COHERENT (VISIBLE) LIGHT EMISSION FROM Ga(As1−xPx) JUNCTIONS,” *AIP*, 1962.

[11] D. P. J. Bergh A. A., “Light Emitting Diodes,” *Oxford, Clarendon Press*, p. 598 p, 1976.

[12] M. Arik, C. A. Becker, S. E. Weaver, and J. Petroski, “Thermal management of LEDs: package to system,” no. January 2004, p. 64, 2004.

[13] S. Nakamura, M. Senoh, N. Iwasa, and S. I. Nagahama, “High-brightness InGaN blue, green and yellow light-emitting diodes with quantum well structures,” *Jpn. J. Appl. Phys.*, vol. 34, no. 7, pp. L797–L799, 1995.

[14] “United States Secretary of Energy,.” .

[15] “Lumileds,” 2003. [Online]. Available: www.lumileds.com,.

[16] N. C. Chen, C. M. Lin, Y. K. Yang, C. Shen, T. W. Wang, and M. C. Wu, “Measurement of junction temperature in a nitride light-emitting diode,” *Jpn. J. Appl. Phys.*, vol. 47, no. 12, pp. 8779–8782, 2008.

[17] U. Z. Uras, “Thermal Issues Posed by Compact Packaging and IoT for Next Generation SSL,” no. 64, pp. 44–51, 2017.

[18] L. Pérez-Lombard, J. Ortiz, and C. Pout, “A review on buildings energy consumption information,” *Energy Build.*, vol. 40, no. 3, pp. 394–398, 2008.

[19] C. J. Weng, “Advanced thermal enhancement and management of LED packages,” *Int. Commun. Heat Mass Transf.*, vol. 36, no. 3, pp. 245–248, 2009.

[20] L. Yuan, S. Liu, M. Chen, and X. Luo, “Thermal analysis of high power LED array packaging with microChannel cooler,” *2006 7th Int. Conf. Electron. Packag. Technol. ICEPT ’06*, pp. 6–10, 2007.

[21] M. Arik, J. Petroski, and S. Weaver, “Thermal challenges in the future generation solid state lighting applications: light emitting diodes,” *ITherm 2002. Eighth Intersoc. Conf. Therm. Thermomechanical Phenom. Electron. Syst. (Cat. No.02CH37258)*, pp. 113–120, 2002.

[22] M. Arik, Y. Utturkar, and S. Weaver, “Immersion cooling of light emitting diodes,” *2010 12th IEEE Intersoc. Conf. Therm. Thermomechanical Phenom.*

Electron. Syst. ITherm 2010, 2010.

[23] M. Ha and S. Graham, “Microelectronics Reliability Development of a thermal resistance model for chip-on-board packaging of high power LED arrays,” vol. 52, pp. 836–844, 2012.

[24] P. Mashkov, B. Gyoch, S. Penchev, and H. Beloev, “Method for In – Situ Power LEDs ’ Junction Temperature Measurements T sp,” no. 2, pp. 95–100, 2012.

[25] J. Barbosa, D. Simon, and W. Calixto, “Design Optimization of a High Power LED Matrix Luminaire,” *Energies*, vol. 10, no. 5, p. 639, 2017.

[26] E. F. Schubert and J. K. Kim, “Solid-state light sources getting smart,” *Science (80-.).*, vol. 308, no. 5726, pp. 1274–1278, 2005.

[27] L. Jayasinghe, T. Dong, and N. Narendran, “Is the thermal resistance coefficient of high-power LEDs constant?,” *Proc. SPIE*, vol. 6669, no. September 2007, pp. 666911-666911–6, 2007.

[28] D. Todorov and L. Kapisazov, “LED thermal management,” *Electronics*, pp. 139–144, 2008.

[29] Tamdogan E. and Arik M., “Natural convection immersion cooling and optical degradation of liquid cooled LED systems,” *ASME J. Electron. Packag.*, vol. Vol. 137, no. Issue 4.

[30] K. R. Shailesh, C. P. Kurian, and S. G. Kini, “Junction temperature measurement of a LED street light using forward voltage method,” *2014 Int. Conf. Adv. Electron. Comput. Commun. ICAECC 2014*, 2015.

[31] M. Arik, C. Royce, and K. S. Kulkarni, “D eveloping a S tandard M easurement and C alculation P rocedure for H igh B rightness LED J unction T emperature (□ C/□),” no. 1, 2014.

[32] Y. Gu and N. Narendran, “A noncontact method for determining junction

temperature of phosphor-converted white LEDs," no. January 2004, p. 107, 2004.

[33] B. Siegal, "Practical Considerations in High Power LED Junction Temperature Measurements," *2006 Thirty-First IEEE/CPMT Int. Electron. Manuf. Technol. Symp.*, pp. 62–66, 2006.

[34] A. M. Muslu, O. Burak, T. Ense, and A. Mehmet, "Impact of Junction Temperature Over Forward Voltage Drop for Red, Blue and Green High Power Light Emitting Diode Chips," *16th IEEE ITHERM Conf.*, vol. 7, 2017.

[35] M. I. R. Imaging, E. Tamdogan, G. Pavlidis, S. Graham, and M. Arik, "A Comparative Study on the Junction Temperature Measurements of LEDs With Raman Spectroscopy , Forward Voltage Methods," pp. 1–9, 2018.

[36] A. Poppe and M. Unit, "Testing of Power LEDs: The Latest Thermal Testing Standards from JEDEC," *Electron. Cool.*, no. September, pp. 1–11, 2013.

[37] Z. Wang-yang, C. Chun-feng, H. Yan, and L. Qian, "THE ANALYSIS TECHNIQUE OF THERMAL MANAGEMENT FOR LEDS BASED ON THERMAL RESISTANCE," pp. 1–4.

[38] M. J. Wen, S. Subramani, M. Devarajan, and F. Sulaiman, "Effect of ethyl cellulose on thermal resistivity of thixotropic ZnO nano-particle paste for thermal interface material in light emitting diode application," *Mater. Sci. Semicond. Process.*, vol. 58, no. November 2016, pp. 61–67, 2017.

[39] A. Hanß, M. Schmid, E. Liu, and G. Elger, "Transient thermal analysis as measurement method for IC package structural integrity," *Chinese Phys. B*, vol. 24, no. 6, p. 068105, 2015.

[40] E. Juntunen, O. Tapaninen, A. Sitomaniemi, and V. Heikkinen, "Effect of phosphor encapsulant on the thermal resistance of a high-power COB LED module," *IEEE Trans. Components, Packag. Manuf. Technol.*, vol. 3, no. 7, pp.

1148–1154, 2013.

[41] JEDEC Standard JESD51-50, “Overview of Methodologies for the Thermal Measurement of Single- and Multi-Chip, Single- and Multi-PN Junction Light-Emitting Diodes (LEDs).” [Online]. Available: www.jedec.org/sites/default/files/docs/jesd51-50.pdf.

[42] S. J. P. O. Ueda, “Materials and Reliability Handbook for Semiconductor Optical and Electron Devices,.” .

[43] “Lapshere.” [Online]. Available: http://halmapr.com/news/labsphere/page/4/.

[44] A. Alexeev, G. Martin, and V. Hildenbrand, “Structure function analysis and thermal compact model development of a mid-power LED,” *2017 33rd Therm. Meas. Model. Manag. Symp.*, pp. 283–289, 2017.

[45] “No Title.” [Online]. Available: www.optotherm.com.

[46] B. Ozluk, A. M. Muslu, and M. Arik, “A Comparative Study for the Junction Temperature of Green Light Emitting Diodes (LED) s,” pp. 1–11.

[47] “No Title.” [Online]. Available: https://www.vision-systems.com/articles/print/volume-21/issue-8/features/choosing-a-camera-for-infrared-imaging.html.

[48] G. H. Feng, C. C. Sharp, Q. Zhou, W. Pang, E. S. Kim, and K. K. Shung, “Fabrication of MEMS ZnO dome-shaped-diaphragm transducers for high frequency ultrasonic imaging,” *Proc. - IEEE Ultrason. Symp.*, vol. 3, pp. 1950–1953, 2004.

[49] “No Title.” [Online]. Available: httpswww.ansys.comproductselectronicsansys-icepak.

[50] *TSE (Power Supply) and Tübitak UME (Spektrometer). .*

[51] *http://www.cormusa.org/uploads/Scharpf-2015.pdf. .*

[52] ISO and GUM, *Guide to the Expression of Uncertainty in Measurement, (1995), with Supplement 1, Evaluation of measurement data, JCGM 101: 2008*. Geneva, Switzerland: Organization of Standardization, 2008.

APPENDIX A

DATA SHEET OF CREE XP-E2 LEDs

Characteristics

Characteristics	Unit	Minimum	Typical	Maximum
Thermal resistance, junction to solder point - white, royal blue, blue	°C/W		9	
Thermal resistance, junction to solder point - green	°C/W		15	
Thermal resistance, junction to solder point - PC amber	°C/W		9	
Thermal resistance, junction to solder point - amber	°C/W		7	
Thermal resistance, junction to solder point - red-orange, red	°C/W		5	
Viewing angle (FWHM) - white	degrees		110	
Viewing angle (FWHM) - royal blue, blue, green	degrees		135	
Viewing angle (FWHM) - PC amber	degrees		110	
Viewing angle (FWHM) - amber, red-orange, red	degrees		130	
Temperature coefficient of voltage - white	mV/°C		-2.3	
Temperature coefficient of voltage - royal blue, blue	mV/°C		-3.3	
Temperature coefficient of voltage - green	mV/°C		-3.8	
Temperature coefficient of voltage - PC amber	mV/°C		-2.5	
Temperature coefficient of voltage - amber, red-orange, red	mV/°C		-1.8	
ESD withstand voltage (HBM per Mil-Std-883D)- white, royal blue, blue, green	V			8000
ESD classification (HBM per Mil-Std-883D) - PC amber, amber, red-orange, red			Class 2	
DC forward current	mA			1000
Reverse voltage	V			5
Forward voltage (@ 350 mA, 85 °C) - white	V		2.9	3.25
Forward voltage (@ 700 mA, 85 °C) - white			3.05	
Forward voltage (@ 1000 mA, 85 °C) - white			3.15	
Forward voltage (@ 350 mA, 25 °C) - royal blue, blue	V		3.1	3.5
Forward voltage (@ 1000 mA, 25 °C) - royal blue, blue	V		3.4	
Forward voltage (@ 350 mA, 25 °C) - green	V		3.2	3.8
Forward voltage (@ 1000 mA, 25 °C) - green	V		3.7	
Forward voltage (@ 350 mA, 25 °C) - PC amber	V		3.05	3.5
Forward voltage (@ 1000 mA, 25 °C) - PC amber	V		3.28	
Forward voltage (@ 350 mA, 25 °C) - amber, red-orange, red	V		2.2	2.6
Forward voltage (@ 1000 mA, 25 °C) - amber, red-orange, red	V		2.65	
LED junction temperature	°C			150

Flux Characteristics

Color	Minimum Luminous Flux (lm) @ 350 mA		Dominant Wavelength (nm)				Order Codes
			Minimum		Maximum		
	Group	Flux (lm)	Group	DWL (nm)	Group	DWL (nm)	
Blue	K2	30.6	B3	465	B6	485	XPEBBL-L1-0000-00Y01
			B3	465	B5	480	XPEBBL-L1-0000-00Y02
			B4	470	B5	480	XPEBBL-L1-0000-00Y05
	K3	35.2	B3	465	B6	485	XPEBBL-L1-0000-00Z01
			B3	465	B5	480	XPEBBL-L1-0000-00Z02
			B4	470	B5	480	XPEBBL-L1-0000-00Z05
	M2	39.8	B3	465	B6	485	XPEBBL-L1-0000-00201
			B3	465	B5	480	XPEBBL-L1-0000-00202
			B4	470	B5	480	XPEBBL-L1-0000-00205
	M3	45.7	B3	465	B6	485	XPEBBL-L1-0000-00301
			B3	465	B5	480	XPEBBL-L1-0000-00302
			B4	470	B5	480	XPEBBL-L1-0000-00305

Color	Minimum Luminous Flux (lm) @ 350 mA		Calculated Minimum PPF (µmol/s)	Dominant Wavelength (nm)				Order Codes
				Minimum		Maximum		
	Group	Flux (lm)		Group	DWL (nm)	Group	DWL (nm)	
Green	Q2	87.4	0.80	G2	520	G4	535	XPEBGR-L1-0000-00A01
				G2	520	G3	530	XPEBGR-L1-0000-00A02
				G3	525	G4	535	XPEBGR-L1-0000-00A03
	Q3	93.9	0.86	G2	520	G4	535	XPEBGR-L1-0000-00B01
				G2	520	G3	530	XPEBGR-L1-0000-00B02
				G3	525	G4	535	XPEBGR-L1-0000-00B03
	Q4	100	0.91	G2	520	G4	535	XPEBGR-L1-0000-00C01
				G2	520	G3	530	XPEBGR-L1-0000-00C02
				G3	525	G4	535	XPEBGR-L1-0000-00C03
	Q5	107	0.98	G2	520	G4	535	XPEBGR-L1-0000-00D01
				G2	520	G3	530	XPEBGR-L1-0000-00D02
				G3	525	G4	535	XPEBGR-L1-0000-00D03
	R2	114	1.04	G2	520	G4	535	XPEBGR-L1-0000-00E01
				G2	520	G3	530	XPEBGR-L1-0000-00E02
				G3	525	G4	535	XPEBGR-L1-0000-00E03
	R3	122	1.11	G2	520	G4	535	XPEBGR-L1-0000-00F01
				G2	520	G3	530	XPEBGR-L1-0000-00F02
				G3	525	G4	535	XPEBGR-L1-0000-00F03

Performans Characteristics

Color	DWL Group	Minimum DWL (nm) @ 350 mA	Maximum DWL (nm) @ 350 mA
Royal Blue	D3	450	455
	D4	455	460
	D5	460	465
Blue	B3	465	470
	B4	470	475
	B5	475	480
	B6	480	485
Green	G2	520	525
	G3	525	530
	G4	530	535
Amber	A2	585	590
	A3	590	595
Red-Orange	O3	610	615
	O4	615	620
Red	R2	620	625
	R3	625	630

Performans Groups – Forward Voltages

Forward Voltage Group	Minimum Forward Voltage (V) @ 350 mA	Maximum Forward Voltage (V) @ 350 mA
B	1.75	2.0
C	2.0	2.25
D	2.25	2.5
E	2.5	2.75
F	2.75	3.0
G	3.0	3.25
H	3.25	3.5
J	3.5	3.75

Performans Groups – Luminous Flux

Group Code	Minimum Luminous Flux (lm) @ 350 mA	Maximum Luminous Flux (lm) @ 350 mA
K2	30.6	35.2
K3	35.2	39.8
M2	39.8	45.7
M3	45.7	51.7
N2	51.7	56.8
N3	56.8	62.0
N4	62.0	67.2
P2	67.2	73.9
P3	73.9	80.6
P4	80.6	87.4
Q2	87.4	93.9
Q3	93.9	100
Q4	100	107
Q5	107	114
R2	114	122
R3	122	130
R4	130	139

Performans Groups – Radiant Flux

Group	Minimum Radiant Flux (mW) @ 350 mA	Maximum Radiant Flux (mW) @ 350 mA
30 (J)	450	475
31 (K)	475	500
32 (L)	500	525
33 (M)	525	550
34 (N)	550	575
35 (P)	575	600
36 (Q)	600	625
37 (R)	625	650
38 (S)	650	675
39 (T)	675	700

Thermal Design

Green

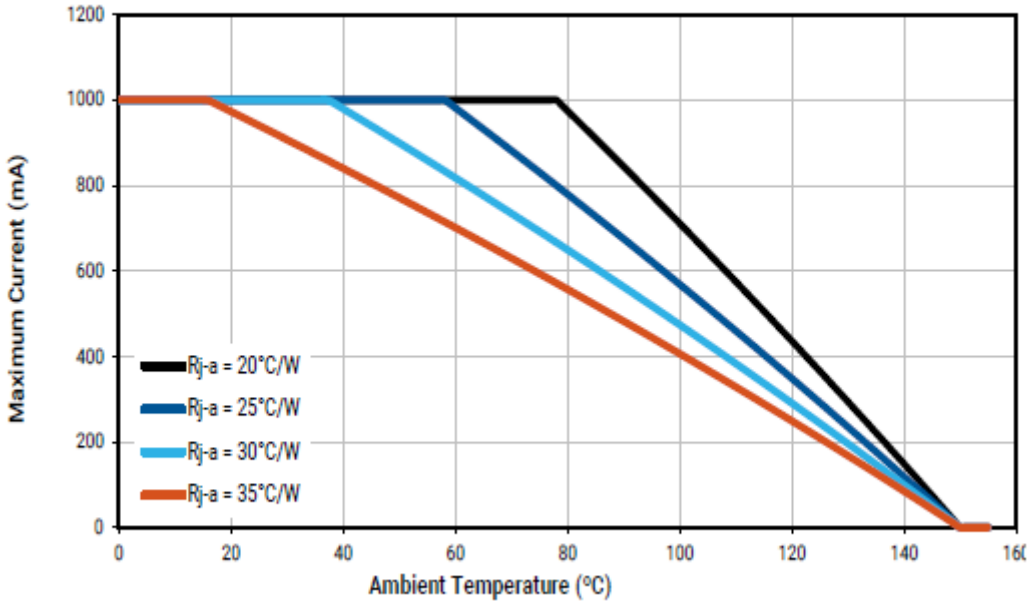

Royal Blue, Blue

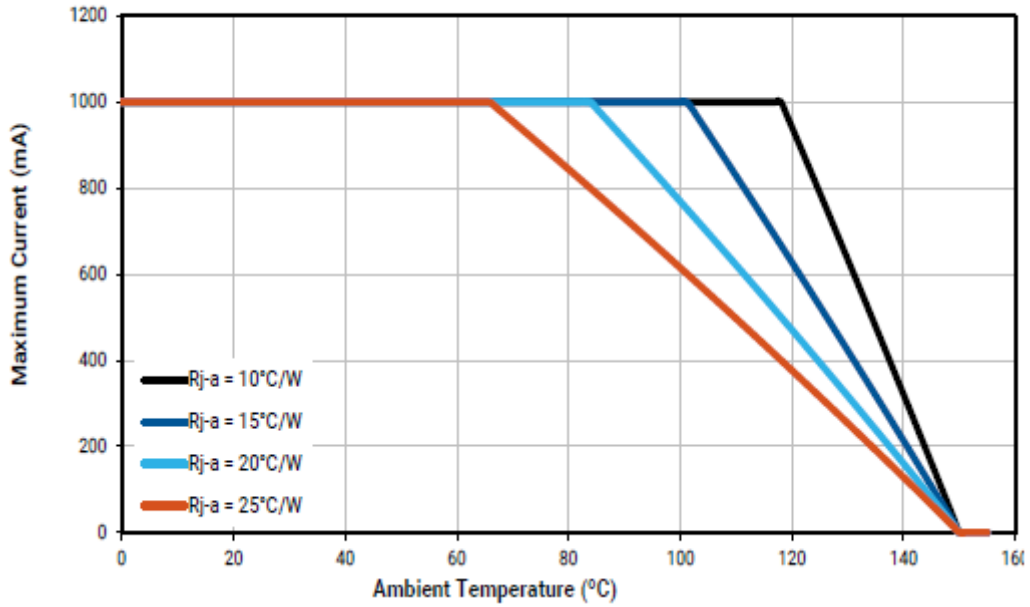

APPENDIX B

UNCERTAINITY ANALYSIS

The measurement uncertainty of parameters (T_j, V_f, P, Φ_e and $\lambda_{Dom)}$ was calculated with an analytical study. The calibration certificates of devices were used to determine contribution of each component to the uncertainty calculation. With regard to the observations and standard deviations calculated in measurements, uncertainties for the oven system and source meter are added.

The uncertainty value for the spectrometer, SCL 1400 lamp, LPS 150 power supply and Agilent power supply are taken from the calibration certificates issued by the certified institutions for the integration of radiant power and dominant wavelength measurements. [50], while SCL 1400 lamp life uncertainty values, nonlinearity spectrometers, spectrometer drift, spectrometer stray light, sphere near field absorption and sphere non-uniformity are obtained from a guide presented by Labsphere [51]. In calculations, variations in temperature and air flow in the laboratory are also taken into account. The uncertainties for individual Luminous Flow, CCT and CRI measurements are calculated in accordance with the " Guide for the Expression of Uncertainty in Measurement (GUM, 2008) " within a 95% confidence interval for which the uncertainties are set out in Table 1, Table 2 and Table 3 [52].

In addition, the conducted uncertainty for the measurement of the blue chip's junction temperature is also given in Table 18. Results have shown that the calculation of the junction temperature is done with the forward voltage change method below the range specified in the previous study.

Detailed measurements equations are shown below;

"T_jx= Junction temperature measurement"
"V_fx= Steady forward voltage value"
"T_jo= First junction temperature"
"V_fo= First forward voltage"
"KVT= Voltage-temperature coefficient"

$$T_{jx} = T_{jo} + \frac{V_{fx} - V_{fo}}{KVT}$$

"V_f1 and V_f2; Forward voltage measurements at ambient temperatures of T_1 and T_2"
"T_j1 and T_j2; Junction temperatures after thermal equilibrium"

$$KVT = \frac{V_{f1} - V_{f2}}{T_{j1} - T_{j2}}$$

"The standard uncertainty of junction temperature TJ is given by;"

$$A = U^2$$

$$A_{Tj} = A_{Tjo} + \frac{1}{KVT^2} \cdot (A_{Vfx} + A_{Vfo}) + \frac{(V_{fx} - V_{fo})^2}{KVT^4} \cdot A_{KVT}$$

"The standard uncertainty of the voltage-temperature coefficient; KVT, is given by;"

$$A_{KVT} = \left[\frac{(V_{f1} - V_{f2})^2}{(T_{j1} - T_{j2})^4}\right] \cdot (A_{Tj1} + A_{Tj2}) + \frac{1}{(T_{j1} - T_{j2})^2} \cdot (A_{Vf1} + A_{Vf2})$$

Table Appendix B.1 Integrating sphere – Luminous flux (Lm) measurement uncertainty

	Given or Expected Data	*Distribution Type*	*Standard Measurement Uncertainty*	*Sensitivity Constant*	*Uncertainty Constant*	*Variant*
Reference Device or Related Uncertainty Components						
Spectrometer (Wavelength Calibration)	0,7	Normal	0,35	1	0,35	0,1225
SCL 1400 Lamp	1,00	Normal	0,5	1	0,5	0,25
LPS 150 Power Supply (Direct Voltage)	0,005	Normal	0,0025	1	0,0025	0,00000625
LPS 150 Power Supply (Direct Current)	0,005	Normal	0,0025	1	0,0025	0,00000625
LPS 100 Power Supply (Direct Voltage)	0,005	Normal	0,0025	1	0,0025	0,00000625
LPS 100 Power Supply (Direct Current)	0,005	Normal	0,0025	1	0,0025	0,00000625
Agilent Power Supply (AC Voltage)	0,06	Normal	0,03	1	0,03	0,0009
Agilent Power Supply (Frequency)	0,01	Normal	0,005	1	0,005	0,000025
SCL 1400 Lamp Lifetime Uncertainty Constant	3,2332E-05	Rectangle	1,8667E-05	1	1,8667E-05	3,4844E-10
Spectrometer Non-linearity Uncertainty Constant	0,06	Normal	0,03	1	0,03	0,0009
Spectrometer Light Leakage Uncertainty Constant	0,05	Rectangle	0,02886751	1	0,02886751	0,00083333
Spectrometer Drift Based Uncertainty	0,05	Normal	0,025	1	0,025	0,000625
Sphere Space Absorptivity Uncertainty Constant	0,5	Normal	0,25	1	0,25	0,0625
Sphere Non-uniformity Uncertainty Constant	0,2	Normal	0,1	1	0,1	0,01
Method Based Uncertainty						
Temperature Based Uncertainty	0,77558493	Rectangle	0,44778417	1	0,44778417	0,20051066
Air Velocity Based Uncertainty	0	Rectangle	0	1	0	0
Experiment Repeatability Based Uncertainty	2,51197134	Normal	1,25598567	1	1,25598567	1,5775
						2,61022598
Overall Measurement Uncertainty:			1,61561938			
Expanded Measurement Uncertainty:			3,23123876			

Table Appendix B.2 Integrating sphere – CCT measurement uncertainty

	Given or Expected Data	*Distribution Type*	*Standard Measurement Uncertainty*	*Sensitivity Constant*	*Uncertainty Constant*	*Variant*
Reference Device or Related Uncertainty Components						
Spectrometer (Wavelength Calibration)	0,7	Normal	0,35	1	0,35	0,1225
SCL 1400 Lamp	0,23	Normal	0,115	1	0,115	0,013225
LPS 150 Power Supply (Direct Voltage)	0,005	Normal	0,0025	1	0,0025	6,25E-06
LPS 150 Power Supply (Direct Current)	0,005	Normal	0,0025	1	0,0025	6,25E-06
LPS 100 Power Supply (Direct Voltage)	0,005	Normal	0,0025	1	0,0025	6,25E-06
LPS 100 Power Supply (Direct Current)	0,005	Normal	0,0025	1	0,0025	6,25E-06
Agilent Power Supply (AC Voltage)	0,06	Normal	0,03	1	0,03	0,0009
Agilent Power Supply (Frequency)	0,01	Normal	0,005	1	0,005	0,000025
SCL 1400 Lamp Lifetime Uncertainty Constant	3,2332E-05	Rectangle	1,8667E-05	1	1,87E-05	3,48E-10
Spectrometer Non-linearity Uncertainty Constant	0,06	Normal	0,03	1	0,03	0,0009
Spectrometer Light Leakage Uncertainty Constant	0,05	Rectangle	0,02886751	1	0,028868	0,000833
Spectrometer Drift Based Uncertainty	0,05	Normal	0,025	1	0,025	0,000625
Sphere Space Absorptivity Uncertainty Constant	0,5	Normal	0,25	1	0,25	0,0625
Sphere Non-uniformity Uncertainty Constant	0,2	Normal	0,1	1	0,1	0,01
Method Based Uncertainty						
Temperature Based Uncertainty	0,77558493	Rectangle	0,44778417	1	0,447784	0,200511
Air Velocity Based Uncertainty	0	Rectangle	0	1	0	0
Experiment Repeatability Based Uncertainty	3,46	Normal	1,73	1	1,73	2,9929
						9,016845
Overall Measurement Uncertainty:			3,002806195			
Expanded Measurement Uncertainty:			6,005612389			

Table Appendix B.3 Integrating sphere – CRI measurement uncertainty

	Given or Expected Data	*Distribution Type*	*Standard Measurement Uncertainty*	*Sensitivity Constant*	*Uncertainty Constant*	*Variant*
Reference Device or Related Uncertainty Components						
Spectrometer (Wavelength Calibration)	0,7	Normal	0,35	1	0,35	0,1225
SCL 1400 Lamp	1,3	Normal	0,65	1	0,65	0,4225
LPS 150 Power Supply (Direct Voltage)	0,005	Normal	0,0025	1	0,0025	0,00000625
LPS 150 Power Supply (Direct Current)	0,005	Normal	0,0025	1	0,0025	0,00000625
LPS 100 Power Supply (Direct Voltage)	0,005	Normal	0,0025	1	0,0025	0,00000625
LPS 100 Power Supply (Direct Current)	0,005	Normal	0,0025	1	0,0025	0,00000625
Agilent Power Supply (AC Voltage)	0,06	Normal	0,03	1	0,03	0,0009
Agilent Power Supply (Frequency)	0,01	Normal	0,005	1	0,005	0,000025
SCL 1400 Lamp Lifetime Uncertainty Constant	3,2332E-05	Rectangle	1,8667E-05	1	1,8667E-05	3,4844E-10
Spectrometer Non-linearity Uncertainty Constant	0,06	Normal	0,03	1	0,03	0,0009
Spectrometer Light Leakage Uncertainty Constant	0,05	Rectangle	0,02886751	1	0,02886751	0,00083333
Spectrometer Drift Based Uncertainty	0,05	Normal	0,025	1	0,025	0,000625
Sphere Space Absorptivity Uncertainty Constant	0,5	Normal	0,25	1	0,25	0,0625
Sphere Non-uniformity Uncertainty Constant	0,2	Normal	0,1	1	0,1	0,01
Method Based Uncertainty						
Temperature Based Uncertainty	0,77558493	Rectangle	0,44778417	1	0,44778417	0,20051066
Air Velocity Based Uncertainty	0	Rectangle	0	1	0	0
Experiment Repeatability Based Uncertainty	0,14	Normal	0,07	1	0,07	0,0049
						0,23774999
Overall Measurement Uncertainty:			0,487596136			
Expanded Measurement Uncertainty:			0,975192271			

Table A.5 Uncertainty analysis for the junction temperature of green chip

No	*Component*	*Symbol*	*Standard Uncertainty*	*Type*	*Sensitivity Coefficient*	*Contribution*
1	Initial junction temperature	T_{j0}	0.2	A	1	0.2
2	Steady voltage	V_f'	1	B	-0.8	0.8
3	Initial voltage	V_{f0}	1	B	0.8	0.8
4	Voltage-temperature coefficient	K_{VT}	0.006	B	15.12	0.089
4.1	Calibration junction temperature 1	T_{J1}	1	A	0.4	
4.2	Calibration junction temperature 2	T_{J2}	1	A	-0.4	
4.3	Calibration voltage 1	V_{f1}	1	B	-0.5	
4.4	Calibration voltage 2	V_{f2}	1	B	0.5	
	Total uncertainty					$u(T_j) = 1.15$
	Expanded uncertainty (k = 2)					$U(T_j) = 2.31$

Table A.5 Uncertainty analysis for the junction temperature of blue chip

No	*Component*	*Symbol*	*Standard Uncertainty*	*Type*	*Sensitivity Coefficient*	*Contribution*
1	Initial junction temperature	T_{j0}	0.2	A	1	0.2
2	Steady voltage	V_f'	1	B	-0.8	0.8
3	Initial voltage	V_{f0}	1	B	0.8	0.8
4	Voltage-temperature coefficient	K_{VT}	0.006	B	15.12	0.089
4.1	Calibration junction temperature 1	T_{J1}	1	A	0.4	
4.2	Calibration junction temperature 2	T_{J2}	1	A	-0.4	
4.3	Calibration voltage 1	V_{f1}	1	B	-0.5	
4.4	Calibration voltage 2	V_{f2}	1	B	0.5	
	Total uncertainty					$u(T_j) = 1.33$
	Expanded uncertainty (k = 2)					$U(T_j) = 2.66$

BIOGRAPHY

Burak Özlük

Research Areas
Developing junction temperature measurement methods for green and blue LED chips.
(CFD analysis, experimental and analytical studies)

M. Sc. Graduate
Özyeğin University, 2018

B. Sc. Graduate
Selçuk University, 2016

Burak Ozluk received the B.Sc. in mechanical engineering department from Selcuk University, Konya, Turkey, in 2016. Throughout his undergraduate education, he had participated for a long-term international exchange program and studied in Politechnica Lubelska Technical University, Lublin, Poland, between 2013-2014. He has also experienced short-term team works in the USA between 2013-2016.

Currently, he is pursuing the M.Sc. degree with the University of Ozyegin, Istanbul, Turkey, focusing on developing an LED thermal characterization setup for the junction temperature measurements of green and blue LEDs. During his master education, he also worked as a teaching and research assistant at Ozyegin University.

At the end of his study, 2 journals (submitted), 1 conference paper, 1 USA patent application have been served to the literature. Moreover, he has been assigned in the TÜBİTAK 1005 Project during his master study.